Basic Energy Sciences Roundtable

Foundational Science for Carbon-Neutral Hydrogen Technologies

Technology Status Document

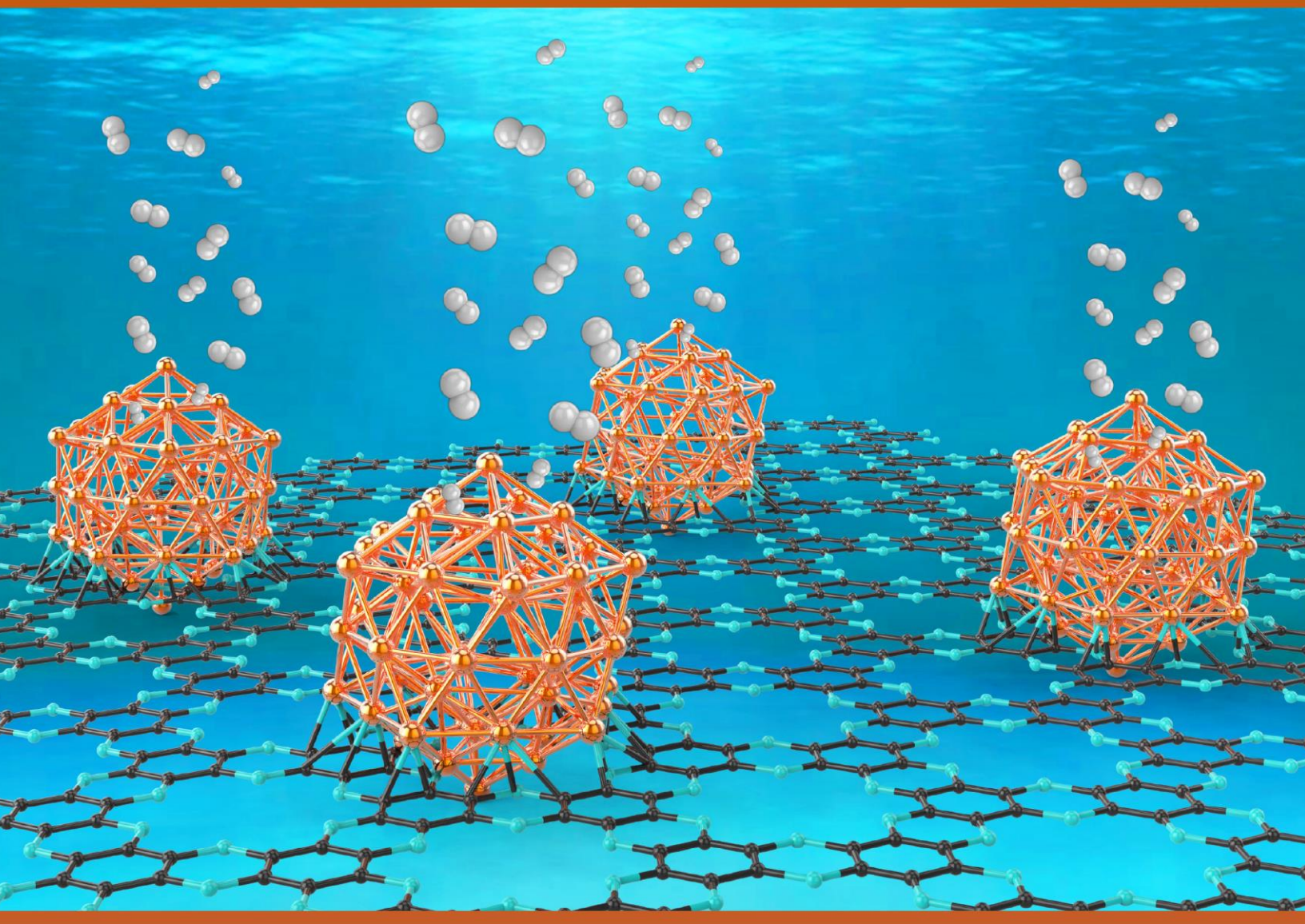

Transformative research for carbon-neutral hydrogen production, chemical- and materials-based hydrogen storage, and utilization for hydrogen technologies

Cover reprinted with permission of Fuel Cells Works *https://fuelcellsworks.com/*

Foundational Science for Carbon-Neutral Hydrogen Technologies
Technology Status Document

Basic Energy Sciences Virtual Roundtable Co-Chairs
Morris Bullock, Pacific Northwest National Laboratory
Karren More, Oak Ridge National Laboratory

Lead author
Deborah J. Myers, Argonne National Laboratory, Lemont, IL

Contributing authors
Rajesh K. Ahluwalia, Argonne National Laboratory, Lemont, IL
Mark D. Allendorf, Sandia National Laboratories, Livermore, CA
Harry Atwater, California Institute of Technology, Pasadena, CA
Thomas Autrey, Pacific Northwest National Laboratory, Richland, WA
Kathy Ayers, Nel Hydrogen, Wallingford, CT
Rodney Borup, Los Alamos National Laboratory, Los Alamos, NM
Mark E. Bowden, Pacific Northwest National Laboratory, Richland, WA
Katherine J. Chou, National Renewable Energy Laboratory, Golden, CO
Hiroyasu Furukawa, Lawrence Berkeley National Laboratory, Berkeley, CA
Thomas Gennett, National Renewable Energy Laboratory, Golden, CO
Jeffrey Goldmeer, General Electric, Boston, MA
Bri-Mathias Hodge, National Renewable Energy Laboratory, Golden, CO
Theodore Krause, Argonne National Laboratory, Lemont, IL
Jeffery R. Long, Lawrence Berkeley National Laboratory, Berkeley, CA
Anna S. Lord, Sandia National Laboratories, Albuquerque, NM
Pin-Ching Maness, National Renewable Energy Laboratory, Golden, CO
Anthony McDaniel, Sandia National Laboratories, Livermore, CA
Pinakin Patel, T2M Global, Danbury, CT
Bryan Pivovar, National Renewable Energy Laboratory, Golden, CO
Christopher San Marchi, Sandia National Laboratories, Livermore, CA
Prabhakar Singh, University of Connecticut, Storrs, CT
Vitalie Stavila, Sandia National Laboratories, Livermore, CA
John Hu, West Virginia University, Morgantown, WV

Acknowledgement to DOE, Energy Efficiency & Renewable Energy, Hydrogen and Fuel Cell Technologies Office
Eric Miller, DOE-EERE-HFTO
Ned Stetson, DOE-EERE-HFTO
Zeric Hulvey, DOE-EERE-HFTO
Neha Rustagi, DOE-EERE-HFTO

Contents

Abbreviations

AEM	alkaline electrolyte membrane or anion-exchange membrane
AEM-WE	anion-exchange membrane or alkaline electrolyte membrane water electrolyzer
AmC	amorphous carbon
BET	Brunauer–Emmett–Teller
BF/BOF	blast furnace/basic oxygen furnace
CCL	cathode catalyst layer
CNT	carbon nanotube
COF	covalent-organic framework
CS	chemical storage
DFT	density functional theory
DOE	US Department of Energy
DRI/EAF	direct reduced iron/electric arc furnace
EERE	Energy Efficiency and Renewable Energy
FCEV	fuel cell electric vehicle
GE	General Electric
GH_2	gaseous hydrogen
GR	graphitic carbon
HDO	hydrodeoxygenation
HER	hydrogen evolution reaction
HFTO	Hydrogen and Fuel Cell Technologies Office
HyMARC	Hydrogen Materials Advanced Research Consortium
LA	liquid alkaline
LA-WE	liquid alkaline water electrolyzer
LH_2	liquid hydrogen
LHV	lower heating value
LOHC	liquid organic hydrogen carrier
MEA	membrane-electrode assembly
MOF	metal-organic framework
OER	oxygen evolution reaction
ORR	oxygen reduction reaction
PAF	porous aromatic framework
PEC	photoelectrochemical cell
PEM	polymer electrolyte or proton-exchange membrane
PEMFC	polymer electrolyte or proton-exchange membrane fuel cell
PEM-WE	proton-exchange or polymer electrolyte membrane water electrolyzer
PFSA	perfluorosulfonic acid
PGM	platinum group metal
R&D	research and development
SMR	steam methane reforming
SOFC	solid oxide fuel cell
SO-WE	solid oxide water electrolyzer
TC	turbostratic carbon
TCD	thermal catalytic decomposition
WE	water electrolysis or electrolyzer
YSZ	yttria-stabilized zirconia

1. Introduction

The purpose of this technology status document is to provide the status of carbon-neutral hydrogen technologies. **Figure 1** illustrates the potential sources of hydrogen and many of the pathways for hydrogen production, delivery and storage scenarios, and the myriad end uses of hydrogen, as summarized by the US Department of Energy (DOE).[1, 2] The state of the art in the implementation, limitations, and challenges of the majority of these technologies—and others not depicted in this figure—is summarized in this document, which is arranged by the three broad categories depicted in **Figure 1**: production, storage and transport, and utilization.

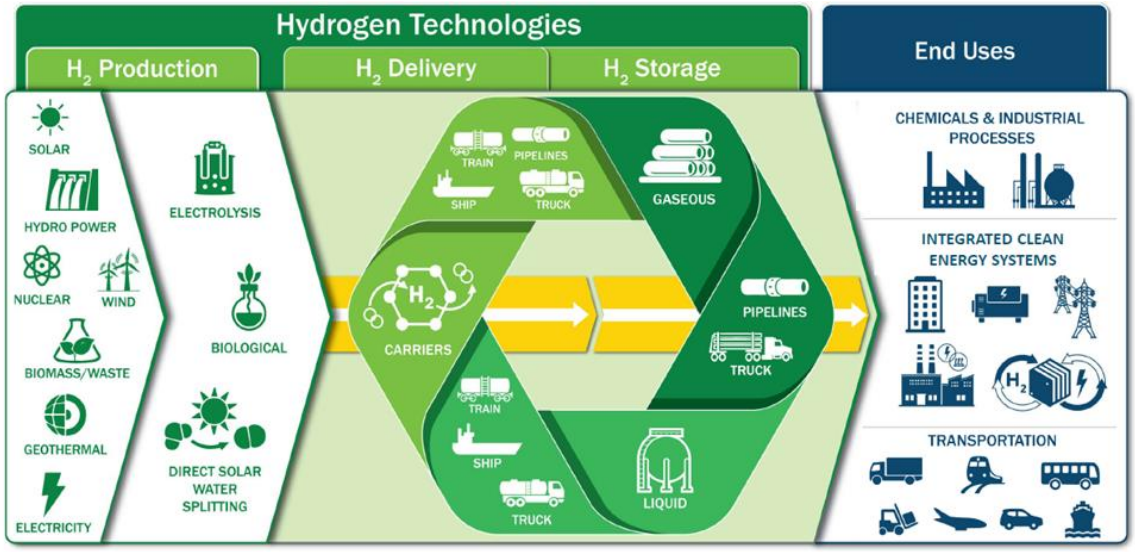

Figure 1. Overview of hydrogen production, delivery and storage, and utilization technologies. Source: [1] Image courtesy of the U.S. Department of Energy.

2. Hydrogen Production

Hydrogen can be extracted from a variety of sources, such as fossil fuels, biomass and waste, and water. Hydrogen is currently produced primarily by using thermochemical processes, such as reforming, pyrolysis, and gasification of hydrocarbon feedstocks. High-temperature catalytic steam methane reforming (SMR) is the dominant process, accounting for approximately 75% of the hydrogen produced globally in 2019.[3] Other processes with smaller production volumes that are in earlier stages of development but with greater potential for implementation as carbon-neutral or carbon-free pathways are electrochemical water splitting and microbial fermentation of biomass.

2.1 Production of Hydrogen by Electrochemical Water Splitting

Electrochemical processes can be used to dissociate water into hydrogen and oxygen. The energy to drive this endothermic reaction can either be electricity—ideally produced using renewable, carbon-neutral processes—input to an electrolyzer or light coupled directly with a photoelectrochemical cell (PEC). Although <0.1% of the hydrogen production worldwide in 2019 used electrolysis,[3] production capacities have increased dramatically over the last decade. As of 2019, the worldwide installed water electrolysis capacity was ~75 MW, and over 40 GW of installations are planned by 2030 as of February 2021.[4] There are three types of commercial water electrolyzers (WEs) and one type of electrolyzer in the developmental stage: proton-exchange or polymer electrolyte membrane (PEM-WE), liquid alkaline (LA-WE), solid oxide (SO-WE), and anion-exchange membrane or alkaline electrolyte membrane (AEM-

WE), respectively.[5] PEM-WEs, LA-WEs, and AEM-WEs operate at less than ~100 °C, and SO-WEs operate at ~800 °C. LA-WEs are generally less expensive than PEM-WEs because they use platinum group metal-free (PGM-free) electrocatalysts rather than iridium and platinum, but they are less efficient and typically operate at lower current densities. The high operating temperatures of SO-WEs allow a significant portion of the energy required to split water to be provided from thermal energy by using sources, such as solar energy and nuclear power plants.[5] PEC water splitting is considered a long-term technology with enormous potential for carbon-free hydrogen production.[2]

2.1.1 Proton Exchange Membrane Water Electrolysis

The components and design of a PEM electrolyzer cell and stack are shown in **Figure 2**.[6] The cell unit comprises a titanium mesh flow field and platinum-coated titanium porous transport layer, an iridium oxide anode catalyst, a perfluorosulfonic acid (PFSA) membrane, a cathode of carbon-supported platinum nanoparticles, and carbon-based porous gas diffusion layers and flow field. The status of the design and materials used for PEM electrolyzers are still influenced by its development legacy, starting from limited numbers of small-scale units for oxygen generation for life support. The criticality of the application drove a high design margin, and the low production volumes led to the adaptation of existing materials vs. the development of electrolysis-specific materials.

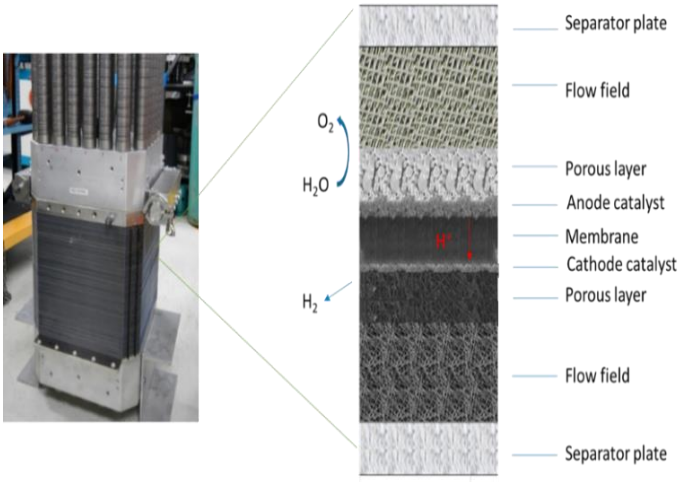

Figure 2. Components of a PEM electrolyzer cell and stack. Source: Ref. [6] (Left): Image courtesy of Nel Hydrogen US. (Right): Reprinted from International Journal of Hydrogen Energy, Vol 44, Villagra, et. al., "An Analysis of PEM Water Electrolysis Cells Operating at Elevated Current Densities," 9708-9717 (2019) with permission from Elsevier.

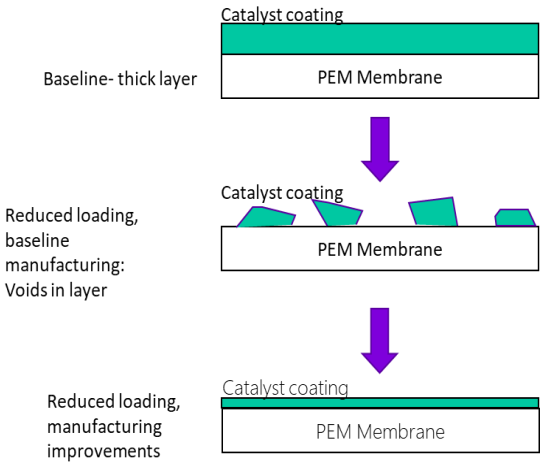

Figure 3. Schematic of PEM electrolyzer catalyst-coated membrane illustrating issues in coating uniformity when anode catalyst loading is reduced. Source: Image courtesy of Nel Hydrogen US.

For example, porous transport layers for the water-oxygen side of the cell are still derived from filter materials used in oil and gas applications. Most membrane development has focused on PEM fuel cells (PEMFCs), optimizing parameters for hot, dry operation and freeze-thaw cycling rather than developing membranes for full liquid hydration and differential pressure. Therefore, electrolyzers still use relatively thick perfluorosulfonic acid (PFSA) membranes that have not changed since the development of chemically stabilized Nafion in the early 2000s. Low volumes have also driven relatively low-speed, labor-intensive manufacturing methods that result in low process capability and high catalyst loadings (thicker layers are required to achieve uniformity in coatings; see **Figure 3**).

Capital cost reductions and efficiency improvements are being pursued to serve emerging energy markets and reach parity with fossil fuel for hydrogen from water

electrolysis. The capital cost is driven by labor and material demands, and the efficiency is driven by the activation overpotential for the oxygen evolution reaction (OER) and the membrane thickness. Promising pathways for increasing OER activity include increasing the catalyst surface area and adding higher-activity components, such as ruthenium. However, such changes often also decrease stability. Specific alloying approaches and extended structures could overcome these challenges but are not yet completely developed. On the membrane side, knowledge of the variables that can be tuned from fuel cell work are being leveraged to develop electrolyzer-specific materials that have less susceptibility to swelling in water, appropriate reinforcements for differential pressure, and low hydrogen permeability.

The electrolyzer cell involves interacting components (**Figure 2**), complicating the introduction of new materials. The interfaces between components must be considered, and the component manufacturing methods must be compatible. For example, a membrane process that involves hydrating the membrane may preclude subsequent dry-coating steps. Thus, co-optimization is often required to enable new advancements. From an electrochemical standpoint, the oxygen and hydrogen electrodes contain much more catalyst than is needed to support the reaction; however, the catalysts in the layers must be accessible, so they must be electrically connected within the cell. In the PEMFC, this connectivity is achieved by using carbon supports to disperse the catalyst particles within the coated catalyst layer and using microporous layers for the gas diffusion layers to bridge across the catalyst layer. The manufacturing method also plays a key role, as shown in **Figure 3**. For the electrolyzer anode, neither stable catalyst supports nor microporous layers on the titanium porous transport layer have been significantly developed to date, although some niobium- and titanium-based supports have shown promise for the iridium-based catalyst.[7]

Ongoing activities in materials development for PEM electrolyzers include optimized membrane chemistry, high-activity catalysts, and stable support structures. In addition to the material composition, the material design activities must also take into account material form to optimize electrode layer structures, including catalyst extended structures and porous transport layers. For example, mechanical optimizations for compressive strength and creep properties are being performed concurrently with the optimization of chemical properties, such as conductivity. Process fundamentals must go hand in hand with materials development to enable the consistent and rapid fabrication of large components with precise features. These efforts involve significant basic research in areas such as reaction dynamics and modeling thermal gradients in large vessels to understand their impacts on resulting catalyst surface structure and particle sizes, as well as to understand how different types of inks (i.e., metal blacks, metals on carbon, and oxides) affect absorption and the resulting rheology behavior. Degradation mechanisms for catalyst and polymer materials, as well as coatings, should be characterized in detail and understood to more effectively define accelerated tests for predicting long-term performance; similarly, methods for measuring small changes can assist in extrapolating lifetimes.[7, 8]

2.1.2 Alkaline and Anion-Exchange Membrane Water Electrolysis

Alkaline electrolyzers can be classified into two types: one using a liquid potassium hydroxide electrolyte at concentration of 25–30% imbibed into a porous separator and the other using a polymer membrane electrolyte with cationic functional groups, termed an *anion-exchange membrane* (AEM), that selectively conducts hydroxyl ions. Liquid alkaline water electrolysis (LA-WE) is an established technology that currently has the largest share of the global electrolysis market. A 2018 review listed 20 leading LA-WE manufacturers in order of their production capacity.[9] The ranking was based on a company's status as of 2017 for producing the following:

- an electrolyzer providing 16 bar hydrogen at a rate of 1,000 Nm^3/h (Normal Cubic Meters per hour ; "normal" conditions are 0 °C and 1 atm) with a 4.7 MW power input or less, a lower heating value (LHV) efficiency of 64%, and an approximate lifetime of 8 years;

- an electrolyzer providing 30 bar hydrogen at a rate of 1,000 Nm^3/h with a <4.5 MW power input and LHV efficiency of 79%; and
- an electrolyzer providing 30 bar hydrogen at a rate of 2,230 Nm^2/h given 10 MW, resulting in an LHV efficiency of 64% and a 10 year stack lifetime.[9-12]

The technology has continued to grow and improve since these reviews were published in 2017. For example, a commercial LA-WE can produce up to 3,800 Nm^3 of hydrogen given 2.2 MW.[13] This technology has been used in a few recent projects on the order of tens of megawatts.[14-16]

LA-WEs have a relatively slow response time compared with either PEM-WEs or AEM-WEs, making it difficult to for them adapt to transient power loads from solar and wind energy.[17] Furthermore, dynamic operation can reduce gas purity when only a fraction of rated power is being used owing to manifold electrolysis.[18] The two major contributions to overpotentials that limit LA-WE performance are caused by bubble formation on the electrode–electrolyte interface that blocks electron transfer and by the high ionic resistance of the thick diaphragm.[19-21] Circulating the electrolyte and modifying the electrode with pathways for bubble escape can help relieve the issues related to bubble formation.[19-21] An ideal separator must have high chemical stability, high wettability, low electrical resistance, and high resistance to permeation by hydrogen.[22] Typical separators are either glass-reinforced polyethylene sulfide, Ryton, or polysulfone-bonded ZrO_2, Zirfon.[23] For example, Zirfon has an approximate thickness of 460 μm and resistance of 281 $m\Omega\ cm^2$.[17, 22] It is almost one order of magnitude thicker than typical AEMs.[24] The thinness of this separator is limited by the cross-permeation of gases, which lowers the current efficiency.[17] Separators also prevent the possibility of higher pressure at the anode than at the cathode, which can reduce oxygen cross-permeation flux and reduce the Nernst voltage.[17] With state-of-the-art LA-WEs design, Zirfon Perl showed a performance of 750 mA cm^{-2} at 1.8 V.[17]

High-pressure operation is desirable to reduce the need for downstream compression and transport and to enable the storage of hydrogen in a volumetrically efficient manner. The majority of AEM-WE demonstrations added a hydroxide salt to the water feed (i.e., a liquid alkaline electrolyte) to enhance the hydroxyl conductivity of the cathode and catalyst use. However, it is highly desirable to operate AEM-WEs with water instead of an electrolyte solution to avoid shunt currents and corrosion. Shunt currents through the electrolyte or in the water supply between cells in a stack can cause current loss, but they can be minimized to a negligible amount by electrolyzer design.[25] The diffusivity in alkaline solutions at high concentrations means that a 30 wt % KOH solution is close to the maximum conductivity of the aqueous KOH solution at 80 °C.[23] Also, KOH in solution can form K_2CO_3 precipitates when exposed to CO_2, which can reduce the anodic reaction, lower ionic conductivity, and block ion transfer.[26-29] However, using water instead of a liquid electrolyte can reduce the interface between the catalyst and the anion-conducting phase.

AEM-WE technology is still largely in the research and development (R&D) stage. Demonstrations of this technology by using a modular stack design have provided up to 35 bar hydrogen at a rate of 0.5 Nm^3h^{-1} given 2.4 kW.[30] There have been continued improvements in AEM technology. A recently developed, commercially available, 80 μm thick AEM offers an area-specific resistance of 45 $m\Omega\ cm^2$, which is over six times lower than that of the incumbent AEM technology.[31] Several groups have demonstrated 400 mA cm^{-2} at 1.8 V AEM-WE performance in operation with pure water.[24, 32-35] Los Alamos National Laboratory developed an ammonium-enriched quaternized polystyrene anion exchange ionomer (TMA-70) that demonstrated a performance of 2.7 A cm^{-2} at 1.8 V in water; however, it demonstrated limited durability. The TMA-70 was unable to retain the catalyst particles during continuous operation, so an alternative ionomer, TMA-53, was used to demonstrate 160 h of durability.[29] High ion-exchange capacity (IEC) is desirable for AEMs and ionomers to improve anion conductivity, but excessively high IEC capacity can lead to ionomer dissolution during operation.[24] Recent AEM material development has included a novel poly(aryl piperidinium) that, when combined with an

Fe_xNi_yOOH-20F anode, resulted in a performance of 1.02 A cm^{-2} at 1.8 V in water and over 160 h of continuous operation at 200 mA cm^{-2}.[24] To summarize, the advantages of AEM-WEs over LA-WEs are that AEM-WEs can support pressurized operation, transient input power, and notably higher current densities.[9] The primary challenge for AEM-WE development is finding and mitigating degradation mechanisms to achieve competitive durability.

2.1.3 Solid Oxide Water Electrolysis

Research and development efforts have led to the successful development and operation (i.e., design, selection of candidate cell component materials, fabrication processes) of laboratory-scale and commercial prototypical ceramic oxygen-ion and proton-conducting solid-state steam electrolysis systems.[36-39] SO-WE cells with oxygen ion-conducting electrolyte is the more mature of the two technologies and typically uses a yttria-stabilized zirconia (YSZ) electrolyte, a Ni-YSZ composite cathode, and a lanthanum strontium manganate anode. Early development of proton-conducting SO-WEs used strontium-doped ceria electrolytes, and later development used barium-zirconium and barium-cerium-doped yttria electrolytes.[37] Early efforts in the development of proton-conducting cells used Pt electrodes; subsequent efforts replaced Pt with more active materials, such as strontium-samarium-doped cobalt oxide for the anode and Ni as the cathode.[37] One advantage of proton-conducting cells is that proton mobility is more facile than oxygen ion mobility, allowing for lower cell-operating temperatures (400–700 °C vs. 700–1,000 °C). Another advantage is that hydrogen is produced on the dry side of the cell, eliminating the need to separate hydrogen from water in the effluent and allowing for electrochemical compression.[37] The lower operating temperatures allow more robust, less expensive metallic ancillary and support system components to be used instead of ceramic components and also decrease the degradation processes rates.[37] Experimental cells for both technologies meet DOE performance and cost targets.[40] On a fundamental level, a mechanistic understanding of electrode processes for both types of SO-WEs has been developed[41, 42] to account for anodic and cathodic polarizations.[43, 44]

Electrochemical performance improvement and long-term performance stability are active areas of SO-WE research. Processes related to bulk, surface, and interface degradation in cells, stacks, and balance-of-plant components and subsystems, resulting from prolonged exposure to elevated temperatures and complex gas atmospheres, are areas of active research but remain largely unknown.[45] Anodic and cathodic atmospheres commonly used in steam electrolysis can accelerate metal corrosion, change oxide defect chemistry, and modify bulk metal microstructures. Hydrogen dissolution, transport, and precipitation—as well as the reaction of dissolved hydrogen with oxygen—may accelerate corrosion. The formation of an H_2-H_2O redox leads to the modification of oxide defect chemistry and promotes localized corrosion due to short circuit diffusion.[46]

Several electrochemically active and electron- and ion-conducting functional perovskites and related compounds show extensive chemical and morphological degradation, including exsolution of dopants, in the complex SO-WE atmosphere.[47] A mechanistic understanding of chemical and morphological degradation and dopant exsolution in multi-cation oxide electrode under complex atmospheres is incomplete, and thermochemical models, along with experimental validation of exsolution processes, are also not yet fully developed.[47]

Hydrogen and steam present in cathodic and anodic atmospheres could develop trace levels (parts per billion to parts per million) of intrinsic and extrinsic gaseous contaminants in the feed gas streams. Such contaminants—which contain Cr, Si, B, and S species—can lead to electrode poisoning due to surface coverage, reaction product formation, and deactivation of the triple phase boundary. For example, at high steam partial pressures in the cathodic atmosphere, gaseous silica species are formed. These species are transported to and deposit on the electrode surface, leading to electrode deactivation over time.[48] The

identification and quantification of gaseous contaminants, the interaction of these contaminants with the electrode materials, their long-term accumulative effects, and methods for the capture of both intrinsic and extrinsic contaminants are areas of active research.[49]

In summary, the implementation of SO-WE technology will be limited without the development of long-term stable processes and approaches for identifying advanced ceramic and metallic materials chemistry and fabrication processes that remain compatible with ambient and high-pressure hydrogen production through steam electrolysis at elevated temperatures. Heterogeneous catalysis and electrocatalysis on complex multi-cation oxides¸ electrode poisoning and deactivation due to cation exsolution and trace gas contaminants, and metal-hydrogen interaction in hydrogen and bi-polar exposure conditions are all current areas of research. The evaluation of the evolution of ceramic and metallic materials—with an emphasis on surface morphological and chemical rearrangement, trace gas phase contaminant interaction, and electrochemical deactivation—is also a topic currently being studied.[50-52] The role of hydrogen in the modification of surface corrosion and bulk structure modification remains a topic of interest for hydrogen production at elevated pressure.[53] Promising R&D approaches are in the areas of computational materials, system-based solutions, advanced experimental techniques to interrogate solid-gas reactions, ion-electron exchange processes, and surface adsorption of trace contaminants.

2.1.4 Photoelectrochemical Water Splitting

The efficiency of systems for hydrogen production by photoelectrochemical water splitting is limited chiefly by the performance and durability of the photoelectrodes, the catalysts for central reactions involved in hydrogen generation—namely the OER and the hydrogen evolution reaction (HER)—and membranes used for product separation. These reactions can be indirectly coupled to sunlight (e.g., photovoltaics+electrolysis), which provides a means of independently optimizing the light-harvesting and catalytic processes that produce hydrogen. They can also be directly coupled via integrated photoelectrochemical water-splitting systems, offering advantages for the chemical control and use of energy from sunlight. Although challenges exist in integrating the light-harvesting, photovoltage-generating, and water-splitting components of integrated systems, integrated systems are being actively developed because of the advantages of decreased cost and complexity compared with separate units and the ease of electric field generation at the semiconductor/water interface.[54]

In many direct solar fuels systems, bulk semiconductors absorb light and generate the photovoltage to drive fuel-forming electrochemical reactions. The photovoltage required to split water at high (>10%) solar-to-fuel efficiencies can be achieved only by using multiple photoabsorbers in a tandem configuration.[54] Because of their exceptionally high photovoltages, multijunction III–V semiconductors have been a popular choice for over two decades and have yielded solar-to-hydrogen efficiencies >19% (**Figure 4**).[55] Silicon, which is dominant in the microelectronics and photovoltaic industries, has also been used extensively. Some of the earliest work on photoelectrochemical systems involved metal chalcogenide, chalcopyrite-type, and kesterite-type semiconductors because their tunable bandgaps are ideal for solar fuel generation (1.0–2.4 eV).[56] Computation, high-throughput synthesis, and data mining have accelerated the discovery and

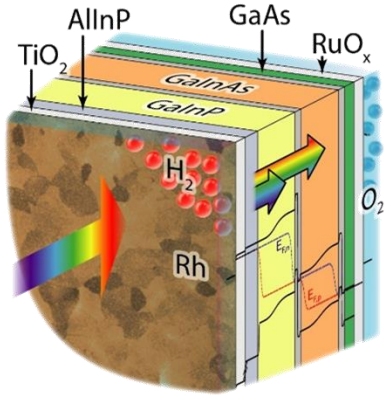

Figure 4. Solar fuel generator for photoelectrochemical water splitting with a >19% solar-to-fuel efficiency. (Source: Ref. [55]). Reprinted with permission from Cheng, et. al. "Monolithic Photoelectrochemical Device for Direct Water Splitting with 19% Efficiency," *ACS Energy Lett.* **3**, 1795–1800, (2018). Copyright 2018 American Chemical Society.

development of new semiconductor materials[57, 58] with some successes in improving stability and performance.

One key challenge is that all these semiconductors undergo corrosion in aqueous electrolytes when used as photocathodes, limiting their reported durability to a range from hours to days.[59]

Semiconductor photoelectrodes can be protected by using inert overlayers, such as TiO_2,[60, 61] with flaws and defects in the coatings as the factor that is currently limiting their durability. Quantitative methods for studying corrosion rates were developed by detecting degradation products in the electrolyte[62] or by measuring the mass loss of the component directly.[63] In situ observation of corrosion processes by scanning probe techniques is also possible and, when combined with theory, can reveal underlying corrosion mechanisms.[64] Many materials are metastable with respect to anodic and cathodic corrosion processes under water-splitting conditions,[65, 66] and corrosion resistance is an important selection criterion in computational and experimental searches for new photocathode materials.

The performance of OER and HER catalysts for photoelectrochemical water splitting can be compared by compiling information regarding catalyst activity, stability, and specific activity in which the primary figure of merit is the overpotential necessary to achieve 10 mA cm^{-2} current density. This is the typical current density at the electrodes of a 10% efficient integrated solar-to-hydrogen prototype under 1 sun illumination[54, 67-76] because the best catalysts are expected to achieve 10 mA cm^{-2} current densities at low overpotential, maintain constant activity over time, and have low surface roughness (i.e., high specific activity). The performance of HER and OER catalysts made of Earth-abundant materials in 1 M NaOH and 1 M H_2SO_4,[77, 78] conditions relevant to solar water-splitting devices, as well as LA-WE, AEM-WE, and PEM-WE, are summarized in **Figure 5**. In 1 M NaOH, most OER catalysts investigated show roughly similar activities, achieving 10 mA cm^{-2} current densities at overpotentials of $0.3\ V \leq \eta \leq 0.5\ V$.

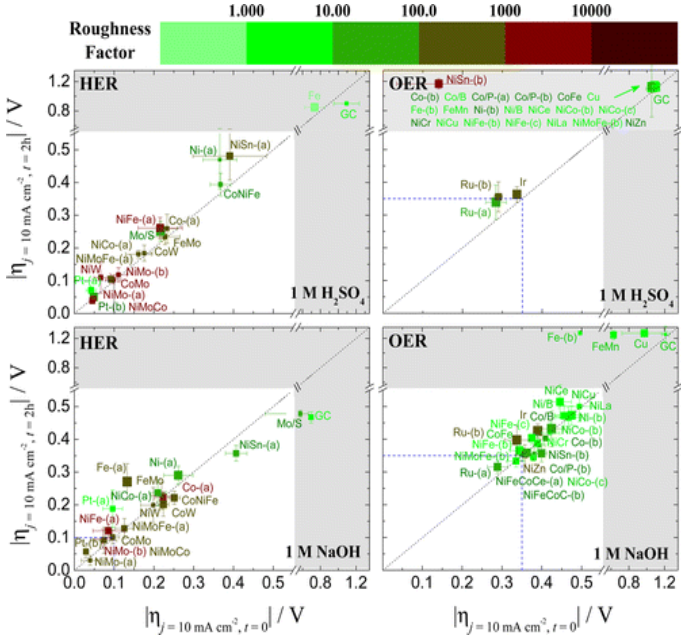

Figure 5. Plots of catalytic activity, stability, and electrochemically active surface area for HER (left) and OER (right) electrocatalysts in acidic (top) and alkaline (bottom) solutions. The x-axis is the overpotential required to achieve 10 mA cm^{-2} per geometric area at time t = 0. The y-axis is the overpotential required to achieve 10 mA cm^{-2} per geometric area at time t = 2 h. The diagonal dashed line is the expected response for a stable catalyst that does not change in activity during 2 h of constant polarization. The color of each point represents the roughness factor of the catalyst with a bin size of one order of magnitude; light green represents RF = 1, and dark red represents $RF > 10^4$. Source: Refs. [77] Reprinted with permission from McCrory, et. al., "Benchmarking Hydrogen Evolving Reaction and Oxygen Evolving Reaction Electrocatalysts for Solar Water Splitting Devices," *J. Amer. Chem. Soc.* **137**, 4347–-4357 (2015). Copyright 2015 American Chemical Society.

In the case of the OER, most catalysts investigated are oxidatively unstable in acidic conditions. Therefore, the utility of a solar water-splitting prototype operating in acidic solution could be limited by the lack of non–noble metal catalysts that are oxidatively stable in acidic solution. Recent work on antimony-manganese based OER catalysts suggested a potential for stable OER catalysts operating in

acidic conditions.[79] Several known Earth-abundant HER catalysts show good activity and stability in acidic and basic electrolytes, as illustrated in **Figure 5**. Thus, a reduction in the overpotential for the OER currently represents a more significant challenge for water splitting than does an improvement in catalysts for the HER.

2.2 Biological Hydrogen Production

The path to renewable H_2 production using waste plant biomass (i.e., lignocellulose) as a feedstock presents a mid- to long-term technology, although production costs are still too high.[80, 81] Presently, the DOE Hydrogen and Fuel Cell Technologies Office (HFTO) invests in developing microbial fermentation technology to use primarily the sugars embedded in lignocellulosic biomass as the energy source to fuel microbial growth and H_2 biosynthesis. This approach bypasses the need for light as the energy source. Guided by technoeconomic analysis, efforts to enable economical biological H_2 production have identified the challenges as the reduction of capital costs associated with major facilities and equipment (e.g., bioreactors), increasing the rates of H_2 production, and increasing the currently low H_2 molar yield (mol H_2/mol sugar consumed) to decrease capital costs and the cost of waste biomass feedstock per unit of hydrogen.[82]

An approach demonstrated to increase both hydrogen yield and production rate is the genetic engineering of a bacterial species, *Clostridium thermocellum*, which is recognized for its rapid growth and solubilization of cellulosic biomass to co-use hemicellulose components of plant biomass (i.e., corn stover).[83, 84] Because cellulose accounts for 38–50% of corn stover and hemicellulose accounts for 23–32%, the co-fermentation of cellulose and hemicellulose increased the total amount of H_2 produced by 33% (reaching 4.1 L of H_2/liter of bioreactor volume) and improved the average H_2 production rate over a 24 h fermentation period by 39% (reaching 3.1 L of H_2/liter of reactor volume per day) by using a baseline strain that can use only the cellulosic portion of the biomass (unpublished data). This increase was demonstrated with fermentation at a moderately high loading of 88.4 g/L of real and pretreated biomass, known as deacetylated and mechanically refined biomass, containing 30 g/L as cellulose in 500 mL of fermentation volume. Challenges remain in further optimizing the strain and bioreactor performance at high solids loading. Increasing the solid biomass loading will reduce the bioreactor volume required to achieve the target H_2 production and reduce the capital expense of the process. Ongoing research efforts include process and bioreactor engineering and bacterial strain development to tolerate high-solids conditions and sustain high hydrogen production rates.

Another approach to reducing feedstock costs is to maximize H_2 molar yields for every mole of sugar (i.e., glucose, xylose) used by the microbe to produce H_2. This is achieved by eliminating other natural fermentation by-products that compete with H_2 biosynthesis for electrons. The reduced and competing organic compounds include ethanol and lactic acid. The theoretical maximum H_2 molar yield per mole of hexose is 4 M.[85] Currently, the highest molar yield using *C. thermocellum,* which is capable of effectively solubilizing and fermenting cellulose, is 3.1 M for low concentrations of hexose sugars. However, under most laboratory conditions that use higher and more realistic concentrations of hexose sugars, H_2 molar yields fall below 3 M.[86] Genetic manipulations of bacteria using metabolic engineering and synthetic biology approaches are being investigated to effectively channel the electrons made available from the glycolysis reaction (i.e., the breakdown of sugars) to the hydrogenase enzymes that catalyze the reduction of protons (i.e., H^+) to generate H_2. However, specific limiting steps and the regulatory mechanisms cells employ to channel electrons toward different metabolites (i.e., H_2 vs. organic compounds) in response to varying environmental conditions remain unclear and are areas of active research.

Hydrogenase enzymes that can be classified as either [NiFe]- or [FeFe]-type, named for the metals in the catalytic center, are central to biological H_2 production.[87-89] These enzymes use either NAD(P)H or

reduced ferredoxin as the electron donor. More recently, an [FeFe]-bifurcating hydrogenase was discovered in numerous anaerobes, including *C. thermocellum*, employing both NAD(P)H and reduced ferredoxin to produce H_2.[90] The combined use of both sources of electron carriers was thought to drive H_2 production against the otherwise thermodynamically uphill reaction if only NAD(P)H was used. Yet mechanistic details governing bifurcating hydrogenases remain elusive and this is a barrier to improved H_2 production yields. *C. thermocellum* also contains the NiFe-type, energy-yielding hydrogenase, which presumably yields energy during proton reduction. The underlying catalytic mechanisms of these enzymes are lacking, especially the mechanism by which H_2 production and redox cofactors are coupled for energy conservation.

2.3 Thermochemical Hydrogen Production

Thermochemical routes for producing hydrogen span an extremely large space akin to the breadth of the chemical processing industry. The emergence of technologies that provide renewable, high-temperature industrial-process heat via concentrated solar power[91] could radically transform both conventional and notional water-splitting chemical processes into carbon-neutral sources for hydrogen at a large scale. These opportunities were recognized and research needs prioritized in recent DOE Basic Research Needs reports[92, 93] and will be discussed to a greater extent here.

Detailed process chemistry for many cycles that have been proposed and/or demonstrated at various scales—from laboratory to small pilot—can be found in seminal works dating from 2003.[94-97] Thematically, thermochemical water-splitting cycles are categorized by the number of reactions required to complete the cycle and by the method of treatment (i.e., purely thermochemical or hybridized approaches that invoke electrochemistry or photochemistry to complete reaction steps within the cycle[98, 99]). For example, a simple two-step cycle that uses metal/metal oxide as a stoichiometric redox pair can be generalized as

$$M_xO \rightarrow xM + \tfrac{1}{2}O_2, \qquad \text{(step 1, reduction)}$$

followed by

$$xM + H_2O \rightarrow M_xO + H_2, \qquad \text{(step 2, oxidation)}$$

and for a two-step cycle that uses metal oxide as a nonstoichiometric redox pair generalized as

$$MO_x \rightarrow MO_{x-\delta} + \delta/2O_2, \qquad \text{(step 1)}$$

followed by

$$MO_{x-\delta} + \delta H_2O \rightarrow MO_x + \delta H_2, \qquad \text{(step 2),}$$

where *M* is a metal element, and δ is a measure of the oxygen deficiency in the lattice. There are hundreds of examples of more complicated purely thermochemical cycles that involve several chemical species participating in a reaction network that nets water splitting; in some instances, the network cycles through different phases of matter.[94, 100] Finally, there are concepts that invoke chemical looping[101] or hybridized approaches in which electrochemical steps within the cycle promote the oxidation or reduction of chemical species other than direct water electrolysis.[90, 94, 96, 98] Thermochemical routes for producing hydrogen via water splitting span an extremely large concept space with opportunities for guidance from fundamental studies to advance the state of the art.

The technology readiness levels of the aforementioned thermochemical cycles have not progressed substantially since the 2003, the year of the first hydrogen Basic Research Needs report.[92, 93] The primary challenges are (1) the understanding of the behavior of materials in extreme environments (e.g., materials subject to harsh chemical and thermal stresses), (2) novel methods for improving the efficiency of separations in harsh environments (e.g., transport membranes), (3) thermodynamic data and modeling, and (4) novel catalyst formulations for a subclass of these cycles to promote efficiency and durability.

R&D efforts have yet to be fully realized that exploit high-performance computing, computational material science, ab initio theory, and fundamental science to develop an atomistic understanding of redox processes to discover new redox materials for thermochemical cycles or to develop concepts that hybridize these cycles. For example, the solar thermochemical fuels community has gravitated toward simple, two-step nonvolatile metal oxide cycles by using nonstoichiometric oxides.[102, 103] These oxides are essentially oxygen storage materials that consist of highly defective crystal structures in their reduced state (i.e., percentage-level oxygen vacancy concentrations). Thermal reduction is achieved at extremely high temperatures (~1,500 °C) and low oxygen gas-phase chemical potential (μ_{O2} gas ~10^{-5} atm). For the subsequent reaction between reduced oxide and water vapor that produces H_2 to be spontaneous, these materials must be able to reoxidize in a mixed H_2O–H_2 environment that is more reducing than that the thermal reduction environment (μ_{O2} gas ~10^{-14} atm). Although there are many examples of off-stoichiometric oxides releasing and reabsorbing lattice oxygen when exposed to various partial pressures of O_2 at temperature, very few oxides are known to reabsorb lattice oxygen when exposed to mixtures of H_2O and H_2. The commercial viability of this technology is critically dependent on the additional discovery of high-capacity redox active oxides that can efficiently conduct cycle chemistry at lower reduction temperatures (ideally <1,350 °C) while producing H_2 at the low gas-phase oxygen chemical potentials established at H_2O/H_2 ratios <10.

Significant R&D activities in this arena focused on material discovery are using high-throughput computational screening,[104, 105] materials by design using density functional theory (DFT),[106, 107] and DFT-driven machine learning[108, 109] to identify compound formulations that exhibit a high efficacy for thermochemical water splitting in the two-step metal oxide cycle (e.g., optimizing a trade-off between H_2 production capacity and H_2 yield predicated on engineering defect thermodynamics). There are also examples emerging from this community of the use of synchrotron X-ray scattering measurements and other advanced electron scattering techniques (e.g., transmission electron microscopy, electron energy loss spectroscopy) to reveal how the electronic structure and other crystallographic features are perturbed upon oxygen defect formation; some of these efforts are in situ or operando.[110, 111] The main goal of the most current R&D is to obtain an atomistic understanding of the bulk redox processes that engender desirable defect thermodynamics to establish design rules for the discovery and improvement of thermochemical water-splitting materials. Such insight will reveal structure-property and composition-property relationships critical to material performance.

2.4 Catalytic and Thermal Hydrocarbon and Biomass Conversion

The high-temperature catalytic conversions of hydrocarbons, primarily methane, are currently the dominant processes for producing hydrogen with CO_2 as a by-product. Efforts to eliminate or reduce CO_2 emissions from methane-to-hydrogen or hydrocarbon-to-hydrogen processes include carbon capture and sequestration, thermal catalytic decomposition (TCD), and thermal plasma technologies. Biomass can also be converted to hydrogen or synthesis gas (H_2 + CO) by using biological or thermal chemical processes, including gasification coupled with steam reforming, pyrolysis, photolysis, and fermentation. Many of these processes produce valuable by-products, such as carbon, as discussed in detail in Section 4.2.6.

2.4.1 Hydrocarbon Conversion

The majority of global H_2 is produced via SMR, leading to average CO_2 emissions of 10 kg CO_2/kg H_2.[112, 113] Partial oxidation, which is similar to SMR, has been developed and targets syngas production rather than hydrogen alone.[114] Owing to environmental and potential future regulatory concerns, it is desirable to develop a process for near-zero CO_2 production of hydrogen that is economically viable. Stoichiometrically, TCD produces two molecules of hydrogen and one atom of carbon from one methane molecule, whereas SMR releases twice the amount of hydrogen due to the conversion of water vapor. From a purely economic consideration, the value of the carbon product must offset the loss of hydrogen; this technoeconomic aspect of TCD vs. SMR has been studied, also considering the cost of carbon capture and sequestration for SMR.[115, 116]

TCD of methane was developed by Universal Oil Products in the 1960s. It is known as the *HyPro process* and targets hydrogen production for refineries.[117] Recent research has focused on improving the efficiency the TCD of methane, which produces solid carbon as a by-product:[118-122]

$$CH_4(g) \rightarrow C(s) + 2H_2(g),\ \Delta H^\circ_{298} = 74.85\ \text{kJ/mol of } CH_4.$$

The TCD of CH_4 can proceed without a catalyst at temperatures as low at 300 °C, according to thermodynamics; however, temperatures of 1000–1200 °C are required to achieve reasonable rates for commercial applications because of kinetic limitations and the high activation energy required to break the stable C-H bond.[116, 123] Higher temperatures and longer residence times favor the production of C and H_2.[124] Lower temperatures and shorter contact times favor more gaseous products with higher yields of olefins and aromatics. Lower pressure favors higher conversion of CH_4 but tends to produce more olefins, which further decompose to C and H_2 with increasing residence time. Addition of a catalyst significantly lowers the activation energy, enabling the reaction to proceed at temperatures ranging from 600 to 900 °C, which is similar to the temperature range for SMR.

Several excellent articles provide reviews of CH_4 cracking and include discussions of catalysts, reaction mechanisms, kinetics, and engineering design considerations.[123, 125-133] The majority of catalyst studies focus on selecting metals, catalyst supports, metal-support interactions,[125, 134-138] and catalyst preparation methods.[139, 140] Transition metals and carbonaceous catalysts have also been investigated.[116, 123, 125-130] It has been reported that the rate of CH_4 decomposition on metal catalysts decreases in the order: Co, Ru, Ni, Rh > Pt, Re, Ir > Pd, Cu, W, Fe, Mo.[125] Nickel, iron, and cobalt have been extensively investigated because of their relative abundance and lower price compared with PGM catalysts.[116, 123, 125, 130] Nickel exhibits high activity but rapidly deactivates because the carbon product encapsulates its active sites. Cobalt also exhibits high activity but is more expensive and toxic than nickel. Iron has acceptable activity, and its higher carbon diffusion capacity makes it more resistant to deactivation at higher temperatures than nickel or cobalt. Several studies of bimetallic catalysts have targeted alloys with higher surface areas, which provide more active sites and exhibit increased diffusion of carbon products to reduce carbon deposition on the active sites compared with the individual metals.[123] Metal-support interactions play a key role in the formation of carbon nanomaterials and affect hydrogen production rates.[121] Metal catalysts have been supported on SiO_2, TiO_2, Al_2O_3, and MgO to enhance catalytic activity and hinder metal agglomeration.[123] Studies have been performed to determine the mechanism of the formation of carbon nanomaterials on metal-supported catalysts[141-144] and to determine the fundamental reaction pathways via DFT for carbon nanotube (CNT)-supported binary metal catalysts.[115, 145] To increase energy efficiency, microwave catalytic processing has been reported in which microwave energy is directly delivered to metal active sites to facilitate methane decomposition and the formation of CNTs.[146] The selective microwave heating reduces heat transfer limitations and avoids the heat loss that results from conventional heating.

Coking is the major cause of TCD catalyst deactivation.[116, 123, 125, 130] Nickel, cobalt, and iron form CNTs or fibers at a rate of formation that depends on the temperature and particle size. Catalysts with higher carbon diffusion capacities and lower carbon solubilities are more resistant to deactivation but eventually deactivate. Regeneration processes using steam or air to oxidize carbon can be employed to recover catalyst activity; however, the high temperatures generated by the oxidation processes tend to change the catalyst morphology so that the catalyst activity falls below acceptable levels after multiple regenerations.[123] Processes are being developed to recover the carbon product when regenerating the catalyst, such as mechanical separation by attrition by using a fluidized-bed reactor. Thus far, the technique has yielded low separation efficiency.[147] Acid treatment is commonly used to separate and purify grown CNTs from catalysts;[148] in that process, the oxide support and the metal on the support are dissolved in acid, making metal recovery difficult. A TCD process that consists of cyclic reaction-regeneration was experimentally demonstrated for a Ni-Pd/CNT catalyst.[115] As illustrated in **Figure 6**, the Ni-Pd/CNT catalyst can be regenerated and reused, a small fraction of product CNTs can be used as catalyst supports, and the process is self-sustaining without using an externally added catalyst.[115]

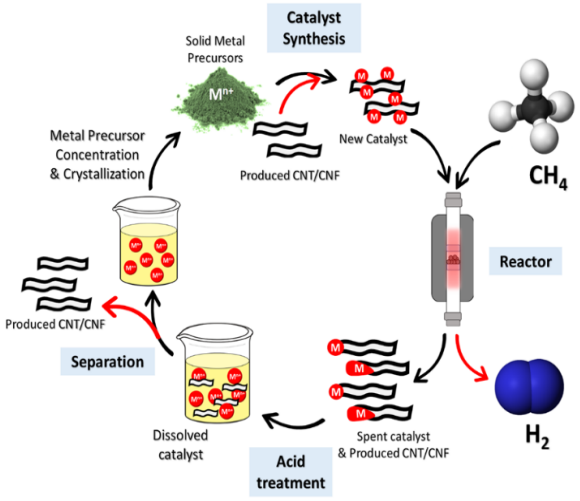

Figure 6. Cyclic CH_4 TCD process consisting of CH_4 decomposition reaction, catalyst-carbon separation, and catalyst regeneration steps. Source: Ref. [115] Used with permission of Royal Society of Chemistry, from "Catalytic Decomposition of Methane Into Hydrogen and High-Value Carbons: Combined Experimental and DFT Computational Study," Wang, et. al., *Catal. Sci. Technol.* **11**, (2021); permission conveyed through Copyright Clearance Center, Inc.

Carbonaceous catalysts (e.g., activated char, biochar, coal char, carbon black) have been investigated.[116, 123, 125, 130] Carbonaceous catalysts offer several advantages, including lower cost, higher resistance to high temperatures, tolerance of impurities such as sulfur, and self-catalytic effects of the carbon product.[123] The performance of carbonaceous catalysts is lower than that of metal catalysts; the activity of the latter tends to decrease after a few hours in stream owing to morphology changes and pore blockage. But unlike the activity of metal catalysts, the activity of carbonaceous catalysts stabilizes after the initial decrease.[123]

Thermal plasma technologies are used to dissociate hydrogen from various hydrogen-containing compounds, such as methane.[149, 150] The process is operated at very high temperatures, producing hydrogen and carbon black with yields approaching 100%. A plasma reactor is about one order of magnitude smaller than traditional thermal reactors.[151, 152] The disadvantages of this technology are related to the energy required to crack CH_4 all the way to solid carbon because the relatively high fraction of methyl radical enables the formation of stable hydrocarbons and polymeric species, as well as to the use of electrical energy.[151, 153]

Molten metal processes in which CH_4 is bubbled through a molten metal bath were studied.[123] The main advantage of the molten metal process is that the lower density of carbon allows it to float to the surface of the bath, which facilitates its recovery and allows for a continuous process. Other advantages include improved heat transfer due to the high heat capacity of the molten media and increased residence times due to liquid viscosity. The gas stream contains primarily H_2 with lesser amounts of unreacted CH_4 and other byproducts. The major disadvantage is the high temperatures required. In addition to molten metals,

molten salts have been studied for methane reforming and may also be useful for methane decomposition.[154, 155]

Concentrated solar energy allows for reaction temperatures approaching 2000 °C, which enhance methane conversion.[116, 123] Catalysts may be used to promote the kinetics, but the harsh conditions limit the choice of catalysts. Catalytic-based solar processes have issues similar to those of other catalytic-based thermochemical conversion processes, such as the recovery of the carbon from the catalyst and regeneration of the catalyst.

2.4.2 Biomass Conversion

Biomass can be converted to hydrogen by biological and thermal chemical conversion.[156, 157] Most reported methods are based on biomass gasification, steam reforming, and pyrolysis. Literature reports have compared hydrogen production rates and yields for these processes.[158, 159] Other hydrogen production processes from biomass include bio-photolysis,[160] fermentation,[161] and chemical looping approaches.[162] A major issue involved in biomass conversion to hydrogen is deoxygenation, largely because oxygen can be removed either as H_2O, which can cause a loss of H_2 yield, or as CO_2. The balance between the formation of H_2O and CO_2 is critical in hydrogen production. To increase hydrogen yields, a recent study explored synergistic methane-activated catalytic biomass gasification in which 5–15% CH_4 was co-processed with biomass.[163] A novel in situ bi-reforming approach that produces hydrogen-rich syngas by using biomass and flare gas with CO_2 use was reported.[164] **Figure 7** illustrates the reaction mechanism.

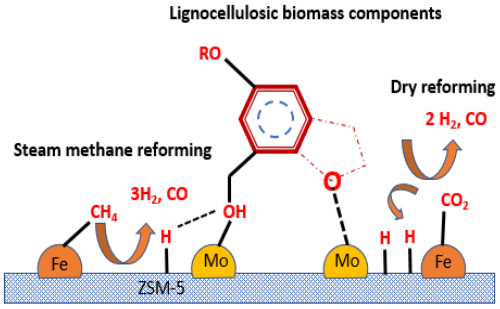

Figure 7. In situ bi-reforming approach for biomass conversion to H_2-rich syngas.Source: Ref. [164] Reprinted from Chem. Eng. J. Vol 385, Lalsare, et. al., "Biomass – Flare Gas Synergistic Co-Processing in the Presence of Carbon Dioxide for the controlled Production of Syngas (H_2:CO ~ 2-2.5)," 123783, Copyright 2020, with permission from Elsevier.

Self-regenerable, graphene-supported Fe/Ni, β-Mo_2C nanoparticles were used as catalysts for the coprocessing of lignin with CH_4 (**Figure 8**).[165, 166] Furthermore, DFT modeling was conducted to elucidate synergistic hydrogen production mechanisms presented in the coprocessing of lignin and CH_4.[166] The present research targets solving the issues of low hydrogen yield in biomass conversion and reducing gas flaring in stranded shale gas fields.

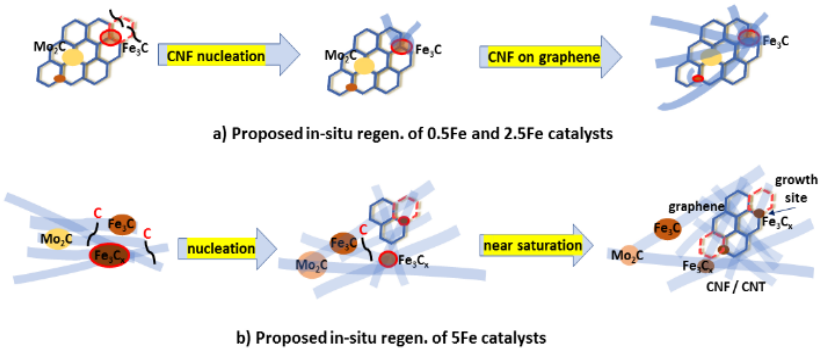

Figure 8. In situ self-regeneration mechanism for (a) 0.5Fe and 2.5Fe catalysts and (b) 5Fe catalysts. Source: Ref. [166] Reprinted from *Appl. Catal. B*, Vol 282, Lalsare, et. al., "Self-Regenerable Carbon Nanofiber Supported Fe-Mo_2C Catalyst for CH_4-CO_2 Assisted Reforming of Biomass to Hydrogen Rich Syngas," 119537, Copyright 2021, with permission from Elsevier.

3. Hydrogen Storage and Transport

Efficiently transporting and storing hydrogen are major challenges facing a hydrogen-based energy economy. Although elemental hydrogen has the highest gravimetric energy density of any fuel, its volumetric density is much lower than conventional fuels (**Figure 9**).[167] Consequently, very high pressures or cryogenic temperatures are required to store amounts sufficient for practical applications. In contrast, material-based hydrogen storage is an area of vigorous research. Materials-based storage systems could store hydrogen at lower pressures and at near-ambient conditions than liquid or 700 bar compressed hydrogen, thus simplifying storage systems, tanks, and delivery infrastructure.

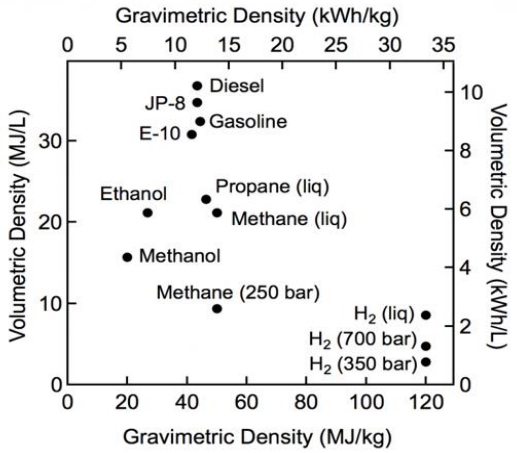

Figure 9. Comparison of specific energy (energy per mass or gravimetric density) and energy density (energy per volume or volumetric density) for several fuels based on lower heating values. Source: Ref. [167] Image courtesy U.S. Department of Energy.

Research concerning these materials encompasses many energy-related applications, including hydride batteries;[168-170] bulk transport (e.g., liquid organic hydrocarbons,[171-174] ammonia,[175, 176] formate[177]); hydrogen compressors;[178, 179] thermal energy storage; heat pumps; stationary applications, such as microgrids and server farms;[179, 180] and transportation,[171, 181, 182] including material handling equipment, such as forklifts[183, 184] and rail transport.[185-188] This section provides a brief overview of the primary strategies for storing hydrogen: materials based, compressed gas or cryogenic liquid, and geological. Of these, cryogenic and pressurized gas are mature technologies, although material compatibility issues persist. Currently available light-duty fuel cell electric vehicles (FCEVs) store gaseous hydrogen (GH_2) at 700 bar in fiber-reinforced tanks that are the largest contributor to the cost of the fuel storage system.

3.1 Material-Based and Chemical-Based Hydrogen Storage

Material-based hydrogen storage continues to be of interest because of the cost and low density of pressurized gas. Between 2005 and 2010, DOE Energy Efficiency and Renewable Energy (EERE) HFTO-supported Centers of Excellence focused on materials for onboard hydrogen storage. Starting in FY16, HFTO initiated the Hydrogen Materials Advanced Research Consortium (HyMARC)[189] to perform foundational scientific research aimed at understanding and solving key issues blocking the development of storage materials that meet materials targets, such as those for light-duty vehicles.[190] HyMARC is now in its second phase (FY18–22). Although originally focused on storage for light-duty vehicles, the HyMARC mission now includes heavy-duty vehicles, stationary hydrogen storage, and hydrogen transport (e.g., from point of production to end use).

There are three primary classes of storage materials.

- Physisorption materials (e.g., metal-organic frameworks [MOFs] and related materials).
- Chemical storage (CS) materials. These can be further subdivided into metal hydrides with either hydridic (i.e., anionic) bonds (e.g., $NaAlH_4$) or ionic bond (e.g., LiH) and "chemical hydrides," such as BH_3NH_3, in which bonds to hydrogen are covalent.

- Liquid or gaseous small molecules, including ammonia, liquid organic hydrogen carriers (LOHCs), and anionic systems, such as formate.

In all cases, the process of material discovery has been inhibited by the complex nature of the chemical and physical processes involved. Consequently, machine learning and data science research are increasingly of interest.[191-194]

3.1.1 Storage Based on Physisorption

In the last two decades, significant effort has been focused on developing novel porous adsorbents, such as MOFs, for physisorptive H_2 storage. Hydrogen uptake in these materials is typically reported as gravimetric uptake capacity (wt %) or volumetric uptake capacity (g/L) at a range of pressures and temperatures, and these metrics are critical for evaluating practical adsorbent performance. A typical high-pressure gas adsorption measurement yields what is known as the *excess gravimetric capacity*, which can be considered is the total uptake of the material less than the quantity of H_2 present in the void space of the sample. The total uptake is then commonly expressed as (total uptake) = (excess uptake) + (bulk density of H_2) × (pore volume). However, the amount of H_2 that is actually accessible for end use will be lower than the total uptake estimated in this way because the minimum delivery pressure to the fuel cell system is typically set around 5 bar. The system capacity will be even lower. Finally, volumetric usable capacity is typically estimated from the gravimetric usable capacity and the crystallographic density of a guest-free material. Because the packing density of adsorbent crystals within a structured form is generally somewhat lower than in single crystals, the actual usable volumetric capacity is also expected to be lower than this calculated value.[195]

Following the empirical observation that the excess H_2 adsorption capacity for carbonaceous microporous materials is nearly proportional to the surface area (known as *Chahine's rule*),[196, 197] early materials development was devoted to preparing materials with high Brunauer–Emmett–Teller (BET) surface areas (>6000 m^2/g), such as MOF-210 and NU-100 (**Table 1** and **Figure 10).**[198, 199] These two materials take up more than 14 wt % H_2 at 77 K and 70 bar. However, because of their low densities (<0.3 g/cm^3), their volumetric adsorption capacities (~40 g/L) did not increase with the increment of gravimetric capacities and BET surface areas. A consensus was established in recent years that for light-duty vehicles, the volumetric density more strongly impacts the amount of energy that can be stored than the gravimetric density.[195, 196, 200] Therefore, research has focused on developing adsorbent materials that exhibit high volumetric capacities without sacrificing gravimetric capacities and vice versa.[197, 201] With advances in computational screening and machine learning approaches, it has also been possible to predict material properties that will optimize gravimetric and volumetric performance,[191, 197] such as framework density ranging from 0.4 to 0.5 g/cm^3, pore volumes ranging from 1 to 2 cm^3/g, and pore diameters ranging from 10 to 20 Å.

Furthermore, materials that exhibit both high gravimetric and volumetric BET surface areas are preferred, and this can be ascertained without high-pressure analysis.[201] Recent analysis also suggests that to achieve the ultimate deliverable capacity, a material that can undergo a nonporous-to-porous transformation will be required.[202]

Table 1 summarizes the structural properties of representative MOFs and their gravimetric and volumetric usable capacities achieved by pressure swing or temperature–pressure swing adsorption processes. Data for the prototypical framework, MOF-5 (Zn_4O(benzenedicarboxylate)$_3$), are also included for reference. At 77 K with a 5–100 bar pressure swing, it is clear that the greater the material's BET surface area, the greater the material's gravimetric usable capacity.[201] For all the materials listed in **Table 1**, the usable capacity can be enhanced by more than 30% by increasing the discharge temperature—in this case, adsorption at 77 K/100 bar and desorption at 160 K/5 bar. Under these

conditions, the highest usable volumetric capacity was achieved by MOF-5 (51.9 g/L on a material basis, not accounting for the packing density losses).[196] The capacities achieved were approximately 50% higher than the bulk density of H_2 gas. However, the additional temperature controlling units required for higher-temperature desorption would reduce the system-level performance because of the system weight and tank precooling before recharging.[181]

Table 1. Structural properties of representative porous adsorbents and their gravimetric and volumetric usable capacities achieved by pressure swing or temperature–pressure swing adsorption processes.

Adsorbent material	A_{BET} **(m^2/g)**	V_p **(cm^3/g)**	d_{bulk} **(g/cm^3)**	**Usable capacity (77 K/100 bar → 77 K/5 bar)**		**Usable capacity (77 K/100 bar → 160 K/5 bar)**		**$-\Delta H$ (kJ/mol)**	**Ref.**
				wt %	**g/L**	**wt %**	**g/L**		
MOF-5	3,510	1.36	0.59	4.5	31.1	7.8	51.9	4.8	[196, 203]
IRMOF-20	4,070	1.65	0.51	5.7	33.4	9.1	51.0	n.d.	[196]
SNU-70	4,940	2.14	0.41	7.3	34.7	10.6	47.9	5.1	[191, 204]
NU-100	6,050	3.17	0.29	9.9	35.2	13.9	47.6	6.1	[191, 198]
UMCM-9	5,040	2.31	0.37	8.0	34.1	11.3	47.4	n.d.	[191]
NU-1101	4,340	1.72	0.46	6.1	29.9	9.1	46.6	5.5	[205]
NU-1501-Al	7,310	2.91	0.28	10.1	34.8	14.0	46.2	4	[201]
COF-102	3,620	1.55	0.43	5.8[a]	29.0[a]	n.d.	n.d.	3.9	[206]
PAF-1	3,790	2.03	0.35	5.4	21.6	n.d.	n.d.	4.6	[206, 207]
Bulk H_2	n.a.	n.a.	n.a.	n.a.	29.7	n.a.	30.5	n.a.	[208]
Adsorbent material	A_{BET} **(m^2/g)**	V_p **(cm^3/g)**	d_{bulk} **(g/cm^3)**	**Usable capacity (25 °C/100 bar → 25 °C/5 bar)**		**Usable capacity (–75 °C/100 bar → 25 °C/5 bar)**		**$-\Delta H$ (kJ/mol)**	**Ref.**
				wt %	**g/L**	**Wt %**	**g/L**		
Ni_2(*m*-dobdc)	1,320	0.56	1.20	0.90	10.9	1.9	18.2	13.7	[209]
$V_2Cl_{2.8}$(btdd)	1,920	1.12	0.64	1.48	9.6	2.5[b]	16.4[b]	21	[210]
NU-1501-Al	7,310	2.91	0.28	2.75[c]	8.0[c]	5.0[b]	14.9[b]	4	[201]
MOF-5	n.d.	n.d.	0.59	1.45	8.8	2.7	16.5	4.8	[203, 209]
Bulk H_2	n.a.	n.a.	n.a.	n.a.	7.67	n.a.	11.0	n.a.	[208]

A_{BET}, BET surface area; V_p, pore volume; d_{bulk}, single-crystal density of framework; ΔH, adsorption enthalpy; n.d., no data; n.a., not applicable. [a]Data for 77 K/86 bar → 77 K/5 bar. [b]Values are calculated based on the reported temperature-independent parameters. [c]Measured at 296 K.

Highly porous framework materials constructed from all-organic building blocks, such as covalent-organic frameworks (COFs) and porous aromatic frameworks (PAFs), are also of interest for gas storage applications.[206, 211] Computations have predicted that certain structure types may exhibit H_2 storage capacities as high as 50.6 g/L;[212-214] however, only a limited number of materials have been experimentally evaluated to date (**Table 1**).[207, 211] These capacities approach those of the best MOF materials, but further work is needed to improve the conditions that are suitable for large-scale synthesis.

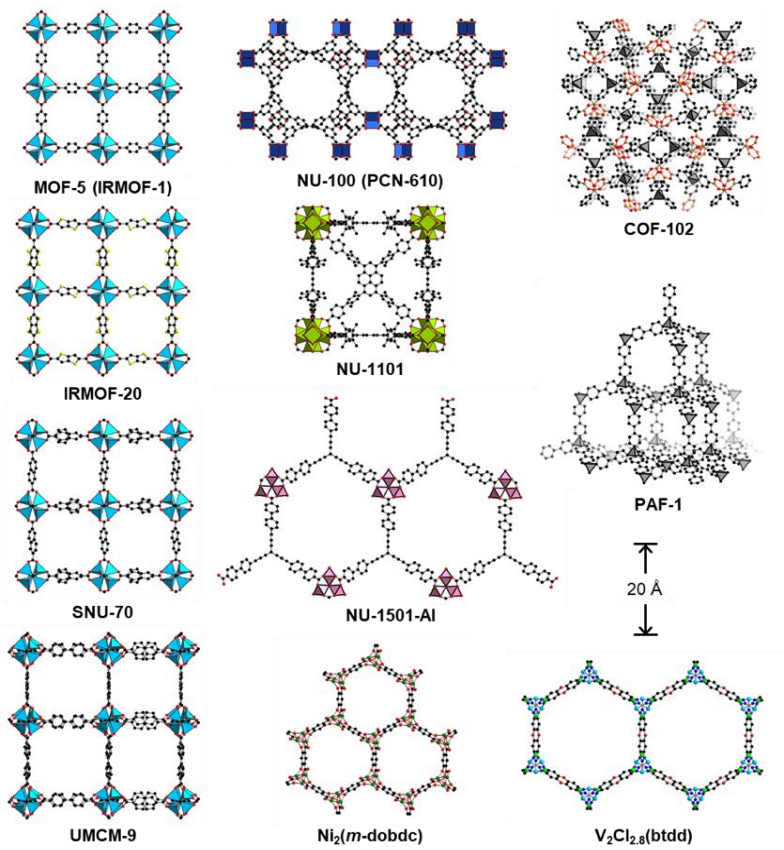

Figure 10. Solid-state structures of representative H_2 adsorbents. All structures are drawn at the same scale. Atom colors: C, black; O, red; N, blue; B, orange; S, yellow; Cl, light green; Ni, green; V, light blue; Zn, blue polyhedra; Cu, navy blue square; Zr, green polyhedra; Al, pink polyhedra; tetrahedral carbons, gray polyhedra. Hydrogen atoms are omitted for clarity. PAF-1 is amorphous, so the structure of the ideal diamond net is shown. Image courtesy of Hiroyasu Furukawa, University of California, Berkeley and Lawrence Berkeley National Laboratory.

As a result of their low H_2 binding enthalpies (−4 to −5 kJ/mol), the aforementioned materials are suitable only for cryogenic H_2 storage. Significant energy savings could be achieved by storing hydrogen near ambient temperatures by controlling the thermodynamic and/or kinetic properties of materials.[215] To realize such strong H_2 binding energies within adsorbents, one promising strategy is to use MOFs featuring coordinatively unsaturated metal sites that can polarize the H_2 molecules, drawing them closer to the surface.[197] The M-MOF-74 or M_2(dobdc)(M = Mg, Fe, Co, Ni, Mn, Zn; $dobdc^{4-}$ = dioxidobenzenedicarboxylate) family of frameworks and structural analogues feature a high density of coordinatively unsaturated metal sites and have been extensively studied for hydrogen storage[216] (**Table 1**).[209] Recently, a vanadium-based MOF, $V_2Cl_{2.8}$(btdd) (btdd = bis(1H-1,2,3-triazolo[4,5-b],[4′,5′-i])dibenzo[1,4]dioxin), was shown to exhibit an optimal binding enthalpy of −21 kJ/mol for ambient temperature H_2 storage.[210] To improve the capacity, the synthesis of MOFs containing low-coordinate metals capable of binding multiple H_2 molecules at each site provides a powerful strategy.[217]

For practical applications, additional properties must be evaluated, including adsorption and desorption kinetics, durability and impurity tolerance, thermal transport properties, formation of dense monoliths from powders, and effects of pelletizing powdered samples. Many of these are currently in early-stage research. Although the use of porous carbon samples has been extensively investigated, materials with controlled heterostructures and hybrid materials are of interest.[197] However, low isosteric heats of adsorption may limit their application to cryo-storage. Catalyst-driven hydrogen spillover on carbon-

based materials has also been extensively explored but was determined to be infeasible for light-duty vehicle storage.[197] However, the observation of C-H bond formation during this process suggests this approach could be useful for long-term hydrogen storage. Issues with reproducibility indicate that fundamental understanding of the spillover mechanisms is lacking.[218, 219] Additionally, simple analysis protocols to estimate the amount of stored H_2 in a tank have yet to be developed.[220]

3.1.2 Chemical Storage

Chemical storage (CS) is broadly defined as storing hydrogen in chemical bonds in contrast to adsorption on a high-surface area material. Because the hydrogen in CS is strongly bound, thermal energy—and, in some cases, a catalyst—are required to enable hydrogen release and uptake. Compounds used for CS cover a broad range of elements. However, materials primarily composed of light main group elements—particularly Li, B, C, N, O, Na, Mg, and Al—are often sought to achieve high-gravimetric densities of hydrogen. There is also renewed interest in CS and LOHCs for nonvehicular applications, given the potential to use existing infrastructure to transport and store hydrogen in this form at ambient pressures and temperatures. Large-scale and long-duration energy storage in chemical bonds is attractive for a wide range of applications, such as emergency backup power for critical infrastructure, and storage and transport of energy derived from intermittent renewable resources.[221]

Metal Hydrides. Metal hydrides are the most extensively investigated class of storage materials and are used commercially for a variety of applications. Subcategories include binary or "simple" hydrides in which the metal is bound only to hydrogen, such as MgH_2 and AlH_3, and complex hydrides in which the metal is bound to a polyatomic anion, such as BH_4^-, AlH_4^-, or NH_2^-. Examples include $LiNH_2$, $Mg(BH_4)_2$, and $NaAlH_4$. Both simple and complex hydrides in their bulk form have been extensively researched for light-duty vehicle transportation.[170, 222] Interstitial hydrides are an extremely large class of materials that has versatility and tunability for both sorption pressures and temperatures. Examples include AB (e.g., TiFe), AB_2 (e.g., $MgNi_2$), and AB_5 stoichiometries (e.g., $LaNi_5H_6$).[180, 223] These materials generally have excellent uptake and release kinetics and high-storage densities. The gravimetric capacity of these is too low for transportation applications, but they have proved to be suitable for stationary applications and in material handling equipment in which the additional weight is an advantage. Key issues to be addressed include improved activation (e.g., for TiFe) and resistance to poisoning by impurities, such as CO, O_2, H_2O, and sulfur-containing species. Reduced hysteresis and microstructure engineering to resist decrepitation would also be key improvements.

Achieving high hydrogen capacity, particularly gravimetric capacity, has traditionally been a major driver for hydride discovery.[170, 224] However, it is now clear that the thermodynamics and kinetics of hydrogen release and uptake are major issues[182] as a result of the multiple physical and chemical processes involved (**Figure 11**).[225] This knowledge has led to a variety of innovative strategies. Nanoscaling in particular is the focus of vigorous research,[170, 224] but high-entropy alloys,[226] metastable hydrides,[227] and composites[228] are also of interest.

Carbon-Based Compounds. Cyclic alkanes as LOHCs have reached a level of maturity that allows them to be used in small-scale industrial applications. By nature of being in a liquid form, LOHCs provide advantages over solid phase materials, such as metal hydrides, because they can transport hydrogen by using existing infrastructure, such as pipelines, tanker trucks, rail, and cargo ships. For example, methylcyclohexane is being used to ship hydrogen internationally from Brunei into the port of Kawasaki in Japan.[229] Platinum supported on oxides is reportedly the best catalyst for releasing H_2 from methylcyclohexane vapor.[230] The compound H18-dibenzyl toluene is also being used as a hydrogen carrier in which a platinum-based catalyst is used to release hydrogen in the liquid phase.[231] Recent reviews have focused on the desirable range of physiochemical properties and thermodynamics of LOHCs,[172, 173, 232] as well as on the kinetic and catalytic challenges.[233, 234]

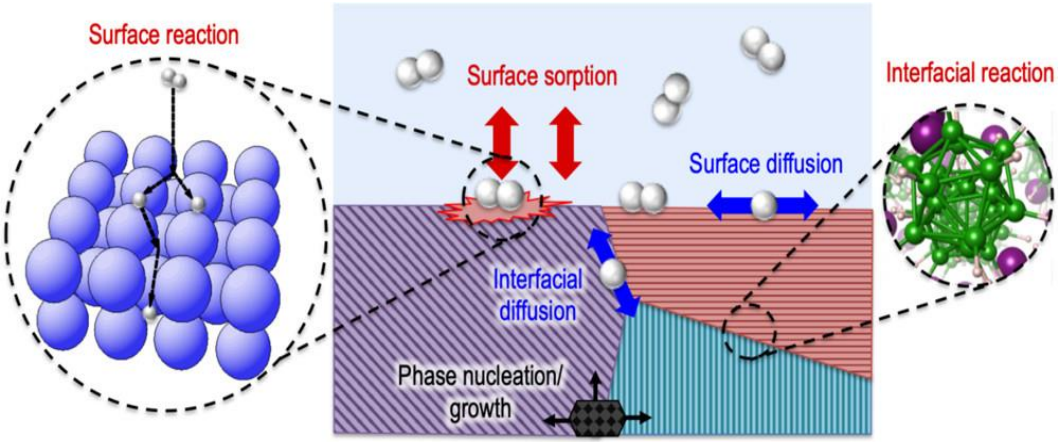

Figure 11. Schematic showing chemical and physical processes occurring during interactions of hydrogen with a chemical storage material, such as a metal hydride.Source: Ref. [225] Reprinted with permission from Wood, et. al., "Beyond Idealized Models of Nanoscale Metal Hydrides for Hydrogen Storage," *Industrial & Engineering Chemistry Research*, **59**, 5786–5796 (2020). Copyright 2020 American Chemical Society.

Boron Compounds. Borohydrides and boranes have drawn considerable interest, particularly ammonia borane, for its high density of hydrogen and the low temperature of H_2 release; however, regeneration is still energy intensive.[235, 236] On the other hand, thermal decomposition of borohydrides forms a mixture of "unstable" borane products that can be hydrogenated to regenerate borohydride under extreme pressure and high temperatures.[237] Saldan describes some of the complex chemistry and how it changes with reaction conditions.[238] Although several studies have described the catalytic activation of B-H bonds in ammonia borane,[239] there is little insight into catalysts to enable H_2 release from borohydrides.

Nitrogen-Containing Compounds. Ammonia and N-heterocyclic arenes have received the greatest attention in this class of materials. A breakthrough in low-temperature ammonia synthesis was recently achieved,[240] reducing the temperature for high catalytic activity from between 300 and 500 °C, as required for the incumbent Haber-Bosch process, to <300 °C by using a bifunctional LiH-transition metal catalyst. It was proposed that the second catalytic site, LiH, acted to break the scaling relationship between adsorption and transition-state energies of intermediates observed with transition metal catalysts.[240] An intriguing process for low-temperature H_2 release using $LiNH_2$[241] was recently reported with 100% conversion of NH_3 to H_2 at <500 °C. The topic was recently reviewed.[242]

Nitrogen substitution into cyclic alkanes reduces the free energy and allows H_2 release at lower temperatures. Crabtree recently reviewed the approach.[243] Notably, in silico methods are being used to identify the optimum candidates using hetero atom substitution.[192, 244] There was interest in cyclic azaborines, carbon-boron-nitrogen compounds, given the favorable thermodynamics; however, it was difficult to find catalysts that could couple the endothermic and exothermic release of hydrogen.[245]

Oxygen Compounds. These CS materials and processes include classic methanol reforming. Low-temperature molecular catalysts have been reported to reform methanol at lower temperatures.[246] A recent focus has been on catalyst development for H_2 release from formic acid[247] and formate salts.[177] Formic acid is intriguing because as the release of H_2 is entropy controlled and provides a chemical approach to generate high-pressure hydrogen. Although not the topic of this roundtable, it is notable that an active field of research is the production of formate or formic acid using electrochemical reduction of CO_2 incorporating water oxidation in the same device, eliminating the separate step of producing hydrogen.[248, 249]

3.2 Physically Based Storage

3.2.1 Compressed Gas Storage and Transport

Hydrogen is commonly stored and transported as a compressed gas, and the technology for this is mature. Suitable materials, material microstructure, and cylinder design for compressed gas hydrogen storage must consider the effects of adsorption and diffusion of hydrogen into the material on the materials' mechanical properties, commonly known as *hydrogen embrittlement*.[250-256] For small-scale uses, hydrogen is currently distributed in standard US Department of Transportation–approved gas cylinders at pressures up to ~150 bar. Special transportable gas cylinders are available at pressures up to ~420 bar. Transportable cylinders are generally Cr-Mo steel (aluminum can also be used for hydrogen service), which has been quenched and tempered to a relatively low-strength condition (tensile strength <850 MPa). Although these materials are strongly affected by hydrogen, especially for fatigue loading, they remain ductile, and the low-wall stresses characteristic of transportable cylinders effectively manages the embrittling effects of hydrogen. Stationary storage for fuel cell applications can approach pressures of 1,000 bar (e.g., in vehicle refueling applications). Steel vessels for these higher-pressure applications require very thick walls to manage the high pressure-induced stresses. Consequently, quenched and tempered Ni-Cr-Mo steels are used to help manufacture the required thick-walled structures. As for transportable gas cylinders, the strength of the steels is relatively low (tensile strength <915 MPa) to manage hydrogen embrittlement.[257] Steel pressure vessels of these types are generally referred to as *Type I vessels* (i.e., all steel) and are relatively inexpensive and extremely heavy.

Hoop-wrapping of steel cylinders with high-strength wire or fibers is an engineering solution to manage stress in large-scale stationary pressure vessels for high-pressure operation (~1000 bar).[258] The pressure-induced hoop stresses are shared between the thick-walled steel structure and the hoop wrapping, typically carbon fiber or high-strength steel wire. Axial stresses are carried principally by the steel. Load-sharing structures of this type are referred to as *Type II vessels*. Type II vessels are essentially Type I vessels with a composite wrapped around the cylindrical section of the vessel. Recent advances in characterizing the mechanical properties of pressure vessel steels in hydrogen suggest that Type II vessels can be designed so that the vessel service life is limited by the aging of the composite, provided that the fatigue stresses in the steel due to pressure cycling are appropriately managed.[259]

Two types of composite overwrapped pressure vessels are used for mobility applications: Type III vessels use a nonstructural metal liner, and Type IV vessels use a polymer liner. These types of composite vessels improve the volumetric and gravimetric efficiency of storage at substantially higher cost.[260] The standard fuel system for light-duty FCEVs includes a Type III or Type IV vessel for onboard storage at a pressure of 700 bar. Type III vessels at 350 bar are also used in FCEVs, such as busses.

There are two principal methods of compressed hydrogen transport: truck and pipelines. The tube trailers used to transport GH_2 by truck are simply bundles of large gas cylinders made of the same steels used for transportable gas cylinders. The use of Type III and Type IV vessels is increasing for hydrogen transport because of the substantially higher payload capacity of the tube trailer. (e.g., ~350 kg H_2 for a jumbo trailer with steel tubes at ~182 bar compared with ~1,000 kg H_2 of composite tubes at 500 bar). The transport of compressed GH_2 in dedicated pipelines is a mature technology, whereas the impact of blending hydrogen into natural gas (HyBlend) remains a lively debate. HyBlend is discussed in detail in Section 3.2.2. Steel pipelines are essentially long pressure vessels that use lower-cost and lower-strength steels. Pipeline steels perform similarly to pressure vessel steels in hydrogen environments. More than 2,500 km of hydrogen pipeline exist in the United States, primarily in the Gulf Coast region, to support the oil, gas, and chemical industries. Even after decades of research, fundamental questions remain concerning the atomistic interactions of metals with dissolved hydrogen. Imaging of hydrogen within the metal lattice is a significant challenge because of the high mobility of H and the compositional

complexity of commercial alloys, whereas surface studies are often confounded by background hydrogen and surface mobility. The surface chemistry of metals exposed to GH_2 represents a rich research topic, especially in the presence of the diverse range of potential oxides on metal surfaces and other species that are present when hydrogen is blended with natural gas (e.g., oxygen, sulfur compounds, carbon monoxide).

Numerous innovations in pressure vessel design are under development (e.g., conformal vessels, Type V, linerless vessels); generally, these invoke creative engineering by using existing materials and manufacturing methods. Advanced third-generation steels—a broadly active area of research—are not targeted toward pressure vessel applications and are unlikely to improve the cost-performance trade space for this application. Innovative microstructural design concepts for low-cost steels (e.g., low-carbon steels) have not been proposed for demanding structural service in harsh environments, but materials design developments could benefit hydrogen technologies for storage and transportation. Fundamental limitations of composite vessels (inclusive of Type II) include the cost and strength of the composite fiber, as well as the stress rupture properties of the fiber.

3.2.2 Blending Hydrogen with Natural Gas in Pipelines

Blending of hydrogen with natural gas in pipeline networks is gaining interest as a means to reduce emissions from the heating and power generation sectors. In 2020, DOE selected the HyBlend project for funding, a 2 year collaboration between six national laboratories and over 20 stakeholders, conducting materials compatibility R&D, cost, and emissions analysis to identify the value proposition and quantify the challenges associated with blending. Additionally, DOE's Building Technologies Office and HFTO are managing the development of an R&D outlook document to identify technical barriers to use for hydrogen blends in building appliances. Currently, several gas system operators worldwide are also conducting pilot tests of blends with hydrogen levels on the order of 5–30 vol % (**Figure 12**), blending either in pipelines or at the point of use (e.g., the natural gas turbine). These demonstrations will identify additional technical and operational barriers to blending.

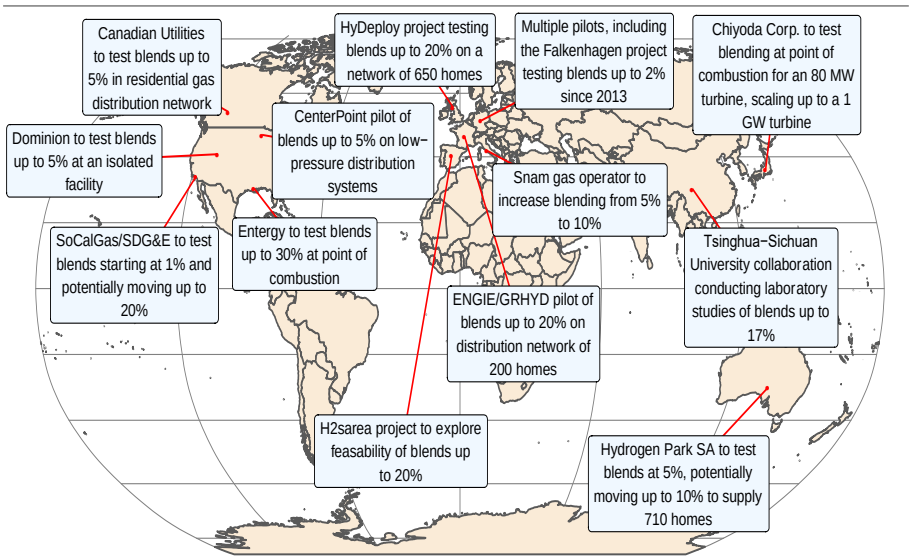

Figure 12. Summary of announced or ongoing pilot programs intended to study the impacts of hydrogen blending on natural gas pipeline systems. This figure summarizes major pilots and is not intended to be comprehensive. Source: Bri-Mathias Hodge, National Renewable Energy Laboratory; B. Cakir Erdener, B. Sergi, O.J. Guerra Fernandez, A. Lazaro Chueca, K. Pambour, C. Brancucci, B-M Hodge, "A review of technical and regulatory limits for hydrogen blending in natural gas pipelines" **(Under review).**

One key concern with regard to blending is that hydrogen can affect the reliability of metallic and polymeric pipeline materials. The magnitude of these effects depends on pipeline operating pressure, operation (e.g., daily pressure fluctuations), pipeline integrity before blending, and pipeline materials. Hydrogen pipelines in service today are designed around relevant codes and standards (e.g., the American Society of Mechanical Engineers B31.12, *Hydrogen Piping and Pipelines*) to manage these risks. However, limited R&D has been conducted to date regarding the performance of legacy natural gas pipeline materials in varying concentrations of hydrogen. One goal of the HyBlend project is to conduct testing across a range of materials and blend pressures to inform the development of a publicly accessible tool that characterizes the risks of blending under user-defined conditions.[261, 262]

Beyond materials, hydrogen blends are also likely to impact gas system operations. The lower calorific value of hydrogen reduces the Wobbe Index of the delivered gas, an indicator of the interchangeability of fuel gases. The range of impacts could be conditional on the natural gas quality (**Figure 13**). Maintaining a consistent energy content delivered to customers could require increased gas flows and pressure levels and thus require modifications to existing equipment. Increasing pressures would also require higher power consumption from compressor stations and could affect reliability and efficiency.[263, 264] Aspects such as leakage rates of hydrogen blends from underground gas storage facilities, metering devices, and regulators are not yet well characterized. End-user restrictions could also limit blend levels. For example, the gas turbines manufactured by some original equipment manufacturers (OEMs) have a limiting value of 5–15%, and others have reported high-efficiency gas turbines fueled by mixes of up to 30% hydrogen, although higher levels could be possible with retrofits or technological advancement.

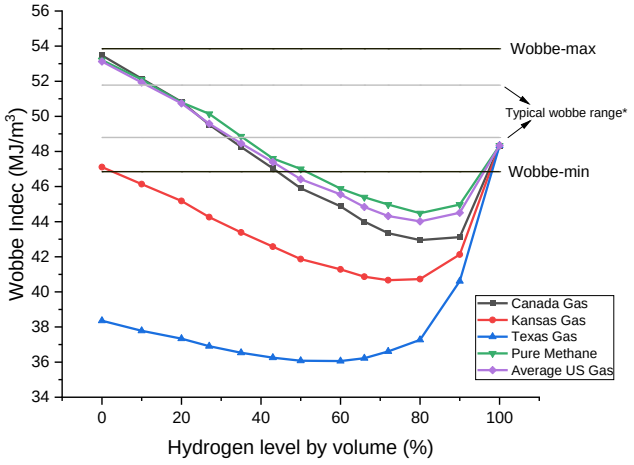

Gas Compositions (%)				
	Canada	Kansas	Texas	Average US
Methane	77.1	73	65.8	92.3
Ethane	6.6	6.3	3.8	3.6
Propane	3.1	3.7	1.7	0.8
Nitrogen	3.2	14.7	25.6	1.8
Others	10	2.3	3.1	1.5

Figure13. Wobbe index values for different hydrogen blending levels and natural gas types based on assumed gas compositions shown in the table. Values are estimated using simulations on a test network with the SAInt gas net modeling software. Source: Bri-Mathias Hodge, National Renewable Energy Laboratory; B. Cakir Erdener, B. Sergi, O.J. Guerra Fernandez, A. Lazaro Chueca, K. Pambour, C. Brancucci, B-M Hodge, "A review of technical and regulatory limits for hydrogen blending in natural gas pipelines" **(Under review)**.

Historically, many gas system operators limited the hydrogen levels (typically 0.1–0.5% in natural gas) to maintain high gas quality. Regulatory limits to hydrogen blending differ by country, ranging from as low as 0.1% in Japan, Sweden, the United Kingdom, and others to as high as 10% in Germany. Data on these limits are available from various sources, including the European Hydrogen Law Database (HyLaw),[265] a survey of European regulators by the Agency for the Cooperation of Energy Regulators (ACER),[266] academic papers,[267, 268] and other sources.[3, 269, 270] Countries without explicit limits, such as the United States, may nonetheless provide implicit constraints on hydrogen blend levels, such as requirements on

the energy content of delivered gas. Many regulators are currently looking to hydrogen blending pilots to evaluate whether to permit higher blending levels.

In terms of the usefulness of blending as a decarbonization strategy, hydrogen has a much lower energy content than natural gas, meaning that larger volumes are needed to provide the same energy services to end users as displaced natural gas. Thus, high levels of blending (i.e., >75% H_2) are likely to be needed to substantially reduce emissions from natural gas.

3.2.3 Liquid Hydrogen Storage and Delivery

There are many potential advantages to building a hydrogen infrastructure using liquid hydrogen (LH_2) rather than GH_2 (**Figure 14**).[271] The higher density of LH_2 leads to a smaller footprint for stationary and onboard storage and lower distribution costs.[272, 273] LH_2 can be transported in barges and overseas on ships; LH_2 pumps can be compact and achieve high throughput with low electricity consumption.[274]

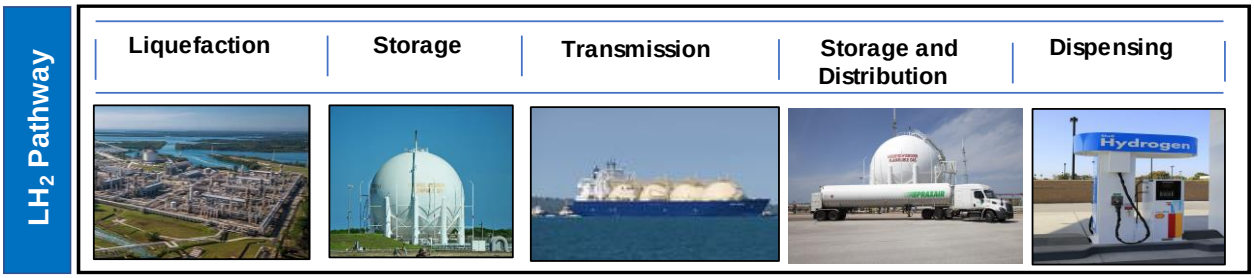

Figure 14. Typical LH_2 pathway showing steps for liquefaction at H_2 production site, storage at port, transmission by ships, storage at receiving terminal, and distribution and dispensing.
Source: Ref. [271] Image L-R: "Aerial of Badak NGL Natural Gas Refinery," (https://commons.wikimedia.org/wiki/File:Aerial_of_Badak_NGL_natural_gas_refinery.jpg), Created by Consigliere Ivan/Flickr, Copyright by Creative Commons Attribution 2.0 Generic (CC BY 2.0) https://creativecommons.org/licenses/by/2.0/deed.en; "Liquid Hydrogen Tank at Cape Canaveral," https://www.flickr.com/photos/warriorwoman531/8155235271/, Created by Heather Paul/Flickr, Copyright by Creative commons Attribution-NoDerivs 2.0 Generic (CC BY-ND 2.0)https://creativecommons.org/licenses/by-nd/2.0/; "Alto Acrux Departs Darwin in June 2012," https://www.flickr.com/photos/40132991@N07/7501108978, Created by Ken Hodge/Flickr, Copyright by Creative Commons Attribution 2.0 Generic (CC BY 2.0), https://creativecommons.org/licenses/by/2.0/; "KSC_20160428-PH_FJM0001_0016," https://www.flickr.com/photos/nasakennedy/26172644733, Created by NASA Kennedy/Flickr, Copyright by Creative Commons: Attribution-Non Commercial-No Drivs 2.0 Generic (CC BY-NC-ND 2.0), https://creativecommons.org/licenses/by-nc-nd/2.0/; "Hydrogen pump," https://www.flickr.com/photos/iip-photo-archive/22724718378/in/photostream/, Created by GPA Photo Archive/Flickr, Copyright by Creative Commons Attribution 2.0 Generic (CC BY 2.0), https://creativecommons.org/licenses/by/2.0/.

For low- to medium-capacity refueling stations, specially designed LH_2 tanks are available to fit into a 40 ft container.[273] These tanks have 11.5 m^3 of internal volume to store 900 kg of H_2 and double-wall construction in which the intervening space is filled with a multilayer vacuum insulation for a <0.6%/day boil-off rate. For early markets with low H_2 demand, smaller tanks are available with 6 m^3 internal volume and 400 kg LH_2 storage capacity. They have a special insulation system to limit the boil-off rate to <0.5%/day.[273] For industrial applications with high H_2 demand, horizontal and vertical tanks are available that can store 4,600 kg of LH_2 and obtain a <0.95%/day boil-off rate using vacuum perlite insulation.[273]

Since the mid-1960s, NASA has operated two 3,218 m^3 spherical tanks at the Kennedy Space Center, each capable of storing >230,000 kg LH_2.[275] These storage tanks consist of an 18.7 m diameter stainless-

steel inner sphere concentrically located inside a 21.6 m diameter carbon steel outer sphere. The annular region is evacuated to 20–60 mTorr and filled with perlite insulation to limit the boil-off rate to <0.035%/day. Numerous concepts were explored to develop zero–boil-off systems for cryogenic storage. Recently, NASA completed a pilot study to demonstrate an integrated refrigeration and storage concept that uses a closed-loop helium refrigeration system.[276] The pilot operated for 13 months to demonstrate zero boil-off and 390 W cooling at 20 K without any liquid nitrogen precooling.

LH_2 can be delivered by road in ~4,000 kg capacity trailers that require 4 h to load and ~1 h to off-load.[273] Nearly 100 kg of H_2 is vented during LH_2 transfer at refueling stations.[277] The off-load time can be cut in half and the transfer losses avoided by transporting LH_2 in 3,000 kg containers that can be swapped at the refueling station.[273] LH_2 can also be transported overseas by using these containers, possibly with liquid N_2 shields for longer holding times.[273] Kawasaki is planning to build and operate two LH_2 carriers to operate on the 9,000 km Australia-to-Japan route.[277] Each carrier will have four 40,000 m^3 spherical tanks for 160,000 m^3 or 10,800 tons of H_2 total capacity. As a comparison, the largest liquified natural gas carriers in commercial use today have 180,000 m^3 capacity obtained with four Moss-type spherical tanks.

An early onboard LH_2 storage system designed and built for light-duty vehicles had 143 L of internal tank volume for 8.1 kg of H_2 capacity at operating pressures of up to 5 bar.[278] The total weight of the system was about 100 kg.[278] A subsequent design using lightweight aluminum instead of steel showed the feasibility of reducing the system weight to 66 kg and improving the gravimetric capacity from 9 to 15%.[278] Recently, conceptual studies were conducted to investigate onboard LH_2 storage for long-haul heavy-duty trucks, freight locomotives, passenger boats, and regional planes.[279, 280] These studies suggest that LH_2 might be attractive in applications that require large amounts of stored H_2 (e.g., locomotives, boats, trucks), have duty cycles that require only 1–3 days of dormancy (e.g., trucks), or are extremely sensitive to weight (e.g., aviation).

3.3 Geological Storage

Geological storage of hydrogen within salt cavities was demonstrated.[281] However, to allow geographically more widespread storage and opportunities to meet ongoing renewable energy needs, additional geological formation types must be considered, such as porous media (**Figure 15**).[282] This will require increased characterization, including understanding technical challenges involved in the subsurface storage of hydrogen. These include (1) the enhanced mobility of hydrogen, which has a viscosity of about half that of natural gas; (2) hydrogen embrittlement of the steel casings typically used in well completions;[283] and (3) the impact and permeability of hydrogen on other well-sealing materials (e.g., elastomers, casing cements[284]). Additional concerns center on the biological[285] and chemical interactions of hydrogen with the host rock and engineering well materials. These could change the permeability of the storage

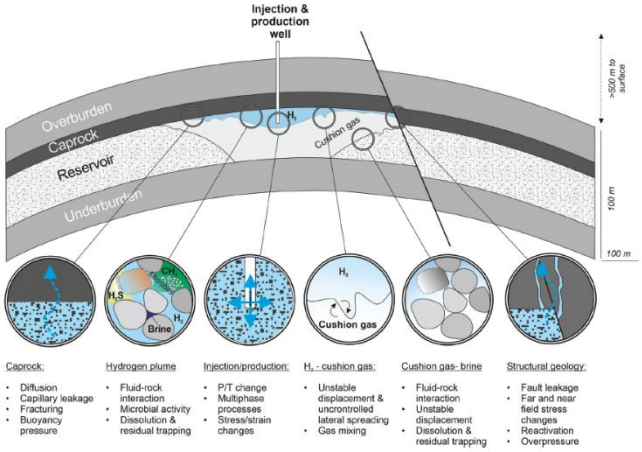

Figure 15. Image depicting the technical challenges to be addressed to ensure the successful storage of hydrogen within porous media. Source: Ref. [282] Used with permission of Royal Society of Chemistry from "Enabling Large-Scale Hydrogen Storage in Porous Media – the Scientific Challenges," Heinemann, et. al., Vol. 14, 2021; permission conveyed through Copyright Clearance Center, Inc.

formation, thereby impacting the reliability of geologic seals and compromising the integrity of the access well.[286, 287]

For the storage of hydrogen in depleted reservoirs (e.g., porous media), literature has discussed the issues in common with storing other gases.[288] These include the need for a cushion gas, migration into the surrounding formation rocks and fluids, contamination of the stored gas, and subsurface chemical reactions. The similarities to natural gas and helium are also evident in simulation work, indicating the importance of understanding gas diffusion and bio-geochemical interactions among the gas phase, the residual water or brine, and the rock matrix.[289] In contrast, other recent modeling has shown that the details of subsurface hydrogen storage are unique and differ from those of natural gas.[290] These differences include the hydrodynamics of the storage system in addition to differences in microbial activity. The main difference between hydrogen and natural gas storage is the higher diffusivity and lower viscosity of hydrogen.[281] With respect to hydrogen storage in salt caverns, virtually no difference was observed in salt permeability between natural gas and hydrogen.[291] The only differences observed were attributed to the differences in viscosity between the gases. Consequently, large-scale permeation of hydrogen into the surrounding salt should not be an issue. Perez et al. discusses work regarding chemical and biologic reactions with the host rock in an assessment of subsurface porous media hydrogen storage in Argentina, but hydrogen embrittlement was considered to be the greatest technical hurdle in implementing this facility.[292]

Beyond subsurface geological storage, the storage of hydrogen underwater is also possible, taking advantage of the pressure generated by the water column and allowing hydrogen to be stored at high pressures without the need for storage vessels that need to tolerate high pressure differentials. This approach was investigated for compressed air storage but offers much greater energy densities in stored hydrogen.[293]

4. Hydrogen Utilization and Conversion

As shown in **Figure 1**, there are a myriad of uses for hydrogen. These technologies are in various stages of development. The processing and production of chemicals (e.g., petroleum refining and ammonia synthesis) are well established, but in many cases, they are energy intensive and need alternative processes to decrease energy use and increase product selectivity. Hydrogen can be used to produce electricity using fuel cells, an established process from an R&D and demonstration standpoint that is an emerging technology in terms of implementing and adopting a variety of applications. Although hydrogen has been used in combustion turbines for power generation for decades, almost all applications and demonstrations use low concentrations of hydrogen to avoid various issues with NO_x emissions and component degradation. Early-stage applications include conversion to other energy carriers via chemical upgrading and commodity production.[2, 4, 8, 294] The common goal of the majority of emerging and early-stage applications is to reduce CO_2 emissions by either decreasing the process energy demands or directly replacing fossil fuels, such as methane and gasoline.

4.1 Conversion to Energy and Electricity

4.1.1 Fuel Cells

Fuel cells electrochemically convert the chemical energy in hydrogen into electrical energy that can be used in applications that range from small portable power to transportation (e.g., cars and trucks) to grid-level stationary power with higher efficiencies than the incumbent combustion processes.[2, 267] The by-product heat from the electrochemical reaction can also be used to increase efficiencies in combined heat and power applications, such as residential power. There are several types of fuel cells that differ in terms

of the materials used in their components—such as the ion-conducting electrolyte—which define their operating temperature range and are categorized in this document as low, intermediate, and high. The operating temperature then dictates the most suitable applications and the required fuel purity. PEM fuel cells (PEMFCs) typically operate in the 20–100 °C temperature range but can provide power at even lower temperatures. Because of these low operating temperatures, their solid-state construction, and their rapid response to changing loads, PEMFCs are suitable for transportation and for portable and stationary power. Solid oxide fuel cells (SOFCs) typically operate at 600–1000 °C, which makes rapid start-up and load cycling challenging. Thus, SOFCs are most suitable for large-scale stationary power applications. There are several other types of fuel cells, such as molten carbonate and phosphoric acid, that are considered mature technologies but that have limitations due to their non–solid-state construction and thus receive less R&D attention.

The total global shipments of fuel cell systems were over 1 GW in 2019, and the transportation sector and stationary applications accounted for 908 MW and 221 MW, respectively.[295] Fuel cells for transportation are in the early stages of commercialization with >10,000 fuel cell cars sold in the United States and more than 40,000 fuel cell vehicles worldwide.[4] A major driving force for the implementation of fuel cells is their capacity to produce zero emissions with water as the only by-product. Countries and municipalities are increasingly passing legislation banning internal combustion engines in favor of zero-emission vehicles. For example, California is requiring that 50% of trucks be zero-emission by 2035 and that 100% of trucks be zero-emission by 2045, as well as plans to ban the sale of gas-powered cars in 15 years.[296] This type of legislation exemplifies the need for new transportation technologies, such as vehicle electrification. Stationary applications of fuel cell systems range from the sub-kilowatt to multi-megawatt scales. These applications include residential power and heat, such as the 300,000 residential fuel cells operating in Japan, and more recent use in data centers.[2] Reversible fuel cells, which are combinations of fuel cells and electrolyzers as either separate or integrated units,[297-299] also offer the potential for energy storage, which could help facilitate the deployment of intermittent renewables, such as solar and wind.

4.1.1.1 Polymer Electrolyte Fuel Cells

There are two major types of low-temperature fuel cells: PEMFCs and Alkaline Exchange Membrane Fuel Cells (AEMFCs). Early commercial fuel cell vehicles adopted PEMFCs exclusively; however, interest in AEMFCs is rapidly growing, as evidenced by the rising rate of publications.[300] For transportation applications, developers have been highly focused on direct hydrogen fuel cells that rely on high-purity hydrogen, whereas distributed generation fuel cell applications use hydrogen from natural gas or liquid petroleum gas. The focus of R&D on PEM transportation fuel cells for the last decade has been on the light-duty vehicle application and meeting the cost and longevity demands of that application. Recently, fuel cells for heavy-duty vehicles have attracted significant attention. R&D efforts have thus shifted to evaluating material performance in terms of enabling higher efficiency (target 72%) and durability (target 30,000 h) rather than a relatively singular focus on material cost reduction.[301]

PEM fuel cells are typically based on membrane electrolytes membranes that facilitate the efficient and selective transport of hydrogen ions from the anode catalyst layer to the cathode catalyst layer (CCL); the anodes contain platinum catalysts for hydrogen oxidation, and the cathodes employ platinum or platinum-alloy catalysts for oxygen reduction. The oxygen reduction reaction (ORR) at the cathode is most often the rate- and performance-limiting process, resulting in an extensive R&D effort to develop highly active and durable cathode catalysts. A representative three-layer membrane-electrode assembly (MEA) is shown in **Figure 16** [301, 302] that also illustrates the hierarchical structure of the electrode, especially the CCL. The catalyst nanoparticles are highly dispersed within the catalyst layers with 2–5 nm particles supported on carbon black particles.[303] Platinum-alloy catalysts were developed that exhibit a high initial activity, including PtCo, PtNi, and PtFe; however, durability and leaching of the transition metal can be problematic because they can degrade the membrane properties and poison other constituents in the

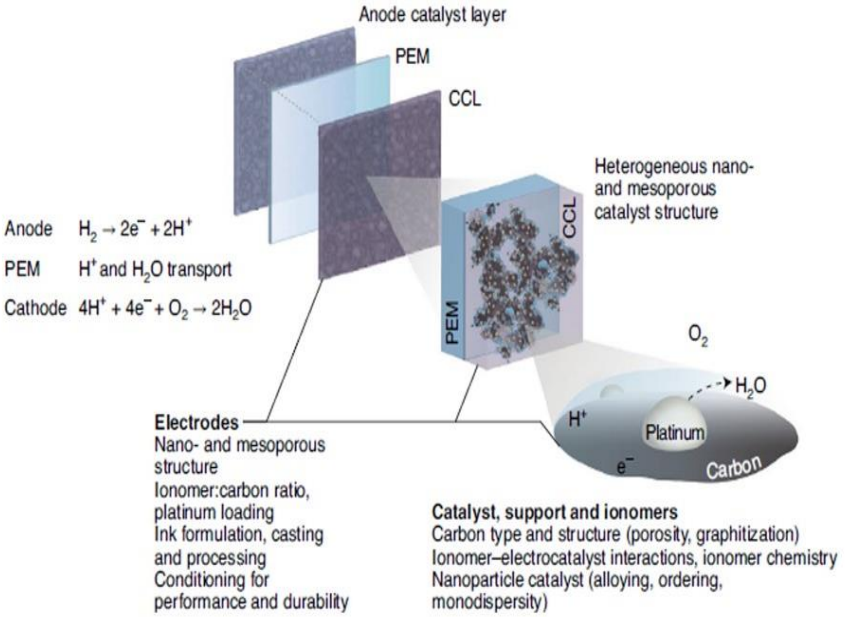

Figure 16. Components and a close-up view of a PEM fuel cell MEA showing materials and cathode catalyst structure. It is shown with anode/cathode reaction and an illustration of the heterogeneous porous structure of the catalyst layer and the interactions between ionomer thin film, carbon support, and platinum catalyst particles. Source: modified from ref. [301] Reprinted by permission from Springer Nature: Cullen, et. al., "New Roads and Challenges for Fuel Cells in Heavy-Duty Transportation," Nat. Energy (2021).

MEA. Ordered intermetallic platinum-alloy catalysts have shown the promise of better stability and long-term performance and are currently being incorporated into CCLs.[304] Research aimed at the development of high-performance PGM-free catalysts for the ORR at the cathode is an ongoing DOE effort to significantly lower the overall cost of PEMFCs.[305] Although the activity and durability of PGM-free catalysts is not yet sufficient to meet performance goals and targets for PEMFC systems, recent progress in this class of catalysts, especially in terms of enhanced durability, is bringing PGM-free catalysts much closer to practical applications.[306, 307]

Although hydrogen oxidation is fast, the anode typically requires high-purity hydrogen so as not to poison the platinum catalyst. Fuel cell electrocatalysts are susceptible to contaminants found in hydrogen and air, including sulfur compounds (e.g., H_2S or SO_x). Strict hydrogen fuel quality standards limit the permissible amount of impurities, such as CO, sulfur-containing compounds, ammonia, and halogenated compounds, which add to the cost of H_2, which can be challenging for H_2 produced by SMR. The membrane in PEMs requires relatively high levels of humidification to be highly proton conductive, and the relatively low operating temperature (80 °C) can pose challenges for vehicle heat rejection; higher-temperature membranes could lead to significant cost and performance benefits. The electrocatalysts, catalyst supports, and membranes making up PEMFC MEAs can degrade during PEMFC operation, and the degradation mechanisms are not fully understood.[308] Therefore, improvements in the performance of materials to enhance durability and extend lifetimes are actively being pursued. Additionally, multiple material interactions within the CCL serve to limit fuel cell performance; for example, ionomer/electrocatalyst surface interactions during CCL preparation can reduce catalytic activity, as summarized in **Figure 17**.[309, 312, 313] Durability, ORR kinetics, tolerance of hydrogen fuel impurities, low relative humidity and/or higher-temperature (~120 °C) operation, ionomer/carbon/catalyst surface interactions, and electrode design optimization all remain active PEMFC R&D areas.[310] In the mid- to long term, achieving stable PEM conductivity under hot (>100 °C) and dynamic fuel cell operating conditions, and achieving high thermal stability and tolerance of water for proton conductors will enable the use of high–energy-density liquid fuels that will increase the payload space for heavy-duty vehicles.[311]

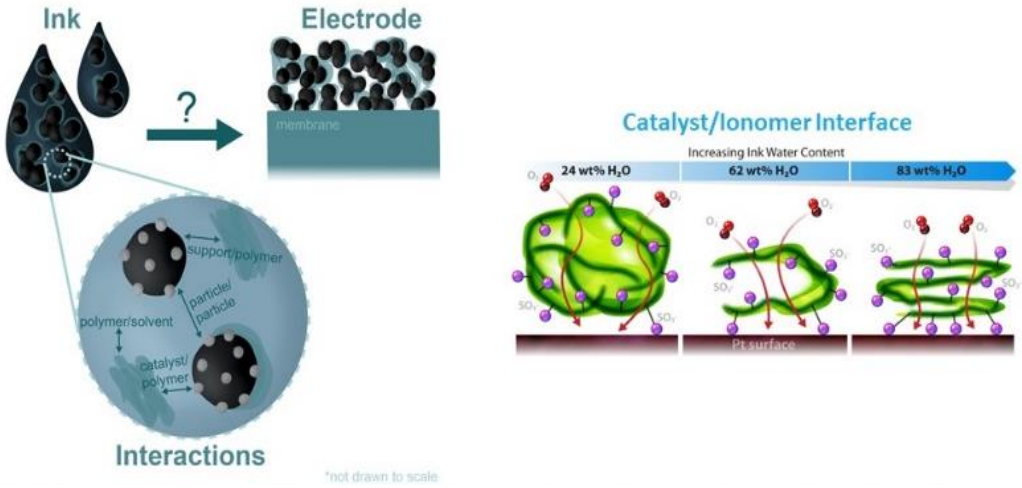

Figure 17. Schematic of how ionomer, water, and solvents interact during the formation of electrocatalyst layers. High water concentration dispersions lead to fewer secondary aggregates and to changes in the ionomer/catalyst structure that affect both gas transport and coverage of the catalyst with the ionomer. Sources: Refs. [312, 313] (Left: Reprinted (adapted) from Berlinger, et. al., "Multicomponent, Multiphase Interactions in Fuel Cell Inks," *Curr. Opin. Electrochem.* **29** (2021). DOI: 10.1016/j.coelec.2021.100744. Right: Reprinted with permission from Van Cleve, et. al., "Dictating Pt-Based Electrocatalyst Performance in Polymer Electrolyte Fuel Cells, from Formulation to Application," *ACS Appl. Mater. Interfaces*, **11**, 46953–46964 (2019). Copyright 2019 American Chemical Society.

AEM fuel cells have attracted attention owing to the improved stability of many materials in alkaline environments vs. acid environments. Non-platinum electrocatalysts exhibit good stability and high activity in alkaline environments; however, the performance of AEM fuel cells greatly depends on the interactions between electrocatalysts and ionomeric binders. Because electrochemically inert perfluorinated anion exchange ionomers are currently unavailable, the adsorption of ionomer fragments can significantly inhibit hydrogen oxidation and ORR (**Figure 18**).[314] The adsorption of anion-exchange ionomers on the catalyst impacts the electrochemical surface area, hydrogen and oxygen permeability, and water transport, depending on the electrode potentials. Unfortunately, the fundamental aspects of ionomer adsorption on PGM-free electrocatalysts are not well understood.

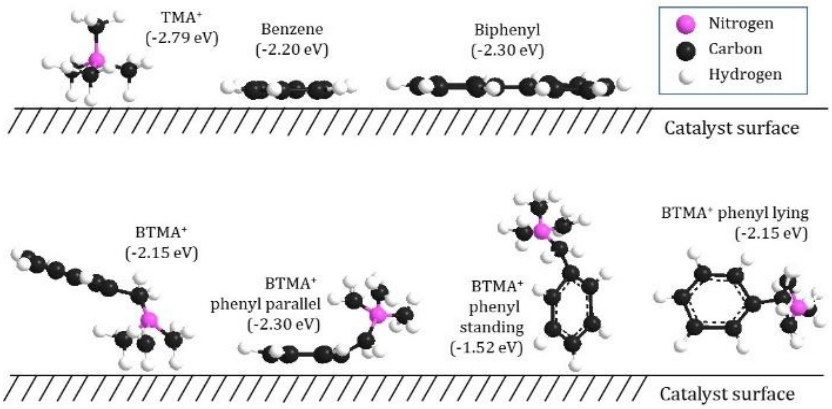

Figure 18. Illustration of the orientation of adsorbed anion-exchange ionomer components; tetramethyl ammonium cations (TMA^+); and benzene, biphenyl, and benzyltrimethyl ammonium cations ($BTMA^+$) on a catalyst surface. Numbers in parentheses denote the adsorption energy of the molecule on Pt(111) calculated by DFT. Source: Ref. [314] Reprinted from *Curr. Opin. Electrochem.*, Vol. 12, Li, et. al., "Impact of Ionomer Adsorption on Alkaline Hydrogen Oxidation Activity and Fuel Cell Performance," 189–195, Copyright 2018, with permission from Elsevier.

The durability of AEMFCs remains the most significant challenge, trailing that of PEMFCs by at least one order of magnitude.[315] AEM-based devices have water and CO_2 management issues that go beyond those of PEM-based devices.[300] Initial AEM fuel cell durability studies showed that the electrochemical oxidation of phenyl group in the anion exchange ionomer at the cathode can also significantly reduce the durability of the AEM fuel cell. Because the product of electrochemical oxidation of phenyl groups is phenol (acidic), the pH of the catalyst-ionomer interface can be significantly lowered from a pH of 13 to 11, resulting in reduced catalytic activity for the ORR.[29, 316] In the near term, more systematic studies to understand water and CO_2 management and the nature of catalyst-ionomer interactions could advance AEM fuel cell technology so that it is competitive with PEMFC technology.

4.1.1.2 Solid Oxide Fuel Cells

Hydrogen-fueled SOFCs offer the potential to efficiently use green hydrogen for centralized and distributed power generation. As discussed previously for SO-WEs, SOFCs can be based on either an oxygen ion-conducting or proton-conducting electrolyte. The most widely-used oxygen ion-conducting electrolyte for SOFCs is yttria-stabilized zirconia (YSZ). The standard anode is a Ni/YSZ cermet, and perovskites, such as lanthanum strontium manganite, are common cathode materials. Doped ferrites have also been widely explored as cathode materials for oxygen ion-conducting SOFCs. Proton-conducting electrolytes for SOFCs include the perovskites, such as doped samaria and yttria (e.g., $Ba_{0.9}Sr_{0.1}Ce_{0.5}Zr_{0.35}Y_{0.1}Sm_{0.05}O_{3-\delta}$, $Ba_{0.5}Sr_{0.5}Ce_{0.6}Zr_{0.2}Gd_{0.1}Y_{0.1}O_{3-\delta}$, $BaCe_{0.9}Y_{0.1}O_3$, and La-doped $BaZrYO_{3-\delta}$).[317]

Research and development efforts have led to the successful development and operation (e.g., design, selection of candidate cell component materials, fabrication processes) of laboratory-scale and commercial ceramic oxygen ion and proton ion-conducting SOFCs.[36-39] Both cells and stacks were fabricated and electrically tested by using dense ceramic electrolytes and metallic/oxide-based electrodes.[52] The operating temperature range for this technology is determined by the temperature dependence of the ionic conductivity of the electrolyte. Oxygen ion-conducting SOFCs operate in the ~600–1000 °C temperature range (classified as *high temperature* from 800 to 1000 °C and *intermediate temperature* from 600 to 800 °C). Proton-conducting SOFCs potentially operate at lower temperatures because protons have lower activation energies for transport through the oxide lattice than oxygen ions (e.g., 300–600 °C).[317, 318] The higher operating temperature range of SOFCs compared with PEM, LA electrolyte, and AEM fuel cells, as well as the susceptibility of the ceramic cell components to both mechanical and thermal shock, has limited their application primarily to large stationary power systems. However, the higher operating temperatures of SOFCs offer the advantage of less stringent hydrogen purity requirements than low-temperature fuel cells.

The technology status of SOFC systems using oxygen ion-conducting electrolytes, such as YSZ electrolytes, is more mature than that of proton-conducting ceramic electrolyte systems, which can be considered to be at the laboratory-scale phase of development. The commercial status of SOFCs can be summarized as follows.

- Cumulative installations of SOFCs of over 500 MW with system sizes ranging from the watt level, kilowatt level, and 100 kW level up to the megawatt level. System costs installed range from $3,000 to $5,000 per kilowatt before incentives.
- Cell-level durability of less than 1 year with the replacement of key components every 2–5 years.
- Power production efficiency is 45–50% in a simple cycle and 50–65% in hybrid cycles.

Within the SOFC cell design space, planar electrolyte-supported cells are the most widely used and are commercially available.[319] Tubular cells have niche market appeal, and anode-supported cells have unique advantages over electrolyte-supported cells, including reduced voltage losses due to electrolyte resistance. A careful assessment of the data for these different cell configurations and of the system-level performance and cost could provide a clear path forward regarding SOFC cell design.

SOFCs face challenges in robustness, durability, high manufacturing and maintenance costs, and operating window limitations. Cell-level durability issues arise both during steady-state operation and during thermal and load cycling.[52] Both ohmic and non-ohmic polarizations of SOFCs increase with operating time.[320] Posttest observations indicate chemical and morphological changes at the electrode and electrolyte surfaces and interfaces, as well as bulk structural modifications. Performance loss has been associated with cathode-side degradation mechanisms (chromium management), interconnect stability, and seal degradation. Bipolar exposure conditions accelerate the corrosion of metallic interconnects.[317, 321] Manufacturing cost challenges arise from high-temperature ceramic processes that require expensive furnaces and from quality assurance.[319, 322] Varying H_2O and H_2 partial pressures in the anode compartment can lead to the gasification of oxides that can be transported to the anode. Trace contaminants poison electroactive sites and form compounds, increasing the overpotential for the hydrogen oxidation reaction.[49, 323]

Active research areas in the fundamental understanding of SOFCs include the interaction of hydrogen (i.e., atomic, molecular, and charged) with metals and oxides at elevated temperatures with regard to surface adsorption, bulk diffusion, and the formation of redox H_2-H_2O at elevated temperatures.[324] At high activity (fugacity) of hydrogen and steam (oxidation) products in the fuel atmosphere, reaction processes with bulk alloy and oxide constituents, surface exsolution, gasification and transport of select oxides, accelerated localized corrosion of alloys, and evaporation of metallic anode are remain relevant research topics.

Beyond the conversion of hydrogen to electricity, ongoing areas of interest to the SOFC R&D community include hybrid systems to maximize power output and tri-gen systems—the coproduction of power, chemicals (hydrogen), and heat. Thermal integration and process intensification are major opportunities for innovation in these areas. Opportunities for SOFC cell and hybrid system development include (1) multifunction components, such as internal-reforming anodes; (2) enabling materials and processing technologies for innovative system applications, such as power, plus other products; and (3) process intensification for chemical, thermal, electrical, electrochemical, and mechanical integration.

4.1.2 Combustion Turbines

Hydrogen has been used as a power generation fuel in combustion turbines (i.e., gas turbines) for over three decades. To date, the major gas turbine OEMs (e.g., Ansaldo, General Electric [GE], Mitsubishi, Siemens, and Solar) have accumulated more than 14.5 million operating hours by using fuels that contain some percentage of H_2.[325-330] **Figures 19–21** show charts from the OEMs that highlight their H_2 fuel experience. However, only a few of these projects included operation on 100% H_2; most, if not all, projects that combust high concentrations of hydrogen use diffusion flame (i.e., mixing H_2 and air occurs in the flame) rather than lean premixed combustion systems, which impacts performance and NO_x emissions, as described as follows.

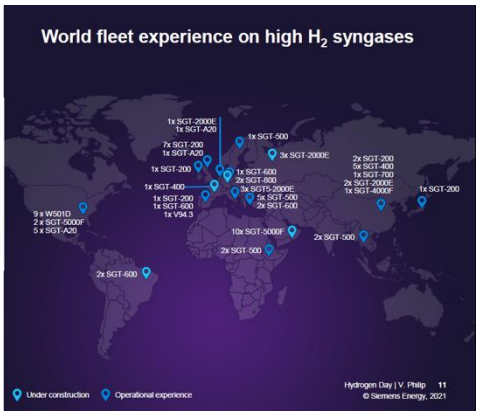

Figure 19. Siemens' high-hydrogen fleet experience. Over 2.5 million operating hours logged on over 53 units since 1979. Source: Ref. [325] Photo use authorized by Siemens Energy.

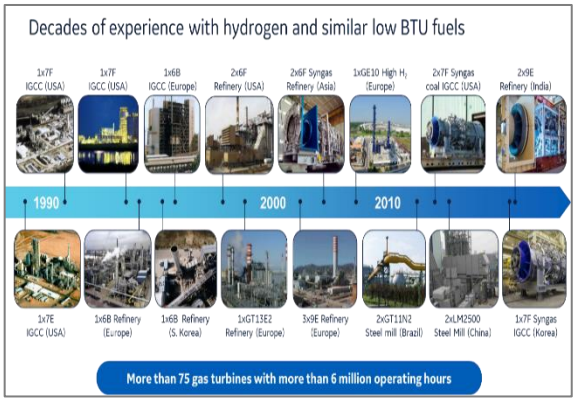

Figure 20. GE Gas Power hydrogen fuel experience. Source: Ref. [326] Photo use authorized by GE Power.

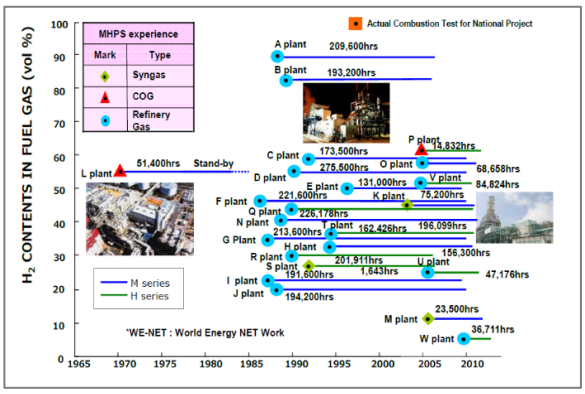

Figure 21. Mitsubishi Gas Power hydrogen fuel experience. Source: Ref. [327] Image courtesy Richard Hamilton, Orlanto Minervino, Narayanaswamy Kv - Mitsubishi Power Europe

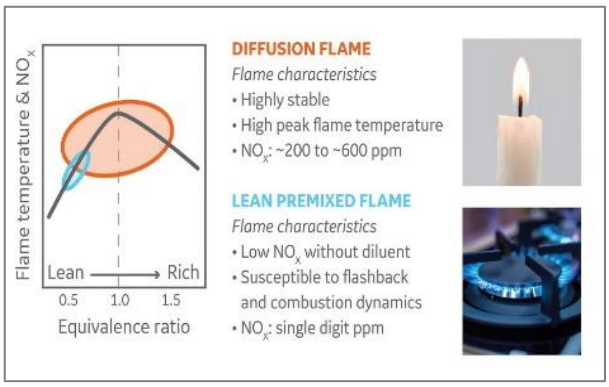

Figure 22. Diffusion vs. lean premixed combustion. Source: Ref. [395] Image courtesy of GE Gas Power.

Modern gas turbines typically operate in a fuel lean mode (fuel/oxidizer equivalence ratio, $\Phi \approx 0.5–0.6$). However, they can also operate with non-premixed (i.e., diffusion) fuel injections in which the flames burn at or near $\Phi = 1$, resulting in increased flame temperatures that drive exponentially higher NO_x emissions (**Figure 22**). Diffusion combustors have historically used a diluent such as water, steam, or nitrogen to reduce the peak (i.e., stoichiometric) flame temperature. This approach reduces net plant efficiency by ~4 or more percentage points. Lean premixed combustion systems—dry low NO_x or dry low emissions—operate at lower Φ, which reduces the flame temperature and lowers NO_x emissions. However, as a result of operability and flashback risks, this approach may limit H_2 content. Flashback (i.e., flame propagation upstream into the pre-mixer) is more likely with H_2-bearing fuels because the flame speed of H_2 (~300 cm/s) is greater than that of methane (~30–40 cm/s).[331] Flashback may cause severe hardware damage and immediate outage. H_2 flames are characterized by greater stoichiometric temperatures, resulting in increased NO_x (**Figure 23**).[326] Avoiding flashback could require additional capital cost for a larger selective catalyst reduction system or reduced performance—due to a reduction in combustor temperature—to mitigate it. Overcoming these challenges requires a new class of combustion systems.

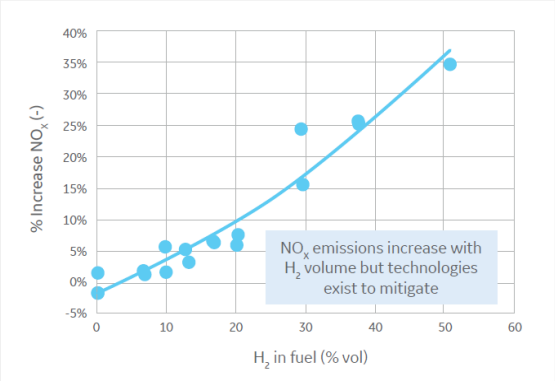

Figure 23. Impact of increased hydrogen on gas turbine NOx emissions. Source: Image courtesy of GE Gas Power. Ref. [395] Image courtesy of GE Gas Power.

These newer combustion systems use different mechanisms for fuel injection, flame stabilization, and emissions mitigation. They include lean direct injection, jet in cross-flow, and sequential combustion.[332-338] **Figure 24** shows full-scale multi-tube (i.e., micro-mix) combustion systems that use a combination of lean-direct-injection and jet-in-cross-flow concepts. These systems have demonstrated the capability to operate on blends of CH_4 and H_2.[326, 327, 334, 336, 337, 339]

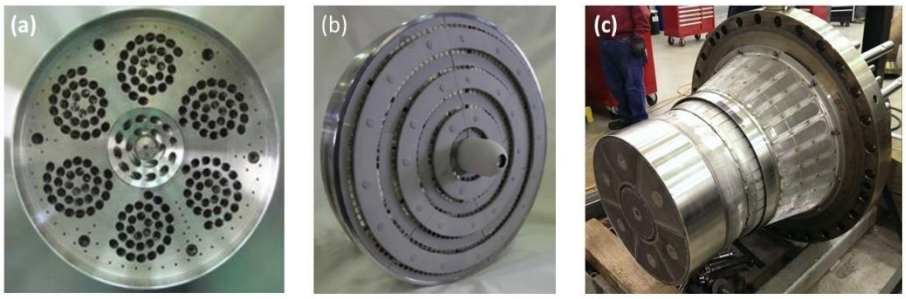

Figure 24. Three types of full-scale multi-tube combustors. Sources: (a) ref. [334], (b) ref. [336], (c) ref. [337]. (a) Reprinted with permission, Dodo, et. al, "Performance of a Multiple-Injection Dry Low NOx Combustor with Hydrogen-Rich Syngas Fuels," *J. Eng. Gas. Turbines Power-Trans*. ASME 135 (2013). Published by ASME; (b) Image courtesy Kawasaki Heavy Industries and NEDO (New Energy and Industrial Technology Development Organization in Japan); (c) Image courtesy of the GE Company.

Operating on blends of H_2 and CH_4 results in different combustion processes compared with operation on 100% H_2. **Figure 25** shows laminar flame speed (S_L) vs. the percent of H_2 in the fuel. At gas turbine conditions and at $f = 1$ (dashed line), S_L is <100 cm/s for all blends but jumps to ~400 cm/s for 100% H_2. As a result, configurations that can operate on H_2/CH_4 blends in the 50–70% vol% range may not be applicable at or near 100% H_2 fuel. The tendency of H_2 to embrittle metals might adversely affect a gas turbine's fuel system; **Figure 26** illustrates the impact of embrittlement. The potential impact of H_2 embrittlement on parts produced via additive manufacturing (i.e., 3D printing) is unknown. Combustion dynamics, which are also called *combustion acoustics*, can cause operational instabilities and damage hardware.[340]

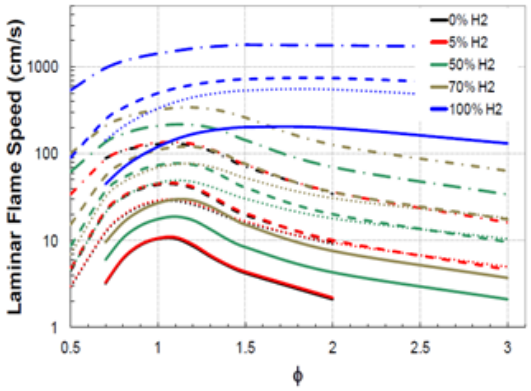

Figure 25. Laminar flame speed as a function of equivalence ratio and percent of hydrogen. Line color indicates the percent of H. Line type indicates test condition: solid line: 15 atm, 300 K; dashed line: 15 atm, 600 K; dotted line: 35 atm, 600 K; dot-dash line: 15 atm, 900 K. Source: Ref. [396] Direct reproduction of this figure has been approved by the authors Brower, et. al., "Ignition Delay Time and Laminar Flame Speed Calculations for Natural Gas/Hydrogen Blends at Elevated Pressures," *ASME TurboExpo*, Copenhagen (2012). Published by ASME.

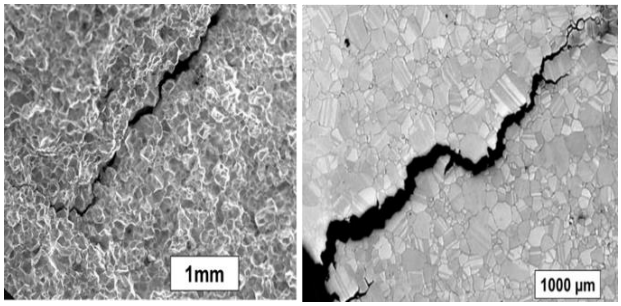

Figure 26. Example of field failure due to hydrogen embrittlement (left), and crack induced by hydrogen embrittlement (right). Source: Ref. [395] Image courtesy of GE Gas Power.

The increasingly demanding requirements of modern power plant operation will likely require new or modified combustion systems as the H_2 content approaches 100%. These requirements include, among others, startup on 100% H_2, stable combustion, low-load turndown, and NO_x emissions compliance. Hydrogen is not only a technology challenge; commercial viability is also a barrier. Today, the price of H_2 is at least two to three times the price of natural gas, and H_2 is unavailable in the volumes required for even a small gas turbine to run for any appreciable length of time. This situation requires new production, transportation, and storage capacity. These challenges must be resolved for a fully operational 100% hydrogen gas turbine.

4.2 Conversion to Energy Carriers, Commodities, and Other Utilization

4.2.1 Conversion of Syn Gas to Hydrocarbons

Synthesis gas, commonly referred to as *syn gas*, is a mixture of hydrogen and CO that can serve as a building block for a wide variety of fuels and chemicals, as shown in **Figure 27**.[342] Currently, mature technologies exist for producing syn gas from feedstocks such as natural gas, petroleum, petroleum derivatives, and coal. Any organic compound or waste can serve as a feedstock. Recently, there has been a growing interest in producing syn gas from non-fossil fuel sources by combining H_2 produced by the electrolysis of water with CO produced by electrochemically reducing CO_2 to CO. [343-346] [347] [355] By using CO_2 captured from an industrial process (e.g., ethanol production or combustion-based power generation) or from the atmosphere, this technology can serve as a means to produce carbon-neutral chemicals and fuels by recycling CO_2. An additional benefit of electrochemical CO_2 reduction is that by separating CO production from H_2 production, the ratio of H_2 to CO can be controlled to produce the optimal ratio for the catalytic process being employed to produce a specific chemical or fuel.

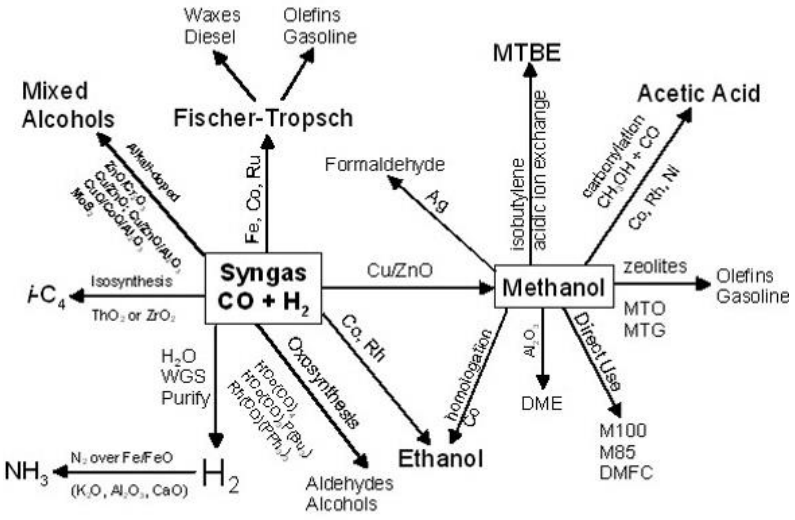

Figure 27. Chemicals and fuels that can be produced from syn gas. Source Ref. [342]. Reprinted with permission from the National Renewable Energy Laboratory, https://www.nrel.gov/docs/fy04osti/34929.pdf, accessed August 31, 2021. The NREL developed figure is not to be used to imply an endorsement by NREL, the Alliance for Sustainable Energy, LLC, the operator of NREL, or the U.S. Department of Energy.

Although a wide variety of chemicals and fuels can be produced directly from syn gas, converting syn gas to methanol—which can be subsequently converted into a wide range of chemicals, including acetic acid, formaldehyde, and dimethyl ether and fuels (e.g., gasoline)—is an attractive option for using carbon-neutral syn gas. The United States produced about 5.7 million metric tons of methanol in 2019.[348] Worldwide, about 148 million metric tons of methanol were produced in 2019, and growth is expected to reach 311 million metric tons by 2030.[349] The $CuO/ZnO/Al_2O_3$ catalyst used in natural gas-based methanol plants needs to be slightly modified to handle the larger amount of water that a carbon-neutral syn gas would produce, and catalyst technology already exists from several catalyst vendors.[350] To produce 1 t of methanol using syn gas—with both CO and H_2 produced by using electrolysis of CO_2 and H_2O, respectively—would require about 1.38 t of CO_2, 0.19 t of H_2 (~1.7 t of H_2), and 12–13 MWh of electricity,[350] the majority of which would be used to electrolyze water. A small-scale methanol plant with a production capacity of 100 tpd would require about ~120–130 MWh of electricity. A mega-methanol plant with a production capacity of 2,500 tpd would require a gigawatt-scale electrolyzer. Today, most new methanol plants are mega-scale for economic reasons. However, small-scale methanol plants in the 100–1000 ton per day range have several advantages compared with large-scale and mega-scale plants.[351] Small-scale plants have lower capital costs, making them attractive to investors and businesses by reducing risk. Because methanol is a liquid chemical that can be easily and cost-effectively transported, small-scale plants can be deployed near wind or solar farms, which are often in remote locations, or near the CO_2 source, eliminating the need to transport CO_2 to the methanol plant.

4.2.2 Conversion of Polymers to Chemicals

Plastics have become an indispensable part of the global society and are used in a wide variety of applications, including packaging, building and construction, transportation, consumer products, textiles, medicine, and electronics.[352] The growing concern regarding the environmental impacts of landfilling or releasing waste plastics into the environment has fueled efforts to develop new process technologies for converting waste plastics into liquid transportation fuels or value-added chemicals.[352-354]

Plastics have a wide range of properties, many of which derive from their thermal and mechanical stability and their resistance to most solvents and chemical reagents, and all of which make them challenging to convert to other products.[352] The conversion of waste polymers to fuels or chemicals presents many challenges. The most abundant class of polymers is polyolefins, which include polyethylene and polypropylene. Polyolefins are thermoplastics that consist of strong carbon-carbon and carbon-hydrogen bonds that make them generally resistant to chemical transformations.[352] These challenges are discussed in detail in a recent DOE BES roundtable report.[352]

Several different process technologies are being developed for waste polymer conversion, including pyrolysis and thermal cracking, hydrocracking and hydrogenolysis, hydrothermal liquefaction, and gasification.[352-354] Because hydrogen is the focus of this technology status document, the discussion to follow is limited to hydrocracking and hydrogenolysis processes that use H_2.

Hydrocracking and hydrogenolysis involve adding H_2 to the thermal cracking or depolymerization processes that typically result in greater yields of higher-quality products than are realized by thermal cracking, particularly if a catalyst is employed.[353] Process conditions can vary but generally require temperatures ranging from 200 to 500 °C and H_2 pressures ranging from 2 to 70 atm. Higher H_2 pressures are typically required to prevent the formation of coke.[355]

One approach for developing hydrogenolysis depolymerization catalysts is to investigate catalysts that consist of Pt, Ir, Rh, or Ru nanoparticles supported on metal oxides that catalyze the hydrogenolysis of small aliphatic hydrocarbons.[352] German researchers in the 1990s catalytically hydrogenated slurries of various plastics to produce aliphatic and aromatic compounds.[356] Oya et al.[357] and Nakaji et al.[358] deconstructed squalane (C_{30}) by regioselective hydrogenolysis of internal C−C bonds into lighter hydrocarbons over Ru/CeO_2 at 240 °C and 60 bar. Celik et al.[359] reported that Pt nanoparticles supported on nano-cuboid $SrTiO_3$ perovskite converted polyethylene (Mn = 8,000−158,000 Da) into high-quality liquid products, such as lubricants and waxes, characterized by a narrow distribution of oligomeric chains at 300 °C and 170 psi of H_2. Product yields as high as 97% were reported. Liu et al.[360] reported that $Pt/WO_3/ZrO_2$ and HY zeolite catalysts selectively converted polyolefins to branched liquid fuels in the gasoline to diesel range at yields up to 85% at temperatures as low as 225 °C and at 30 bar H_2. Tennakoon et al.[361] reported that a mesoporous catalyst with a core-shell Pt/SiO_2 structure selectively converted high-density polyethylene into a narrow distribution of diesel- and lubricant-range alkanes at 300 °C and 1.38 MPa H_2. Zhang et al.[362] developed a tandem hydrogenolysis-aromatization process to produce valuable alkyl aromatics from polyethylene with a Pt/Al_2O_3 catalyst at 280 °C.

Another approach for developing depolymerization catalysts is to use the principles established for developing polymerization and hydrogenation catalysts. Dufaud and Basset[363] reported a highly electrophilic Zr−H species synthesized by surface organometallic chemistry that transformed short-chain (C_{20}−C_{50}) and high molecular weight (Mw = 125,000 Da) polyethylene into fuels and short-chain hydrocarbons. The reaction occurred at temperatures ranging from 150 to 200 °C where unwanted free-radical reactions are not possible.

A review article by Munir et al.[355] provides a more comprehensive review of hydrocracking catalyst development than can be presented here.

To date, no process has been commercialized for the conversion of polyolefin wastes using hydrogen. Current processes still produce a broad distribution of products with yield and selectivity below what is needed for commercialization, and they require significant downstream separations processing. Rates are relatively slow, and some processes have reaction times of 24–72 h. Relatively small changes in operating conditions—such as temperature, pressure, or residence time—often drive the product yield toward unwanted light (C_1–C_4) gases.

The key challenge for the conversion of polymer waste by the hydrocracking and hydrogenolysis processes is that it produces a broad distribution of molecular weights of solid, liquid, and gaseous products that require energy-intensive separations processes to recover.[352] Ideally, upcycling processes should produce one desired product or a well-defined range of products to avoid the energy costs of separations and recovery. Nearly all processes still yield product distributions in the gasoline-to-diesel fuel range. A few processes produce product distributions in the lubricant range, which is a higher-value product than liquid fuel. To date, no process selectively produces one chemical product. New catalysts and chemical processes to increase the selectivity of the reactions are being explored. Catalyst designs should consider incorporating desired functionalization and/or cleavage events with molecular recognition. Introducing reactive functional groups at specific sites in the polymer could provide molecular recognition sites on which catalysts could react.

4.2.3 Ammonia Production

Worldwide production of ammonia was 235 million metric tons in 2019, making it the second-highest produced commodity chemical.[364] About 80% of the NH_3 produced is used in fertilizer production, and the remaining 20% is used in explosives, pharmaceuticals, refrigeration, and other industrial processes.[365] There is a growing interest in using ammonia as a carbon-free fuel for combustion applications or as a hydrogen carrier for fuel cells because of its high volumetric energy density (15.3 MJ/L), high hydrogen content (17.6 wt %), and the existing infrastructure for distribution and storage.[364]

Ammonia is currently produced by the Haber-Bosch process (**Figure 28**).[364-368] The process uses iron-based catalysts that require temperatures of 300–500 °C and pressures of 130–170 bar, or ruthenium-based catalysts that operate at lower pressures (<100 bar).[367] Conversion is low, about 10–15%, despite the harsh reaction conditions. The process is energy intensive, requiring over 30 GJ per metric ton of ammonia produced, and has high greenhouse gas emissions of 2.16 $kgCO_{2\text{-eq}}/kg\ NH_3$ because of the high temperatures and pressures required and the use of natural gas or coal to produce hydrogen.[364] Ammonia production consumes more than 1.4% of the world's energy supply and emits more than 400 million tons of CO_2 annually.[366]

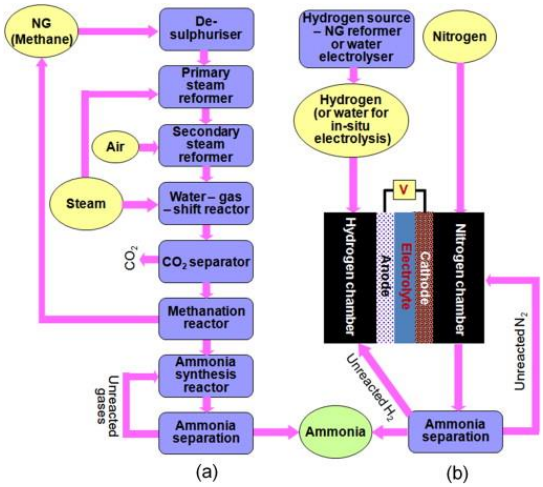

Figure 28. (a) Haber-Bosch process compared with (b) an electrochemical ammonia synthesis process. Source: Ref. [365] Reprinted from *Int. J. Hydrogen Energy* Vol. 38, Giddey, et. al., "Review of Electrochemical Ammonia Production Technologies and Materials," 14576–14594, Copyright 2013, with permission from Elsevier.

Increasing demand for NH_3 is necessitating the development of alternative synthesis processes that are less energy and CO_2 intensive.[364-368] As shown in **Figure 28**, one possible process is the electrochemical reduction of nitrogen by using either hydrogen or water as the source of protons—the latter can be considered a combination of a water and nitrogen electrolyzer.[365] Electrochemical routes could reduce energy consumption by perhaps as much as 20%, simplify reactor design, and reduce overall process complexity and cost. Several excellent reviews that focus on electrochemical NH_3 synthesis processes were recently published.[364-368] Designing catalysts that promote the nitrogen reduction reaction (NRR) while limiting the HER is a main challenge.[364-368] Noble metals (e.g., Ru, Pt, Au, Rh, Pd), transition metals (e.g., Fe, Mo, Co), single-metal-site, bimetallic alloy, transition metal nitride, transition metal carbide, non-noble

metal sulfide/oxide, defect-engineered-oxide and nitride, and defect-rich carbon catalysts have been extensively studied. The HER was the dominant reaction with relatively little NRR activity exhibited by noble metal catalysts in polymer electrolyte membranes or hydroxide-exchange membranes.[369] Production rates of 21.4 $\mu g/h^{-1} \cdot mg^{-1}_{cat}$ were reported by using a gold catalyst.[370] Even if noble metals were able to achieve high catalytic activity, their limited supply and high cost are major concerns.[366] Bimetallic alloy catalysts recently attracted attention based on the potential synergistic effects of combining two metals. A RuPt/C catalyst exhibited an NH_3 formation rate of 3.0×10^{-7} $mol/h^{-1} \cdot cm^{-2}$.[366] Oxide catalysts—including spinel Fe_3O_4 nanorods, MoO_3 nanosheets, Cr_2O_3 microspheres, Mn_3O_4, La_2O_3, V_2O_3-C, and C-doped TiO_2—were reported with NH_3 production rates ranging between 10 and 25 $\mu g/h^{-1} \cdot mg^{-1}_{cat}$.[366]

There is a growing interest in producing "green" ammonia via gas phase catalytic processes. These processes use hydrogen produced by water electrolysis via wind or solar power at a considerably smaller production scale than the Haber-Bosch process, which uses modular process technology.[371] Small-scale ammonia production requires catalyst technology that is more active at lower pressures and temperatures than the current Fe or Ru catalysts to reduce the process energy demand and hence cost. Most experts agree that it would be difficult to develop a new catalyst technology that is more efficient than the current generation of catalysts.[372, 373] However, recently catalysts were discovered that show promise in decoupling the barrier for the initial dissociation of the dinitrogen from the bonding energy of the intermediates, leading to high turnover frequencies at temperatures as low as 150 °C and at lower pressures (<10 atm).[374] Separative reactors are another approach being pursued to lower the pressure by removing ammonia as it is produced to overcome the thermodynamic limitations that require high pressure in the Haber-Bosch process and to eliminate the energy-intensive downstream condensation process for separating ammonia from nitrogen and hydrogen.[375, 376] New membrane or absorbent technologies are required that can be integrated into the synthesis reactor.

4.2.4 Upgrading of Bio-Oils

Fast pyrolysis and hydrothermal liquefaction are two promising processes for converting biomass to a bio-oil that can be subsequently upgraded to produce a renewable liquid transportation fuel. Unfortunately, the bio-oil produced is of poor quality because of the high residual oxygen content (30–50 wt % for pyrolysis oils and 5–20 wt % for hydrothermal liquefaction oils), which contributes to its low thermal stability and high corrosivity. Hydrotreating the bio-oil with hydrogen to reduce the residual oxygen (i.e., hydrodeoxygenation [HDO]) is one method for improving the quality of the bio-oil. Using "green" H_2 in the HDO process results in a bio-oil with a low- to near-zero carbon footprint.

Deep deoxygenation is required to reduce the oxygen content to <1 wt %, which is required for use as a drop-in transportation fuel. Thus, HDO requires a catalyst and is conducted at elevated temperatures that range from 300 to 450 °C and H_2 pressures that range up to 20 MPa. Numerous catalysts reported in the literature include metal oxide and sulfides; noble metals; and metal phosphides, carbides, and nitrides.[377-379] Although catalytic HDO was demonstrated to produce a high-quality bio-oil, there are many challenges, including the high cost and extremely short lifetime of the catalysts, the large amount of H_2 required, and severe reaction conditions.

4.2.5 HySteel

Carbon plays three vital roles in steelmaking by serving as a fuel for heating, a reducing agent, and an alloying agent. Coke is the major carbon source.[380] Globally, steelmaking generates about 1.85 metric tons of CO_2 per metric ton of steel produced.[381] The US steel industry produces about 80–90 million metric tons annually, accounting for ~2% of US energy use and ~4% of US CO_2 emissions.[382] With global demand for steel projected to rise to 2.5 billion metric tons by 2050, it is estimated that annual

emissions from the global steel industry must decrease to about 500 million metric tons by 2050 for the world to meet the goal of the 2015 Paris Climate Agreement.[381]

Using H_2 to reduce iron ore to metallic iron is one option for reducing CO_2 emissions in the steel industry.[383-386] The Baur-Glässner diagram (**Figure 29**) describes the thermodynamics of iron oxide reduction.[384] The diagram displays the stability of different iron oxide phases, depending on the temperature the gas oxidation degree (i.e., the ratio of oxidizable gas components over the sum of oxidized and oxidizable gas components). As indicated by this diagram, reduction using H_2 should be performed at the highest possible temperature as the stability of iron expands with increasing temperature. The kinetics of H_2 reduction depend on several factors, including temperature, pressure, gas composition, grain size, and iron oxide porosity and minerology.

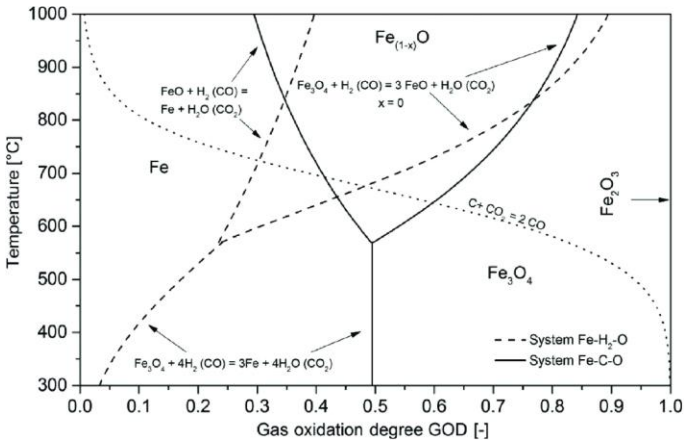

Figure 29. Baur-Glässner diagram for the Fe-O-H_2 and Fe-O-C system. Source: Ref. [384] Reprinted with permission by Wiley Publishing. Spreitzer, et. al., *Steel Res. Int.* Vol 90 (2019). © 2019 The Authors. Published by Wiley – VCH Verlag GmbH & Co. KGaA Weinheim.

The two main processes for producing steel are (1) the blast furnace/basic oxygen furnace (BF/BOF) process, which uses iron ore as a feedstock, and (2) the electric arc furnace (EAF) process, which uses scrap metal and direct reduced iron (DRI) as feedstock (**Figure 30**).[383, 385, 386]

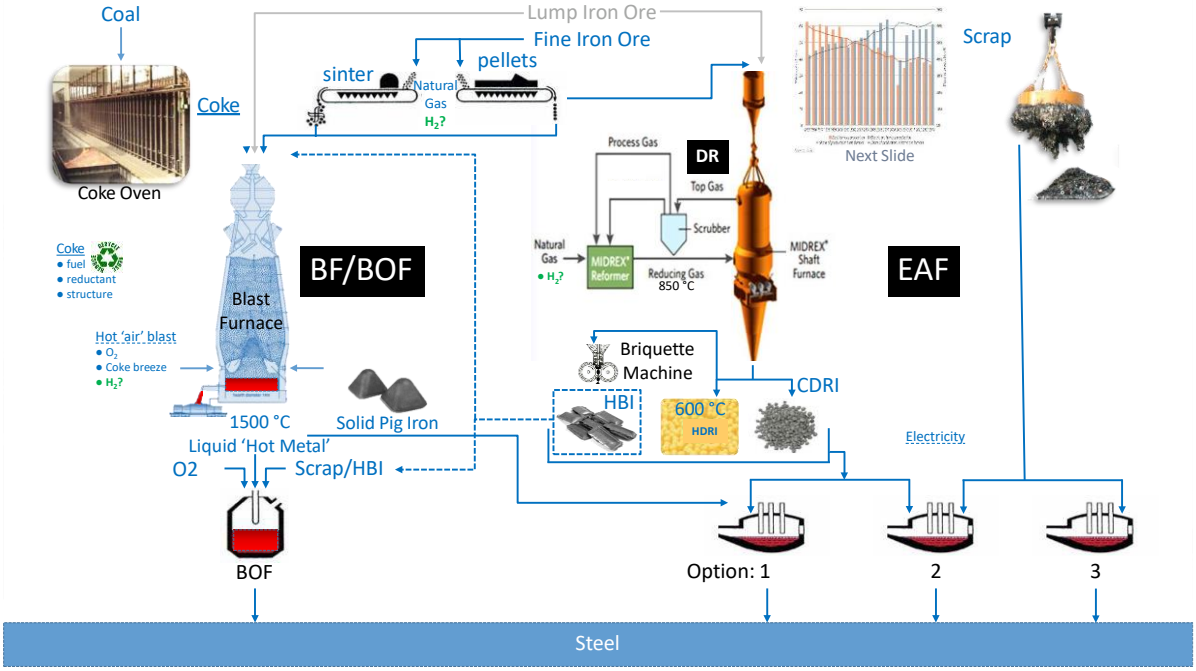

Figure 30. Comparison of the blast furnace (BF)/basic oxygen furnace (BOF) and MIDREX direct reduced iron (DRI) /electric arc furnace (EAF). Source: Ref. [397] Image courtesy of Midrex Technologies, Inc.

Currently, more than 70% of the world's steel is produced by the BF/BOF process, and this process accounts for about 70% of the CO_2 emissions arising from steel production.[384] However, in the United States, over 60% of steel is produced via the EAF process. BF/BOFs cannot operate using only H_2. Coke is still required owing to problems with gas permeability in the cohesive zone of the reactor and gas, slag, and metal drainage in the metallurgical zone. Using H_2 will increase the energy demand compared with the incumbent technology, thus requiring more coke to provide sufficient energy. Injecting synthetic gas mixtures, similar to coke oven gas, that contain H_2 and CO with the CO derived from biomass or waste plastics can reduce the amount of coke required and lead to lower CO_2 emissions.[383] However, this introduces additional problems, such as periphery gas flow within the BF due to rapid combustion, which is detrimental to the wall refractory and lining. Increasing the H_2 content leads to an increase in the water content, which reduces the BF gas calorie content and results in a lower hot-blast temperature. New process concepts are required that can operate only with H_2.[383, 384]

In the DRI/EAF process, the DRI process uses a mixture of H_2 and CO to reduce iron ore to metallic iron.[388] Worldwide, about 100 million tons of steel are produced annually by the DRI process.[389] The higher reactivity of H_2 allows the reduction to occur at a temperature below the melting temperature of iron (1535 °C) so that a molten liquid phase does not develop. DRI offers the advantage of lower capital cost and less complexity in design and operation compared with BFs.[390] The two major DRI processes are the MIDREX and the HYL/Energiron processes;[383, 386] recently, a DRI process that uses 100% H_2 (no CO) was developed called HYBRIT.[391] Pure H_2 reduction reactions have the additional energy demand of preheating the H_2 because these reactions are endothermic.

Recently, there has been interest in using H_2 plasmas to reduce Fe ores.[392-394] The high energy and density of H radicals and excited states help overcome the reaction's activation barrier, and they could realize reduction rates that are one order of magnitude higher than the rates achievable in the BF or DRI processes. An additional benefit is that H_2 plasmas can reduce lump or fine Fe, eliminating the need to pelletize the ore.[394] The high-energy demand of plasma processing and the development of commercial-scale reactor technology are major challenges.

In summary, the key challenges facing the use of H_2 to reduce Fe ores are:

- addressing the increased process energy demand of using H_2 and determining how to effectively introduce energy into the process,
- the impacts of material and gas flows within BF and DRI furnaces—due to the lower density of H_2—on the rate of Fe ore reduction,
- material compatibility issues due to the presence of H_2 at high temperatures, and
- coupling the use of H_2 with biomass and waste plastics as a renewable carbon source for use in existing blast furnaces.

Key challenges for H_2 plasma reduction are the evaluation of heat and mass transfer and kinetics within the plasma to enable reduced energy demand and the development of scalable reactor designs.

4.2.6 Carbon Products

The TCD of methane for hydrogen production is discussed in detail in Section 2.4.1. As discussed previously, the TCD of methane produces solid carbon as a valuable by-product. The morphology of the carbon product is affected by the prevailing decomposition mechanism, which is determined by the

temperature, pressure, catalyst, and residence time (**Figure 31**).[116, 130] A variety of different carbon products can be produced—including carbon black, carbon fibers, CNTs, graphite, graphene, or needle coke—depending on the reactor design and operating parameters. The production of marketable carbon products has been one of the driving forces behind the interest in CH_4 cracking as a means of offsetting the high cost of producing H_2; however, the current markets for carbon are limited compared with the H_2 market.[116, 123] Current markets for carbon products are considerably smaller than the H_2 market. New carbon-based products that target larger markets, such as building materials, must be developed to increase the size of the carbon markets to match the H_2 market.

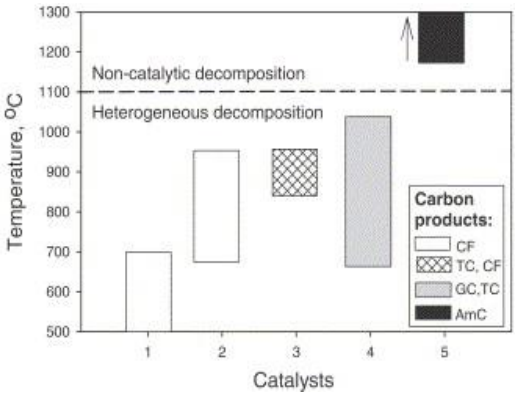

Figure 31. Summary of published data on catalysts, temperature, and carbon products from methane decomposition. Catalysts include (1) Ni based; (2) Fe based; (3) C based; (4) Co, Ni, Pd, Pt, Cr, Ru, Mo, and W catalysts; and (5) noncatalytic decomposition. Carbon products include carbon filaments (CF),turbostratic carbon (TC), graphitic carbon (GC), and amorphous carbon (AmC). Source: Ref. [130]. Reprinted from *Int. J. Hydrogen Energy* Vol. 30, Muradov, et. al., "From Hydrocarbon to Hydrogen-Carbon to Hydrogen Economy," 225–237, Copyright 2005, with permission from Elsevier.

5. Summary

There are numerous sources and processes for producing hydrogen that can broadly be categorized as hydrocarbons or water and catalytic, thermochemical, or electrochemical. Today, the dominant source and process are hydrocarbon and catalytic, making carbon neutrality challenging. Other processes with smaller production volumes and in earlier stages of development—but with greater potential for implementation as carbon-neutral or carbon-free pathways—are electrochemical water splitting and microbial fermentation of biomass. Although WEs are being deployed at increasing rates, most notably in hydrogen fueling stations for FCEVs, they face many fundamental challenges to widescale deployment, primarily in the coupled areas of cost and durability.

Efficient transport and storage of hydrogen is one of the main challenges to a hydrogen-based energy economy. The challenge arises in part from the low volumetric energy density of hydrogen, which necessitates very high pressures or cryogenic temperatures to store sufficient amounts for practical applications. Compressed hydrogen cylinders are the incumbent technology, storing hydrogen at pressures up to 700 bar for light-duty FCEVs, for example. The storage of hydrogen in materials or in chemicals is being pursued to address the issues associated with compression, such as parasitic energy loss and weight, size, and cost of storage containers. The complex nature of the chemical and physical processes involved in the uptake, storage, and release of hydrogen has slowed the discovery of suitable hydrogen storage materials. Both small- and large-scale storage face the challenge of embrittlement of the storage media by hydrogen.

Hydrogen has a myriad of uses that could improve the efficiency of various applications and reduce or eliminate CO_2 emissions. These include the direct electrochemical conversion to electricity, power vehicles and grid-level stationary applications, combustion, and the production of chemicals and commodities. One of the most impactful applications in terms of reducing CO_2 emissions is fuel cell passenger vehicles and heavy-duty vehicles, such as class 8 trucks. Aside from the main issue of the lack

of a hydrogen distribution infrastructure, the challenges facing the widespread deployment of fuel cells are cost and durability. Both issues are primarily related to the fuel cell cathode catalyst. The other uses of hydrogen—including conversion to hydrocarbons, polymer upcycling, and bio-oil upgrading—are at varying stages of maturity and also face fundamental challenges associated with catalytic processes and materials.

6. References

1. N. Stetson, in *U.S. Department of Energy Hydrogen Program 2021 Annual Merit Review and Peer Evaluation Meeting*, Virtual, **2021.** https://www.hydrogen.energy.gov/pdfs/review21/plenary7_stetson_2021_o.pdf
2. U. S. Department of Energy, *Vol. DOE/EE-2128*, **November, 2020.** https://www.hydrogen.energy.gov/pdfs/hydrogen-program-plan-2020.pdf
3. International Energy Agency (IEA), **2019.** https://www.iea.org/publications/reports/thefutureofhydrogen/
4. S. Satyapal, in *U.S. Department of Energy Hydrogen Program 2021 Annual Merit Review and Peer Evaluation Meeting*, Virtual, **2021** https://www.hydrogen.energy.gov/pdfs/review21/plenary5_satyapal_2021_o.pdf
5. S. A. Grigoriev, V. N. Fateev, D. G. Bessarabov, P. Millet, "Current status, research trends, and challenges in water electrolysis science and technology", *International Journal of Hydrogen Energy*, **45**, 26036-26058 (2020). 10.1016/j.ijhydene.2020.03.109
6. A. Villagra, P. Millet, "An analysis of PEM water electrolysis cells operating at elevated current densities", *International Journal of Hydrogen Energy*, **44**, 9708-9717 (2019). 10.1016/j.ijhydene.2018.11.179
7. K. Ayers, N. Danilovic, R. Ouimet, M. Carmo, B. Pivovar, M. Bornstein, "Perspectives on Low-Temperature Electrolysis and Potential for Renewable Hydrogen at Scale", *Annual Review of Chemical and Biomolecular Engineering*, **10**, 219-239 (2019). 10.1146/annurev-chembioeng-060718-030241
8. B. Pivovar, N. Rustagi, S. Satyapal, "Hydrogen at Scale (H2@Scale): Key to a Clean, Economic, and Sustainable Energy System", *The Electrochemical Society Interface* **27**, 47-52 (2018). 10.1149/2.f04181if
9. A. Buttler, H. Spliethoff, "Current status of water electrolysis for energy storage, grid balancing and sector coupling via power-to-gas and power-to-liquids: A review", *Renewable & Sustainable Energy Reviews*, **82**, 2440-2454 (2018). 10.1016/j.rser.2017.09.003
10. Cockerill Jingli Hydrogen, *Vol. 2021* https://www.jinglihydrogen.com
11. Verde LLC, *Vol. 2021* https://www.verdellc.com
12. Sunfire, *Vol. 2021* https://www.sunfire.de/en
13. Nel Hydrogen, *Vol. 2021* https://nelhydrogen.com
14. Cision, *Vol. 2021* https://news.cision.com/nel-asa/r/nel-asa–receivespurchase-order-from-nikola,c3127494
15. Cision 2, *Vol. 2021* https://news.cision.com/nel-asa/r/nel-asa–enters-intoframework-agreement-for-delivery-of-electrolysers-in-france,c3093166
16. Cision 3, *Vol. 2021* https://news.cision.com/nel-asa/r/nel-signs-loi-withstatkraft-for-a-green-hydrogen-project-with-up-to-50mw-of-electrolyser-capacity,c3228323
17. M. Schalenbach, G. Tjarks, M. Carmo, W. Lueke, M. Mueller, D. Stolten, "Acidic or Alkaline? Towards a New Perspective on the Efficiency of Water Electrolysis", *Journal of the Electrochemical Society*, **163**, F3197-F3208 (2016). 10.1149/2.0271611jes
18. M. Lehner, R. Tichler, H. Steinmuller, M. Koppe, in *Power-to-Gas: Technology and Business Models*, Springer Int Publishing Ag, Cham, **2014**, pp. 1-93.
19. R. Abbasi, B. P. Setzler, S. S. Lin, J. H. Wang, Y. Zhao, H. Xu, B. Pivovar, B. Y. Tian, X. Chen, G. Wu, Y. S. Yan, "A Roadmap to Low-Cost Hydrogen with Hydroxide Exchange Membrane Electrolyzers", *Advanced Materials*, **31**, 14 (2019). 10.1002/adma.201805876
20. M. Bodner, A. Hofer, V. Hacker, "H-2 generation from alkaline electrolyzer", *Wiley Interdisciplinary Reviews Energy and Environment*, **4**, 365-381 (2015). 10.1002/wene.150
21. R. L. Leroy, "Industrial Water Electrolysis - Present and Future", *International Journal of Hydrogen Energy*, **8**, 401-417 (1983). 10.1016/0360-3199(83)90162-3

22. P. Vermeiren, W. Adriansens, J. P. Moreels, R. Leysen, "Evaluation of the Zirfon (R) separator for use in alkaline water electrolysis and Ni-H-2 batteries", *International Journal of Hydrogen Energy*, **23**, 321-324 (1998). 10.1016/s0360-3199(97)00069-4
23. R. J. Gilliam, J. W. Graydon, D. W. Kirk, S. J. Thorpe, "A review of specific conductivities of potassium hydroxide solutions for various concentrations and temperatures", *International Journal of Hydrogen Energy*, **32**, 359-364 (2007). 10.1016/j.ijhydene.2006.10.062
24. J. W. Xiao, A. M. Oliveira, L. Wang, Y. Zhao, T. Wang, J. H. Wang, B. P. Setzler, Y. S. Yan, "Water-Fed Hydroxide Exchange Membrane Electrolyzer Enabled by a Fluoride-Incorporated Nickel-Iron Oxyhydroxide Oxygen Evolution Electrode", *ACS Catalysis*, **11**, 264-270 (2021). 10.1021/acscatal.0c04200
25. J. Divisek, R. Jung, D. Britz, "Potential Distribution and Elecrode Stability in Bipolar Electrolysis Cell", *Journal of Applied Electrochemistry*, **20**, 186-195 (1990). 10.1007/bf01033594
26. M. S. Naughton, F. R. Brushett, P. J. A. Kenis, "Carbonate resilience of flowing electrolyte-based alkaline fuel cells", *Journal of Power Sources*, **196**, 1762-1768 (2011). 10.1016/j.jpowsour.2010.09.114
27. E. Gulzow, "Alkaline fuel cells: A critical view", *Journal of Power Sources*, **61**, 99-104 (1996). 10.1016/s0378-7753(96)02344-0
28. E. Gulzow, M. Schulze, "Long-term operation of AFC electrodes with CO_2 containing gases", *Journal of Power Sources*, **127**, 243-251 (2004). 10.1016/j.jpowsour.2003.09.020
29. D. G. Li, E. J. Park, W. L. Zhu, Q. R. Shi, Y. Zhou, H. Y. Tian, Y. H. Lin, A. Serov, B. Zulevi, E. D. Baca, C. Fujimoto, H. T. Chung, Y. S. Kim, "Highly quaternized polystyrene ionomers for high performance anion exchange membrane water electrolysers", *Nature Energy*, **5**, 378-385 (2020). 10.1038/s41560-020-0577-x
30. Enapter, *Vol. 2021* https://www.enapter.com/electrolyser
31. J. J. Kaczur, H. Z. Yang, Z. C. Liu, S. A. Sajjad, R. I. Masel, "Carbon Dioxide and Water Electrolysis Using New Alkaline Stable Anion Membranes", *Frontiers in Chemistry*, **6**, 16 (2018). 10.3389/fchem.2018.00263
32. J. T. Fan, S. Willdorf-Cohen, E. M. Schibli, Z. Paula, W. Li, T. J. G. Skalski, A. T. Sergeenko, A. Hohenadel, B. J. Frisken, E. Magliocca, W. E. Mustain, C. E. Diesendruck, D. R. Dekel, S. Holdcroft, "Poly(bis-arylimidazoliums) possessing high hydroxide ion exchange capacity and high alkaline stability", *Nature Communications*, **10**, 10 (2019). 10.1038/s41467-019-10292-z
33. Y. J. Leng, G. Chen, A. J. Mendoza, T. B. Tighe, M. A. Hickner, C. Y. Wang, "Solid-State Water Electrolysis with an Alkaline Membrane", *Journal of the American Chemical Society*, **134**, 9054-9057 (2012). 10.1021/ja302439z
34. T. Pandiarajan, L. J. Berchmans, S. Ravichandran, "Fabrication of spinel ferrite based alkaline anion exchange membrane water electrolysers for hydrogen production", *Rsc Adv*, **5**, 34100-34108 (2015). 10.1039/c5ra01123j
35. J. Parrondo, C. G. Arges, M. Niedzwiecki, E. B. Anderson, K. E. Ayers, V. Ramani, "Degradation of anion exchange membranes used for hydrogen production by ultrapure water electrolysis", *RSC Advances*, **4**, 9875-9879 (2014). 10.1039/c3ra46630b
36. L. Bi, S. Boulfrad, E. Traversa, "Steam electrolysis by solid oxide electrolysis cells (SOECs) with proton-conducting oxides", *Chemical Society Reviews*, **43**, 8255-8270 (2014). 10.1039/c4cs00194j
37. L. B. Lei, J. H. Zhang, Z. H. Yuan, J. P. Liu, M. Ni, F. L. Chen, "Progress Report on Proton Conducting Solid Oxide Electrolysis Cells", *Advanced Functional Materials*, **29**, 17 (2019). 10.1002/adfm.201903805
38. D. Medvedev, "Trends in research and development of protonic ceramic electrolysis cells", *International Journal of Hydrogen Energy*, **44**, 26711-26740 (2019). 10.1016/j.ijhydene.2019.08.130
39. A. Pandiyan, A. Uthayakumar, R. Subrayan, S. W. Cha, S. B. Krishna Moorthy, "Review of solid oxide electrolysis cells: a clean energy strategy for hydrogen generation", *Nanomaterial Energy*, **8**, 2-22 (2019).

40. S. Satyapal, National Renewable Energy Laboratory, **2018**
41. S. D. Ebbesen, S. H. Jensen, A. Hauch, M. B. Mogensen, "High Temperature Electrolysis in Alkaline Cells, Solid Proton Conducting Cells, and Solid Oxide Cells", *Chemical Reviews*, **114**, 10697-10734 (2014). 10.1021/cr5000865
42. P. Singh, N. Q. Minh, "Solid oxide fuel cells: Technology status", *International Journal of Applied Ceramic Technology*, **1**, 5-15 (2004). 10.1111/j.1744-7402.2004.tb00149.x
43. M. Sohal, Idaho National Laboratory, **2009** https://inldigitallibrary.inl.gov/sites/sti/sti/4247164.pdf
44. P. Mocoteguy, A. Brisse, "A review and comprehensive analysis of degradation mechanisms of solid oxide electrolysis cells", *International Journal of Hydrogen Energy*, **38**, 15887-15902 (2013). 10.1016/j.ijhydene.2013.09.045
45. Y. Wang, W. Y. Li, L. Ma, W. Li, X. B. Liu, "Degradation of solid oxide electrolysis cells: Phenomena, mechanisms, and emerging mitigation strategies-A review", *Journal of Materials Science & Technology*, **55**, 35-55 (2020). 10.1016/j.jmst.2019.07.026
46. M. S.K., "Oxidation Behavior of FeCr Steels Interconnect in Low pO2 Environments of Solid Oxide Electrolysis Cells", *Materials Science* (2016).
47. M. Choi, S. J. Kim, W. Lee, "Effects of water atmosphere on chemical degradation of PrBa0.5Sr0.5Co1.5Fe0.5O5+delta electrodes", *Ceramics International*, **47**, 7790-7797 (2021). 10.1016/j.ceramint.2020.11.124
48. A. Hauch, S. H. Jensen, J. B. Bilde-Sorensen, M. Mogensen, "Silica segregation in the Ni/YSZ electrode", *Journal of the Electrochemical Society*, **154**, A619-A626 (2007). 10.1149/1.2733861
49. A. Aphale, M. Reisert, J. Hong, S. J. Heo, B. Hu, P. Singh, in *49th International Conference on Environmental Systems*, **2019**
50. M. P. Hoerlein, M. Riegraf, R. Costa, G. Schiller, K. A. Friedrich, "A parameter study of solid oxide electrolysis cell degradation: Microstructural changes of the fuel electrode", *Electrochimica Acta*, **276**, 162-175 (2018). 10.1016/j.electacta.2018.04.170
51. S. N. Rashkeev, M. V. Glazoff, "Atomic-scale mechanisms of oxygen electrode delamination in solid oxide electrolyzer cells", *International Journal of Hydrogen Energy*, **37**, 1280-1291 (2012). 10.1016/j.ijhydene.2011.09.117
52. M. Reisert, A. Aphale, P. Singh, "Solid Oxide Electrochemical Systems: Material Degradation Processes and Novel Mitigation Approaches", *Materials*, **11**, 16 (2018). 10.3390/ma11112169
53. M. Palcut, L. Mikkelsen, K. Neufeld, M. Chen, R. Knibbe, P. V. Hendriksen, "Corrosion stability of ferritic stainless steels for solid oxide electrolyser cell interconnects", *Corrosion Science*, **52**, 3309-3320 (2010). 10.1016/j.corsci.2010.06.006
54. M. G. Walter, E. L. Warren, J. R. McKone, S. W. Boettcher, Q. X. Mi, E. A. Santori, N. S. Lewis, "Solar Water Splitting Cells", *Chemical Reviews*, **110**, 6646-6473 (2010). 10.1021/cr1002326
55. W. H. Cheng, M. H. Richter, M. M. May, J. Ohlmann, D. Lackner, F. Dimroth, T. Hannappel, H. A. Atwater, H. J. Lewerenz, "Monolithic Photoelectrochemical Device for Direct Water Splitting with 19% Efficiency", *ACS Energy Letters*, **3**, 1795-1800 (2018). 10.1021/acsenergylett.8b00920
56. K. Sivula, R. van de Krol, "Semiconducting materials for photoelectrochemical energy conversion", *Nature Reviews Materials*, **1**, 16 (2016). 10.1038/natrevmats.2015.10
57. L. Zhou, A. Shinde, D. Guevarra, M. H. Richter, H. S. Stein, Y. Wang, P. F. Newhouse, K. A. Persson, J. M. Gregoire, "Combinatorial screening yields discovery of 29 metal oxide photoanodes for solar fuel generation", *Journal of Materials Chemistry A*, **8**, 4239-4243 (2020). 10.1039/C9TA13829C
58. L. Zhou, A. Shinde, S. K. Suram, H. S. Stein, S. R. Bauers, A. Zakutayev, J. S. DuChene, G. Liu, E. A. Peterson, J. B. Neaton, J. M. Gregoire, "Bi-Containing n-$FeWO_4$ Thin Films Provide the Largest Photovoltage and Highest Stability for a Sub-2 eV Band Gap Photoanode", *ACS Energy Letters*, **3**, 2769-2774 (2018). 10.1021/acsenergylett.8b01514
59. Gurudayal, J. W. Beeman, J. Bullock, H. Wang, J. Eichhorn, C. Towle, A. Javey, F. M. Toma, N. Mathews, J. W. Ager, "Si photocathode with Ag-supported dendritic Cu catalyst for CO2 reduction", *Energy & Environmental Science*, **12**, 1068-1077 (2019). 10.1039/c8ee03547d

60. S. Hu, N. S. Lewis, J. W. Ager, J. Yang, J. R. McKone, N. C. Strandwitz, "Thin-Film Materials for the Protection of Semiconducting Photoelectrodes in Solar-Fuel Generators", *The Journal of Physical Chemistry C*, **119**, 24201-24228 (2015). 10.1021/acs.jpcc.5b05976
61. A. G. Scheuermann, P. C. McIntyre, "Atomic Layer Deposited Corrosion Protection: A Path to Stable and Efficient Photoelectrochemical Cells", *Journal of Physical Chemistry Letters*, **7**, 2867-2878 (2016). 10.1021/acs.jpclett.6b00631
62. L. Chen, J. Yang, S. Klaus, L. J. Lee, R. Woods-Robinson, J. Ma, Y. Lum, J. K. Cooper, F. M. Toma, L.-W. Wang, I. D. Sharp, A. T. Bell, J. W. Ager, "p-Type Transparent Conducting Oxide/n-Type Semiconductor Heterojunctions for Efficient and Stable Solar Water Oxidation", *Journal of the American Chemical Society*, **137**, 9595-9603 (2015). 10.1021/jacs.5b03536
63. B. Mei, A. A. Permyakova, R. Frydendal, D. Bae, T. Pedersen, P. Malacrida, O. Hansen, I. E. L. Stephens, P. C. K. Vesborg, B. Seger, I. Chorkendorff, "Iron-Treated NiO as a Highly Transparent p-Type Protection Layer for Efficient Si-Based Photoanodes", *Journal of Physical Chemistry Letters*, **5**, 3456-3461 (2014). 10.1021/jz501872k
64. F. M. Toma, J. K. Cooper, V. Kunzelmann, M. T. McDowell, J. Yu, D. M. Larson, N. J. Borys, C. Abelyan, J. W. Beeman, K. M. Yu, J. H. Yang, L. Chen, M. R. Shaner, J. Spurgeon, F. A. Houle, K. A. Persson, I. D. Sharp, "Mechanistic insights into chemical and photochemical transformations of bismuth vanadate photoanodes", *Nature Communications*, **7**, 11 (2016). 10.1038/ncomms12012
65. H. Gerischer, "On the stability of semiconductor electrodes against photodecomposition", *Journal of Electroanalytical Chemistry and Interfacial Electrochemistry*, **82**, 133-143 (1977). 10.1016/S0022-0728(77)80253-2
66. S. Chen, L.-W. Wang, "Thermodynamic Oxidation and Reduction Potentials of Photocatalytic Semiconductors in Aqueous Solution", *Chemistry of Materials*, **24**, 3659-3666 (2012). 10.1021/cm302533s
67. M. Gratzel, "Artificial Photosynthesis - Water Cleavage into Hydrogen and Oxygen by Visible-Light", *Accounts of Chemical Research*, **14**, 376-384 (1981). 10.1021/ar00072a003
68. A. J. Bard, M. A. Fox, "Artificial Photosynthesis - Solar Splitting of Water to Hydrogen and Oxygen", *Accounts of Chemical Research*, **28**, 141-145 (1995). 10.1021/ar00051a007
69. J. A. Turner, "Sustainable hydrogen production", *Science*, **305**, 972-974 (2004). 10.1126/science.1103197
70. N. S. Lewis, D. G. Nocera, "Powering the planet: Chemical challenges in solar energy utilization", *Proceedings of the National Academy of Sciences, U. S. A.*, **103**, 15729-15735 (2006). 10.1073/pnas.0603395103
71. N. S. Lewis, "Toward cost-effective solar energy use", *Science*, **315**, 798-801 (2007). 10.1126/science.1137014
72. G. W. Crabtree, M. S. Dresselhaus, "The hydrogen fuel alternative", *MRS Bulletin*, **33**, 421-428 (2008). 10.1557/mrs2008.84
73. H. B. Gray, "Powering the planet with solar fuel", *Nature Chemistry*, **1**, 7-7 (2009). 10.1038/nchem.141
74. T. R. Cook, D. K. Dogutan, S. Y. Reece, Y. Surendranath, T. S. Teets, D. G. Nocera, "Solar Energy Supply and Storage for the Legacy and Non legacy Worlds", *Chemical Reviews*, **110**, 6474-6502 (2010). 10.1021/cr100246c
75. M. F. Weber, M. J. Dignam, "Efficiency of Splitting Water with Semiconducting Photoelectrodes", *Journal of the Electrochemical Society*, **131**, 1258-1265 (1984). 10.1149/1.2115797
76. Y. Gorlin, T. F. Jaramillo, "A Bifunctional Nonprecious Metal Catalyst for Oxygen Reduction and Water Oxidation", *Journal of the American Chemical Society*, **132**, 13612-13614 (2010). 10.1021/ja104587v
77. C. C. L. McCrory, S. Jung, I. M. Ferrer, S. M. Chatman, J. C. Peters, T. F. Jaramillo, "Benchmarking Hydrogen Evolving Reaction and Oxygen Evolving Reaction Electrocatalysts for Solar Water Splitting Devices", *Journal of the American Chemical Society*, **137**, 4347-4357 (2015). 10.1021/ja510442p

78. C. C. L. McCrory, S. H. Jung, J. C. Peters, T. F. Jaramillo, "Benchmarking Heterogeneous Electrocatalysts for the Oxygen Evolution Reaction", *Journal of the American Chemical Society*, **135**, 16977-16987 (2013). 10.1021/ja407115p
79. L. Zhou, A. Shinde, J. H. Montoya, A. Singh, S. Gul, J. Yano, Y. F. Ye, E. J. Crumlin, M. H. Richter, J. K. Cooper, H. S. Stein, J. A. Haber, K. A. Persson, J. M. Gregoire, "Rutile Alloys in the Mn-Sb-O System Stabilize Mn^{3+} To Enable Oxygen Evolution in Strong Acid", *ACS Catalysis*, **8**, 10938-10948 (2018). 10.1021/acscatal.8b02689
80. P. T. Sekoai, K. O. Yoro, M. O. Bodunrin, A. O. Ayeni, M. O. Daramola, "Integrated system approach to dark fermentative biohydrogen production for enhanced yield, energy efficiency and substrate recovery", *Reviews in Environmental Science and Bio-Technology*, **17**, 501-529 (2018). 10.1007/s11157-018-9474-1
81. H. S. Lee, W. F. J. Vermaas, B. E. Rittmann, "Biological hydrogen production: prospects and challenges", *Trends in Biotechnology*, **28**, 262-271 (2010). 10.1016/j.tibtech.2010.01.007
82. B. James, D. Desantis, J. Moton, " H2A: Hydrogen Production Cost from Fermentation", DOE Hydrogen and Fuel Cells Program Record, **2017.**
83. L. R. Lynd, P. J. Weimer, W. H. van Zyl, I. S. Pretorius, "Microbial cellulose utilization: Fundamentals and biotechnology (vol 66, pg 506, 2002)", *Microbiology and Molecular Biology Reviews*, **66**, 506-577 (2002). 10.1128/MMBR.66.3.506–577.2002
84. W. Xiong, L. H. Reyes, W. E. Michener, P. C. Maness, K. J. Chou, "Engineering cellulolytic bacterium Clostridium thermocellum to co-ferment cellulose- and hemicellulose-derived sugars simultaneously", *Biotechnology and Bioengineering*, **115**, 1755-1763 (2018). 10.1002/bit.26590
85. R. K. Thauer, K. Jungermann, K. Decker, "Energy-Conservation in Chemotropic Anaerobic Bacteria", *Bacteriological Reviews*, **41**, 100-180 (1977). 10.1128/mmbr.41.1.100-180.1977
86. E. Lalaurette, S. Thammannagowda, A. Mohagheghi, P. C. Maness, B. E. Logan, "Hydrogen production from cellulose in a two-stage process combining fermentation and electrohydrogenesis", *International Journal of Hydrogen Energy*, **34**, 6201-6210 (2009). 10.1016/j.ijhydene.2009.05.112
87. J. W. Peters, G. J. Schut, E. S. Boyd, D. W. Mulder, E. M. Shepard, J. B. Broderick, P. W. King, M. W. W. Adams, "FeFe - and NiFe -hydrogenase diversity, mechanism, and maturation", *Biochimica Et Biophysica Acta-Molecular Cell Research*, **1853**, 1350-1369 (2015). 10.1016/j.bbamcr.2014.11.021
88. G. J. Schut, M. W. W. Adams, "The Iron-Hydrogenase of Thermotoga maritima Utilizes Ferredoxin and NADH Synergistically: a New Perspective on Anaerobic Hydrogen Production", *Journal of Bacteriology*, **191**, 4451-4457 (2009). 10.1128/jb.01582-08
89. W. Lubitz, H. Ogata, O. Rudiger, E. Reijerse, "Hydrogenases", *Chemical Reviews*, **114**, 4081-4148 (2014). 10.1021/cr4005814
90. W. Buckel, R. K. Thauer, "Energy conservation via electron bifurcating ferredoxin reduction and proton/Na+ translocating ferredoxin oxidation", *Biochimica Et Biophysica Acta-Bioenergetics*, **1827**, 94-113 (2013). 10.1016/j.bbabio.2012.07.002
91. C. A. Schoeneberger, C. A. McMillan, P. Kurup, S. Akar, R. Margolis, E. Masanet, "Solar for industrial process heat: A review of technologies, analysis approaches, and potential applications in the United States", *Energy*, **206**, 18 (2020). 10.1016/j.energy.2020.118083
92. M. Dresselhaus, G. Crabtree, M. Buchanan, T. Mallouk, L. Mets, K. Taylor, P. Jena, F. DiSalvo, T. Zawodzinski, H. Kung, in *Report from the U.S. Department of Energy, Office of Basic Energy Sciences Workshop*, US DOE Office of Science (SC)(United States), Argonne National Laboratory, Lemont, Illinois, **2003**, pp. 16-18, 26-29.
93. C. A. Koval, J. Lercher, S. L. Scott, G. W. Coates, E. Iglesia, R. M. Bullock, T. F. Jaramillo, M. Flytzani-Stephanopoulos, D. Resasco, C. L. Tway, in *Report from the U.S. Department of Energy, Office of Basic Energy Sciences Workshop*, US DOE Office of Science (SC)(United States), Gaithersburg, Maryland, **2017**, pp. 47-50.

94. S. Abanades, P. Charvin, G. Flamant, P. Neveu, "Screening of water-splitting thermochemical cycles potentially attractive for hydrogen production by concentrated solar energy", *Energy*, **31**, 2805-2822 (2006). 10.1016/j.energy.2005.11.002
95. C. Agrafiotis, M. Roeb, C. Sattler, "A review on solar thermal syngas production via redox pair-based water/carbon dioxide splitting thermochemical cycles", *Renewable & Sustainable Energy Reviews*, **42**, 254-285 (2015). 10.1016/j.rser.2014.09.039
96. L. C. Brown, G. Besenbruch, K. Schultz, S. Showalter, A. Marshall, P. Pickard, J. Funk, American Institute of Chemical Engineers, Report No. GA–A24326, **2002.**
97. A. Steinfeld, "Solar thermochemical production of hydrogen - a review", *Solar Energy*, **78**, 603-615 (2005). 10.1016/j.solener.2003.12.012
98. D. Guban, I. K. Muritala, M. Roeb, C. Sattler, "Assessment of sustainable high temperature hydrogen production technologies", *International Journal of Hydrogen Energy*, **45**, 26156-26165 (2020). 10.1016/j.ijhydene.2019.08.145
99. S. Docao, A. R. Koirala, M. G. Kim, I. C. Hwang, M. K. Song, K. B. Yoon, "Solar photochemical–thermal water splitting at 140 °C with Cu-loaded TiO_2", *Energy & Environmental Science*, **10**, 628-640 (2017). 10.1039/C6EE02974D
100. F. Safari, I. Dincer, "A review and comparative evaluation of thermochemical water splitting cycles for hydrogen production", *Energy Conversion and Management*, **205**, 17 (2020). 10.1016/j.enconman.2019.112182
101. M. Luo, Y. Yi, S. Wang, Z. Wang, M. Du, J. Pan, Q. Wang, "Review of hydrogen production using chemical-looping technology", *Renewable and Sustainable Energy Reviews*, **81**, 3186-3214 (2018). 10.1016/j.rser.2017.07.007
102. A. H. McDaniel, "Renewable energy carriers derived from concentrating solar power and nonstoichiometric oxides", *Current Opinion in Greeen and Sustainable Chemistry*, **4**, 37-43 (2017). 10.1016/j.cogsc.2017.02.004
103. M. Kubicek, A. H. Bork, J. L. M. Rupp, "Perovskite oxides - a review on a versatile material class for solar-to-fuel conversion processes", *Journal of Materials Chemistry A*, **5**, 11983-12000 (2017). 10.1039/c7ta00987a
104. A. A. Emery, J. E. Saal, S. Kirklin, V. I. Hegde, C. Wolverton, "High-Throughput Computational Screening of Perovskites for Thermochemical Water Splitting Applications", *Chemistry of Materials*, **28**, 5621-5634 (2016). 10.1021/acs.chemmater.6b01182
105. S. S. Naghavi, J. G. He, C. Wolverton, "CeTi2O6-A Promising Oxide for Solar Thermochemical Hydrogen Production", *ACS Applied Materials & Interfaces*, **12**, 21521-21527 (2020). 10.1021/acsami.0c01083
106. A. M. Deml, A. M. Holder, R. P. O'Hayre, C. B. Musgrave, V. Stevanović, "Intrinsic material properties dictating oxygen vacancy formation energetics in metal oxides", *The Journal of Physical Chemistry Letters*, **6**, 1948-1953 (2015). 10.1021/acs.jpclett.5b00710
107. G. Sai Gautam, E. B. Stechel, E. A. Carter, "Exploring Ca–Ce–M–O (M = 3d Transition Metal) Oxide Perovskites for Solar Thermochemical Applications", *Chemistry of Materials*, **32**, 9964-9982 (2020). 10.1021/acs.chemmater.0c02912
108. C. J. Bartel, C. Sutton, B. R. Goldsmith, R. Ouyang, C. B. Musgrave, L. M. Ghiringhelli, M. Scheffler, "New tolerance factor to predict the stability of perovskite oxides and halides", *Science Advances*, **5**, eaav0693 (2019).
109. N. R. Singstock, C. J. Bartel, A. M. Holder, C. B. Musgrave, "High-Throughput Analysis of Materials for Chemical Looping Processes", *Advanced Energy Materials*, **10**, 2000685 (2020). https://doi.org/10.1002/aenm.202000685
110. S. Zhai, J. Rojas, N. Ahlborg, K. Lim, M. F. Toney, H. Jin, W. C. Chueh, A. Majumdar, "The use of poly-cation oxides to lower the temperature of two-step thermochemical water splitting", *Energy & Environmental Science* (2018). 10.1039/C8EE00050F

111. A. H. McDaniel in U.S. Department of Energy Hydrogen Program 2021 Annual Merit Review and Peer Evaluation Meeting, Virtual, 2021. https://www.hydrogen.energy.gov/pdfs/review21/p148d_mcdaniel_2021_p.pdf, **2021.**
112. B. Parkinson, P. Balcombe, J. F. Speirs, A. D. Hawkes, K. Hellgardt, "Levelized cost of CO2 mitigation from hydrogen production routes", *Energy & Environmental Science*, **12**, 19-40 (2019). 10.1039/c8ee02079e
113. Y. K. Salkuyeh, B. A. Saville, H. L. MacLean, "Techno-economic analysis and life cycle assessment of hydrogen production from natural gas using current and emerging technologies", *International Journal of Hydrogen Energy*, **42**, 18894-18909 (2017). 10.1016/j.ijhydene.2017.05.219
114. M. G. Sobacchi, A. V. Saveliev, A. A. Fridman, L. A. Kennedy, S. Ahmed, T. Krause, "Experimental assessment of a combined plasma/catalytic system for hydrogen production via partial oxidation of hydrocarbon fuels", *International Journal of Hydrogen Energy*, **27**, 635-642 (2002). 10.1016/s0360-3199(01)00179-3
115. I. W. Wang, R. A. Dagle, T. S. Khan, J. A. Lopez-Ruiz, L. Kovarik, Y. Jiang, M. Z. Xu, Y. Wang, C. L. Jiang, S. D. Davidson, P. Tavadze, L. L. Li, J. L. Hu, "Catalytic decomposition of methane into hydrogen and high-value carbons: combined experimental and DFT computational study", *Catalysis Science & Technology*, **11**, 4911-4921 (2021). 10.1039/d1cy00287b
116. R. Dagle, V. Dagle, M. Bearden, J. Holladay, T. Krause, S. Ahmed, **2017.** https://www.osti.gov/servlets/purl/141193
117. J. B. Pohlenz, N. H. Scott, (Ed.: U. S. P. Office), United States, **1966.**
118. D. A. Kutteri, I. W. Wang, A. Samanta, L. L. Li, J. L. Hu, "Methane decomposition to tip and base grown carbon nanotubes and COx-free H-2 over mono- and bimetallic 3d transition metal catalysts", *Catalysis Science & Technology*, **8**, 858-869 (2018). 10.1039/c7cy01927k
119. L. B. Avdeeva, O. V. Goncharova, D. I. Kochubey, V. I. Zaikovskii, L. M. Plyasova, B. N. Novgorodov, S. K. Shaikhutdinov, "Coprecipitated Ni-alumina and Ni-Cu-alumina catalysts of methane decomposition and carbon deposition .2. Evolution of the catalysts in reaction", *Applied Catalysis A-General*, **141**, 117-129 (1996). 10.1016/0926-860x(96)00026-9
120. I. W. Wang, D. A. Kutteri, B. Y. Gao, H. J. Tian, J. L. Hu, "Methane Pyrolysis for Carbon Nanotubes and CO_x-Free H_2 over Transition-Metal Catalysts", *Energy & Fuels*, **33**, 197-205 (2019). 10.1021/acs.energyfuels.8b03502
121. M. Z. Xu, J. A. Lopez-Ruiz, L. Kovarik, M. E. Bowden, S. D. Davidson, R. S. Weber, I. W. Wang, J. L. Hu, R. A. Dagle, "Structure sensitivity and its effect on methane turnover and carbon co-product selectivity in thermocatalytic decomposition of methane over supported Ni catalysts", *Applied Catalysis A-General*, **611**, 117967-117976 (2021). 10.1016/j.apcata.2020.117967
122. A. F. S. Muhammad, A. Awad, R. Saidur, N. Masiran, A. Salam, B. Abdullah, "Recent advances in cleaner hydrogen productions via thermo-catalytic decomposition of methane: Admixture with hydrocarbon", *International Journal of Hydrogen Energy*, **43**, 18713-18734 (2018). 10.1016/j.ijhydene.2018.08.091
123. M. Msheik, S. Rodat, S. Abanades, "Methane Cracking for Hydrogen Production: A Review of Catalytic and Molten Media Pyrolysis", *Energies*, **14**, 3107-3141 (2021). 10.3390/en14113107
124. A. Holmen, O. Olsvik, O. A. Rokstad, "Pyrolysis of Natural Gas - Chemistry and Process Concepts", *Fuel Processing Technology*, **42**, 249-267 (1995). 10.1016/0378-3820(94)00109-7
125. H. F. Abbas, W. Daud, "Hydrogen production by methane decomposition: A review", *International Journal of Hydrogen Energy*, **35**, 1160-1190 (2010). 10.1016/j.ijhydene.2009.11.036
126. A. M. Amin, E. Croiset, W. Epling, "Review of methane catalytic cracking for hydrogen production", *International Journal of Hydrogen Energy*, **36**, 2904-2935 (2011). 10.1016/j.ijhydene.2010.11.035
127. A. Abanades, E. Ruiz, E. M. Ferruelo, F. Hernandez, A. Cabanillas, J. M. Martinez-Val, J. A. Rubio, C. Lopez, R. Gavela, G. Barrera, C. Rubbia, D. Salmieri, E. Rodilla, D. Gutierrez, "Experimental analysis of direct thermal methane cracking", *International Journal of Hydrogen Energy*, **36**, 12877-12886 (2011). 10.1016/j.ijhydene.2011.07.081

128. M. C. Alvarez-Galvan, N. Mota, M. Ojeda, S. Rojas, R. M. Navarro, J. L. G. Fierro, "Direct methane conversion routes to chemicals and fuels", *Catalysis Today*, **171**, 15-23 (2011). 10.1016/j.cattod.2011.02.028
129. N. Z. Muradov, T. N. Veziroglu, ""Green" path from fossil-based to hydrogen economy: An overview of carbon-neutral technologies", *International Journal of Hydrogen Energy*, **33**, 6804-6839 (2008). 10.1016/j.ijhydene.2008.08.054
130. N. Z. Muradov, T. N. Veziroglu, "From hydrocarbon to hydrogen-carbon to hydrogen economy", *International Journal of Hydrogen Energy*, **30**, 225-237 (2005). 10.1016/j.ijhydene.2004.03.033
131. L. Alves, V. Pereira, T. Lagarteira, A. Mendes, "Catalytic methane decomposition to boost the energy transition: Scientific and technological advancements", *Renewable & Sustainable Energy Reviews*, **137**, 20 (2021). 10.1016/j.rser.2020.110465
132. Z. Y. Fan, W. Weng, J. Zhou, D. Gu, W. Xiao, "Catalytic decomposition of methane to produce hydrogen: A review", *Journal of Energy Chemistry*, **58**, 415-430 (2021). 10.1016/j.jechem.2020.10.049
133. S. Schneider, S. Bajohr, F. Graf, T. Kolb, "State of the Art of Hydrogen Production via Pyrolysis of Natural Gas", *ChemBioEng Review*, **7**, 150-158 (2020). 10.1002/cben.202000014
134. U. P. M. Ashik, W. Daud, H. F. Abbas, "Production of greenhouse gas free hydrogen by thermocatalytic decomposition of methane - A review", *Renewable & Sustainable Energy Reviews*, **44**, 221-256 (2015). 10.1016/j.rser.2014.12.025
135. Y. Li, B. C. Zhang, X. W. Xie, J. L. Liu, Y. D. Xu, W. J. Shen, "Novel Ni catalysts for methane decomposition to hydrogen and carbon nanofibers", *Journal of Catalysis*, **238**, 412-424 (2006). 10.1016/j.jcat.2005.12.027
136. M. Pudukudy, Z. Yaakob, Z. S. Akmal, "Direct decomposition of methane over Pd promoted Ni/SBA-15 catalysts", *Applied Surface Science*, **353**, 127-136 (2015). 10.1016/j.apsusc.2015.06.073
137. Y. Shen, A. C. Lua, "Synthesis of Ni and Ni-Cu supported on carbon nanotubes for hydrogen and carbon production by catalytic decomposition of methane", *Applied Catalysis B-Environmental*, **164**, 61-69 (2015). 10.1016/j.apcatb.2014.08.038
138. I. Suelves, J. L. Pinilla, M. J. Lazaro, R. Moliner, J. M. Palacios, "Effects of reaction conditions on hydrogen production and carbon nanofiber properties generated by methane decomposition in a fixed bed reactor using a NiCuAl catalyst", *Journal of Power Sources*, **192**, 35-42 (2009). 10.1016/j.jpowsour.2008.11.096
139. Y. Echegoyen, I. Suelves, M. J. Lazaro, M. L. Sanjuan, R. Moliner, "Thermo catalytic decomposition of methane over Ni-Mg and Ni-Cu-Mg catalysts - Effect of catalyst preparation method", *Applied Catalysis A-General*, **333**, 229-237 (2007). 10.1016/j.apcata.2007.09.012
140. L. Zhou, L. R. Enakonda, M. Harb, Y. Saih, A. Aguilar-Tapia, S. Ould-Chikh, J. L. Hazemann, J. Li, N. Wei, D. Gary, P. Del-Gallo, J. M. Basset, "Fe catalysts for methane decomposition to produce hydrogen and carbon nano materials", *Applied Catalysis B-Environmental*, **208**, 44-59 (2017). 10.1016/j.apcatb.2017.02.052
141. Q. Q. Chen, A. C. Lua, "Kinetic reaction and deactivation studies on thermocatalytic decomposition of methane by electroless nickel plating catalyst", *Chemical Engineerign Journal*, **389**, 124366-124374 (2020). 10.1016/j.cej.2020.124366
142. S. Helveg, C. Lopez-Cartes, J. Sehested, P. L. Hansen, B. S. Clausen, J. R. Rostrup-Nielsen, F. Abild-Pedersen, J. K. Norskov, "Atomic-scale imaging of carbon nanofibre growth", *Nature*, **427**, 426-429 (2004). 10.1038/nature02278
143. E. J. G. Santos, J. K. Norskov, A. R. Harutyunyan, F. Abild-Pedersen, "Toward Controlled Growth of Helicity-Specific Carbon Nanotubes", *Journal of Physical Chemistry Letters*, **6**, 2232-2237 (2015). 10.1021/acs.jpclett.5b00880
144. S. Hofmann, G. Csanyi, A. C. Ferrari, M. C. Payne, J. Robertson, "Surface diffusion: The low activation energy path for nanotube growth", *Physical Review Letters*, **95**, 036101-036104 (2005). 10.1103/PhysRevLett.95.036101

145. M. A. Salam, B. Abdullah, "Catalysis mechanism of Pd-promoted gamma-alumina in the thermal decomposition of methane to hydrogen: A density functional theory study", *Mater. Chem. Phys.*, **188**, 18-23 (2017). 10.1016/j.matchemphys.2016.12.022
146. J. Hu in *U.S. Department of Energy 2021 Hydrogen Program Annual Merit Review (AMR)*,Virtual, **2021.** https://www.hydrogen.energy.gov/pdfs/review21/fe006_hu_2021_o.pdf
147. N. Shah, S. K. Ma, Y. G. Wang, G. P. Huffman, "Semi-continuous hydrogen production from catalytic methane decomposition using a fluidized-bed reactor", *International Journal of Hydrogen Energy*, **32**, 3315-3319 (2007). 10.1016/j.ijhydene.2007.04.040
148. H. Hu, B. Zhao, M. E. Itkis, R. C. Haddon, "Nitric acid purification of single-walled carbon nanotubes", *J. Phys. Chem. B*, **107**, 13838-13842 (2003). 10.1021/jp035719i
149. M. Gautier, V. Rohani, L. Fulcheri, "Direct decarbonization of methane by thermal plasma for the production of hydrogen and high value-added carbon black", *International Journal of Hydrogen Energy*, **42**, 28140-28156 (2017). 10.1016/j.ijhydene.2017.09.021
150. M. Deminsky, V. Jivotov, B. Potapkin, V. Rusanov, "Plasma-assisted production of hydrogen from hydrocarbons", *Pure Appl. Chem.*, **74**, 413-418 (2002). 10.1351/pac200274030413
151. B. W. Longmier, A. D. Gallimore, N. Hershkowitz, "Hydrogen production from methane using an RF plasma source in total nonambipolar flow", *Plasma Sources Sci. Technol.*, **21**, 8 (2012). 10.1088/0963-0252/21/1/015007
152. V. A. Vinokurov, R. G. Sharafutdinov, Y. I. Tychkov, "Plasma-chemical processing of natural gas", *Chem. Tech. Fuels Oils*, **41**, 112-115 (2005). 10.1007/s10553-005-0032-5
153. K. S. Kim, J. H. Seo, J. S. Nam, W. T. Ju, S. H. Hong, "Production of hydrogen and carbon black by methane decomposition using DC-RF hybrid thermal plasmas", *IEEE Trans. Plasma Sci.*, **33**, 813-823 (2005). 10.1109/tps.2005.844526
154. Z. Y. Fan, W. Xiao, "Electrochemical Splitting of Methane in Molten Salts To Produce Hydrogen", *Angewandte Chemie-International Edition*, **60**, 7664-7668 (2021). 10.1002/anie.202017243
155. J. R. Zeng, M. Tarazkar, T. Pennebaker, M. J. Gordon, H. Metiu, E. W. McFarland, "Catalytic Methane Pyrolysis with Liquid and Vapor Phase Tellurium", *Acs Catalysis*, **10**, 8223-8230 (2020). 10.1021/acscatal.0c00805
156. T. A. Milne, C. C. Elam, R. J. Evans, *Vol. IEA/H2/TR-02/001* (Ed.: U. S. D. o. E. Report), **2002** https://www.nrel.gov/docs/legosti/old/36262.pdf
157. W. Liu, C. M. Liu, P. Gogoi, Y. L. Deng, "Overview of Biomass Conversion to Electricity and Hydrogen and Recent Developments in Low-Temperature Electrochemical Approaches", *Engineering*, **6**, 1351-1363 (2020). 10.1016/j.eng.2020.02.021
158. P. Nikolaidis, A. Poullikkas, "A comparative overview of hydrogen production processes", *Renewable & Sustainable Energy Reviews*, **67**, 597-611 (2017). 10.1016/j.rser.2016.09.044
159. Y. K. Salkuyeh, B. A. Saville, H. L. MacLean, "Techno-economic analysis and life cycle assessment of hydrogen production from different biomass gasification processes", *International Journal of Hydrogen Energy*, **43**, 9514-9528 (2018). 10.1016/j.ijhydene.2018.04.024
160. M. Imizcoz, A. V. Puga, "Assessment of Photocatalytic Hydrogen Production from Biomass or Wastewaters Depending on the Metal Co-Catalyst and Its Deposition Method on TiO2", *Catalysts*, **9**, 16 (2019). 10.3390/catal9070584
161. J. L. Wang, Y. A. Yin, "Fermentative hydrogen production using various biomass-based materials as feedstock", *Renewable & Sustainable Energy Reviews*, **92**, 284-306 (2018). 10.1016/j.rser.2018.04.033
162. Y. A. Situmorang, Z. K. Zhao, P. An, T. Yu, J. Rizkiana, A. Abudula, G. Q. Guan, "A novel system of biomass-based hydrogen production by combining steam bio-oil reforming and chemical looping process", *Applied Energy*, **268**, 115122-115131 (2020). 10.1016/j.apenergy.2020.115122
163. A. Lalsare, Y. X. Wang, Q. Y. Li, A. Sivri, R. J. Vukmanovich, C. E. Dumitrescu, J. L. Hu, "Hydrogen-Rich Syngas Production through Synergistic Methane-Activated Catalytic Biomass Gasification", *ACS Sustainable Chemistry & Engineering*, **7**, 16060-16071 (2019). 10.1021/acssuschemeng.9b02663

164. A. Lalsare, A. Sivri, R. Egan, R. J. Vukmanovich, C. E. Dumitrescu, J. L. Hu, "Biomass - Flare gas synergistic co-processing in the presence of carbon dioxide for the controlled production of syngas (H-2:CO similar to 2-2.5)", *Chemical Engineering Journal*, **385**, 123783-123794 (2020). 10.1016/j.cej.2019.123783
165. A. D. Lalsare, T. S. Khan, B. Leonard, R. Vukmanovich, P. Tavazohi, L. L. Li, J. L. Hu, "Graphene-Supported Fe/Ni, beta-Mo2C Nanoparticles: Experimental and DFT Integrated Approach to Catalyst Development for Synergistic Hydrogen Production through Lignin-Rich Biomass Reforming and Reduced Shale Gas Flaring", *ACS Catalysis*, **11**, 364-382 (2021). 10.1021/acscatal.0c04242
166. A. D. Lalsare, B. Leonard, B. Robinson, A. C. Sivri, R. Vukmanovich, C. Dumitrescu, W. Rogers, J. L. Hu, "Self-regenerable carbon nanofiber supported Fe - Mo2C catalyst for CH4-CO2 assisted reforming of biomass to hydrogen rich syngas", *Applied Catalysis B: Environmental*, **282**, 119537-119549 (2021). 10.1016/j.apcatb.2020.119537
167. U.S. Department of Energy, Energy Efficiency and Renewable Energy, Hydrogen and Fuel Cell Technologies Office, **2021.** https://www.energy.gov/eere/fuelcells/hydrogen-storage
168. J. W. Choi, D. Aurbach, "Promise and reality of post-lithium-ion batteries with high energy densities", *Nature Reviews Materials*, **1,** 16013-16028 (2016). 10.1038/natrevmats.2016.13
169. gM. N. Guzik, R. Mohtadi, S. Sartori, "Lightweight complex metal hydrides for Li-, Na-, and Mg-based batteries", *Journal of Materials Research*, **34**, 877-904 (2019). 10.1557/jmr.2019.82
170. R. Mohtadi, S. I. Orimo, "The renaissance of hydrides as energy materials", *Nature Reviews Materials*, **2** 16091-16105 (2017). 10.1038/natrevmats.2016.91
171. P. T. Aaldto-Saksa, C. Cook, J. Kiviaho, T. Repo, "Liquid organic hydrogen carriers for transportation and storing of renewable energy - Review and discussion", *Journal of Power Sources*, **396**, 803-823 (2018). 10.1016/j.jpowsour.2018.04.011
172. P. M. Modisha, C. N. M. Ouma, R. Garidzirai, P. Wasserscheid, D. Bessarabov, "The Prospect of Hydrogen Storage Using Liquid Organic Hydrogen Carriers", *Energy Fuels*, **33**, 2778-2796 (2019). 10.1021/acs.energyfuels.9b00296
173. P. Preuster, C. Papp, P. Wasserscheid, "Liquid Organic Hydrogen Carriers (LOHCs): Toward a Hydrogen -free Hydrogen Economy", *Accounts of Chemical Research*, **50**, 74-85 (2017). 10.1021/acs.accounts.6b00474
174. Y. Sekine, T. Higo, "Recent Trends on the Dehydrogenation Catalysis of Liquid Organic Hydrogen Carrier (LOHC): A Review", *Topics in Catalysis*, **64**, 470-480 (2021). 10.1007/s11244-021-01452-x
175. F. B. Juangsa, A. R. Irhamna, M. Aziz, "Production of ammonia as potential hydrogen carrier: Review on thermochemical and electrochemical processes", *International Journal of Hydrogen Energy*, **46**, 14455-14477 (2021). 10.1016/j.ijhydene.2021.01.214
176. A. Valera-Medina, H. Xiao, M. Owen-Jones, W. I. F. David, P. J. Bowen, "Ammonia for power", *Progress in Energy and Combustion Science*, **69**, 63-102 (2018). 10.1016/j.pecs.2018.07.001
177. A. Bahuguna, Y. Sasson, "Formate-Bicarbonate Cycle as a Vehicle for Hydrogen and Energy Storage", *ChemSusChem*, **14**, 1258-1283 (2021). https://doi.org/10.1002/cssc.202002433
178. M. V. Lototskyy, V. A. Yartys, B. G. Pollet, R. C. Bowman, "Metal hydride hydrogen compressors: A review", *International Journal of Hydrogen Energy*, **39**, 5818-5851 (2014). 10.1016/j.ijhydene.2014.01.158
179. G. Sdanghi, G. Maranzana, A. Celzard, V. Fierro, "Review of the current technologies and performances of hydrogen compression for stationary and automotive applications", *Renewable & Sustainable Energy Reviews*, **102**, 150-170 (2019). 10.1016/j.rser.2018.11.028
180. P. Modi, K. F. Aguey-Zinsou, "Room Temperature Metal Hydrides for Stationary and Heat Storage Applications: A Review", *Frontiers in Energy Research*, **9,** 616115-616139 (2021). 10.3389/fenrg.2021.616115
181. A. Anastasopoulou, H. Furukawa, B. R. Barnett, H. Z. H. Jiang, J. R. Long, H. M. Breunig, "Technoeconomic analysis of metal-organic frameworks for bulk hydrogen transportation", *Energy & Environmental Science*, **14**, 1083-1094 (2021). 10.1039/d0ee02448a

182. L. Z. Ouyang, K. Chen, J. Jiang, X. S. Yang, M. Zhu, "Hydrogen storage in light-metal based systems: A review", *Journal of Alloys and Compounds*, **829,** 154597-154634 (2020). 10.1016/j.jallcom.2020.154597
183. M. V. Lototskyy, I. Tolj, M. W. Davids, Y. V. Klochko, A. Parsons, D. Swanepoel, R. Ehlers, G. Louw, B. van der Westhuizen, F. Smith, B. G. Pollet, C. Sita, V. Linkov, "Metal hydride hydrogen storage and supply systems for electric forklift with low-temperature proton exchange membrane fuel cell power module", *Interntational Journal of Hydrogen Energy*, **41**, 13831-13842 (2016). 10.1016/j.ijhydene.2016.01.148
184. M. V. Lototskyy, I. Tolj, A. Parsons, F. Smith, C. Sita, V. Linkov, "Performance of electric forklift with low-temperature polymer exchange membrane fuel cell power module and metal hydride hydrogen storage extension tank", *Journal of Power Sources*, **316**, 239-250 (2016). 10.1016/j.jpowsour.2016.03.058
185. G. Capurso, B. Schiavo, J. Jepsen, G. A. Lozano, O. Metz, T. Klassen, M. Dornheim, "Metal Hydride-Based Hydrogen Storage Tank Coupled with an Urban Concept Fuel Cell Vehicle: Off Board Tests", *Advanced Sustainable Systems*, **2,** 1800004-18000014 (2018). 10.1002/adsu.201800004
186. S. McWhorter, C. Read, G. Ordaz, N. Stetson, "Materials-based hydrogen storage: Attributes for near-term, early market PEM fuel cells", *Current Opinions in Solid State Materials Science*, **15**, 29-38 (2011). 10.1016/j.cossms.2011.02.001
187. N. A. A. Rusman, M. Dahari, "A review on the current progress of metal hydrides material for solid-state hydrogen storage applications", *International Journal of Hydrogen Energy*, **41**, 12108-12126 (2016). 10.1016/j.ijhydene.2016.05.244
188. J. Yang, A. Sudik, C. Wolverton, D. J. Siegel, "High capacity hydrogen storage materials: attributes for automotive applications and techniques for materials discovery", *Chemical Society Reviews*, **39**, 656-675 (2010). 10.1039/b802882f
189. *HyMARC*, **2021.** https://www.hymarc.org/
190. U.S. Department of Energy, Energy Efficiency and Renewable Energy, Fuel Cell Technologies Office, **2012.** https://www.energy.gov/eere/fuelcells/doe-technical-targets-onboard-hydrogen-storage-light-duty-vehicles
191. A. Ahmed, S. Seth, J. Purewal, A. G. Wong-Foy, M. Veenstra, A. J. Matzger, D. J. Siegel, "Exceptional hydrogen storage achieved by screening nearly half a million metal-organic frameworks", *Nature Communications*, **10,** 1568-1576 (2019). 10.1038/s41467-019-09365-w
192. K. Paragian, B. Li, M. Massino, S. Rangarajan, "A computational workflow to discover novel liquid organic hydrogen carriers and their dehydrogenation routes", *Molecular Systems Design & Engineering*, **5**, 1658-1670 (2020). 10.1039/D0ME00105H
193. M. Witman, G. Ek, S. Ling, J. Chames, S. Agarwal, J. Wong, M. D. Allendorf, M. Sahlberg, V. Stavila, "Data-Driven Discovery and Synthesis of High Entropy Alloy Hydrides with Targeted Thermodynamic Stability", *Chemistry of Materials*, **33**, 4067-4076 (2021). 10.1021/acs.chemmater.1c00647
194. M. Witman, S. L. Ling, D. M. Grant, G. S. Walker, S. Agarwal, V. Stavila, M. D. Allendorf, "Extracting an Empirical Intermetallic Hydride Design Principle from Limited Data via Interpretable Machine Learning", *Journal of Physical Chemistry Letters*, **11**, 40-47 (2020). 10.1021/acs.jpclett.9b02971
195. S. S. Samantaray, S. T. Putnam, N. P. Stadie, "Volumetrics of Hydrogen Storage by Physical Adsorption", *Inorganics*, **9**, 45-69 (2021). 10.3390/inorganics9060045
196. A. Ahmed, Y. Liu, J. Purewal, L. D. Tran, A. G. Wong-Foy, M. Veenstra, A. J. Matzger, D. J. Siegel, "Balancing gravimetric and volumetric hydrogen density in MOFs", *Energy & Environmental Science*, **10**, 2459-2471 (2017). 10.1039/C7EE02477K
197. M. D. Allendorf, Z. Hulvey, T. Gennett, A. Ahmed, T. Autrey, J. Camp, E. Seon Cho, H. Furukawa, M. Haranczyk, M. Head-Gordon, S. Jeong, A. Karkamkar, D.-J. Liu, J. R. Long, K. R. Meihaus, I. H. Nayyar, R. Nazarov, D. J. Siegel, V. Stavila, J. J. Urban, S. P. Veccham, B. C. Wood, "An

assessment of strategies for the development of solid-state adsorbents for vehicular hydrogen storage", *Energy & Environmental Science*, **11**, 2784-2812 (2018). 10.1039/C8EE01085D
198. O. K. Farha, A. O. Yazaydin, I. Eryazici, C. D. Malliakas, B. G. Hauser, M. G. Kanatzidis, S. T. Nguyen, R. Q. Snurr, J. T. Hupp, "De novo synthesis of a metal-organic framework material featuring ultrahigh surface area and gas storage capacities", *Nature Chemistry*, **2**, 944-948 (2010). 10.1038/nchem.834
199. H. Furukawa, N. Ko, Y. B. Go, N. Aratani, S. B. Choi, E. Choi, A. Ö. Yazaydin, R. Q. Snurr, M. O'Keeffe, J. Kim, O. M. Yaghi, "Ultrahigh Porosity in Metal-Organic Frameworks", *Science*, **329**, 424-428 (2010). 10.1126/science.1192160
200. J. A. Mason, M. Veenstra, J. R. Long, "Evaluating metal-organic frameworks for natural gas storage", *Chemical Science*, **5**, 32-51 (2014). 10.1039/c3sc52633j
201. Z. J. Chen, P. H. Li, R. Anderson, X. J. Wang, X. Zhang, L. Robison, L. R. Redfern, S. Moribe, T. Islamoglu, D. A. Gomez-Gualdron, T. Yildirim, J. F. Stoddart, O. K. Farha, "Balancing volumetric and gravimetric uptake in highly porous materials for clean energy", *Science*, **368**, 297-303 (2020). 10.1126/science.aaz8881
202. M. Witman, S. L. Ling, V. Stavila, P. Wijeratne, H. Furukawa, M. D. Allendorf, "Design principles for the ultimate gas deliverable capacity material: nonporous to porous deformations without volume change", *Molecular Systems Design & Engineering*, **5**, 1491-1503 (2020). 10.1039/d0me00122h
203. J. L. C. Rowsell, O. M. Yaghi, "Effects of functionalization, catenation, and variation of the metal oxide and organic linking units on the low-pressure hydrogen adsorption properties of metal-organic frameworks", *Journal of the American Chemical Society*, **128**, 1304-1315 (2006). 10.1021/ja056639q
204. T. K. Prasad, M. P. Suh, "Control of Interpenetration and Gas-Sorption Properties of Metal-Organic Frameworks by a Simple Change in Ligand Design", *Chemistry - A European Journal*, **18**, 8673-8680 (2012). 10.1002/chem.201200456
205. D. A. Gomez-Gualdron, T. C. Wang, P. Garcia-Holley, R. M. Sawelewa, E. Argueta, R. Q. Snurr, J. T. Hupp, T. Yildirim, O. K. Farha, "Understanding Volumetric and Gravimetric Hydrogen Adsorption Trade-off in Metal-Organic Frameworks", *ACS Applied Materials & Interfaces*, **9**, 33419-33428 (2017). 10.1021/acsami.7b01190
206. T. Ben, H. Ren, S. Q. Ma, D. P. Cao, J. H. Lan, X. F. Jing, W. C. Wang, J. Xu, F. Deng, J. M. Simmons, S. L. Qiu, G. S. Zhu, "Targeted Synthesis of a Porous Aromatic Framework with High Stability and Exceptionally High Surface Area", *Angewandte Chemie International. Edition*, **48**, 9457-9460 (2009). 10.1002/anie.200904637
207. S. Rochat, K. Polak-Krasna, M. Tian, L. T. Holyfield, T. J. Mays, C. R. Bowen, A. D. Burrows, "Hydrogen storage in polymer-based processable microporous composites", *Journal of Materials Chemistry A*, **5**, 18752-18761 (2017). 10.1039/c7ta05232d
208. National Institute of Standards and Technology (NIST), **2021.** https://webbook.nist.gov/chemistry/
209. M. T. Kapelewski, T. Runcevski, J. D. Tarver, H. Z. H. Jiang, K. E. Hurst, P. A. Parilla, A. Ayala, T. Gennett, S. A. FitzGerald, C. M. Brown, J. R. Long, "Record High Hydrogen Storage Capacity in the Metal-Organic Framework Ni-2(m-dobdc) at Near-Ambient Temperatures", *Chemistry of Materials*, **30**, 8179-8189 (2018). 10.1021/acs.chemmater.8b03276
210. D. E. Jaramillo, H. Z. H. Jiang, H. A. Evans, R. Chakraborty, H. Furukawa, C. M. Brown, M. Head-Gordon, J. R. Long, "Ambient-Temperature Hydrogen Storage via Vanadium(II)-Dihydrogen Complexation in a Metal-Organic Framework", *Journal of the American Chemical Society*, **143**, 6248-6256 (2021). 10.1021/jacs.1c01883
211. H. Furukawa, O. M. Yaghi, "Storage of Hydrogen, Methane, and Carbon Dioxide in Highly Porous Covalent Organic Frameworks for Clean Energy Applications", *Journal of the American Chemical Society*, **131**, 8875-8883 (2009). 10.1021/ja9015765
212. J. H. Lan, D. P. Cao, W. C. Wang, T. Ben, G. S. Zhu, "High-Capacity Hydrogen Storage in Porous Aromatic Frameworks with Diamond-like Structure", *Journal of Physical Chemistry Letters*, **1**, 978-981 (2010). 10.1021/jz900475b

213. M. M. Tong, W. C. Zhu, J. Li, Z. Y. Long, S. Zhao, G. J. Chen, Y. S. Lan, "An easy way to identify high performing covalent organic frameworks for hydrogen storage", *Chemical Communications*, **56**, 6376-6379 (2020). 10.1039/d0cc01494j
214. X. J. Wu, R. Wang, H. J. Yang, W. X. Wang, W. Q. Cai, Q. Z. Li, "Ultrahigh hydrogen storage capacity of novel porous aromatic frameworks", *Journal of Materials Chemistry A*, **3**, 10724-10729 (2015). 10.1039/c5ta01290b
215. S. K. Bhatia, A. L. Myers, "Optimum conditions for adsorptive storage", *Langmuir*, **22**, 1688-1700 (2006). 10.1021/la0523816
216. M. T. Kapelewski, S. J. Geier, M. R. Hudson, D. Stück, J. A. Mason, J. N. Nelson, D. J. Xiao, Z. Hulvey, E. Gilmour, S. A. FitzGerald, M. Head-Gordon, C. M. Brown, J. R. Long, "M_2(m-dobdc) (M = Mg, Mn, Fe, Co, Ni) Metal–Organic Frameworks Exhibiting Increased Charge Density and Enhanced H_2 Binding at the Open Metal Sites", *Journal of the American Chemical Society*, **136**, 12119-12129 (2014). 10.1021/ja506230r
217. T. Runcevski, M. T. Kapelewski, R. M. Torres-Gavosto, J. D. Tarver, C. M. Brown, J. R. Long, "Adsorption of two gas molecules at a single metal site in a metal-organic framework", *Chemical Communications*, **52**, 8251-8254 (2016). 10.1039/c6cc02494g
218. M. Blanco-Rey, J. I. Juaristi, M. Alducin, M. J. López, J. A. Alonso, "Is Spillover Relevant for Hydrogen Adsorption and Storage in Porous Carbons Doped with Palladium Nanoparticles?", *Journal of Physical Chemistry C*, **120**, 17357-17364 (2016). 10.1021/acs.jpcc.6b04006
219. R. Prins, "Hydrogen Spillover. Facts and Fiction", *Chemical Reviews*, **112**, 2714-2738 (2012). 10.1021/cr200346z
220. A. Iakunkov, A. Klechikov, J. H. Sun, T. Steenhaut, S. Hermans, Y. Filinchuk, A. Talyzin, "Gravimetric tank method to evaluate material-enhanced hydrogen storage by physisorbing materials", *Physical Chemistry Chemical Physics*, **20**, 27983-27991 (2018). 10.1039/c8cp05241g
221. M. Wieliczko, N. Stetson, "Hydrogen technologies for energy storage: A perspective", *MRS Energy & Sustainability*, **7**, 41 (2020). 10.1557/mre.2020.43
222. S. I. Orimo, Y. Nakamori, J. R. Eliseo, A. Zuttel, C. M. Jensen, "Complex hydrides for hydrogen storage", *Chemical Reviews*, **107**, 4111-4132 (2007). 10.1021/cr0501846
223. M. S. Choudhari, V. K. Sharma, M. Paswan, "Metal hydrides for thermochemical energy storage applications", *International Journal of Energy Research*, **45**, 14465-14492 (2021). 10.1002/er.6818
224. A. Schneemann, J. L. White, S. Kang, S. Jeong, L. W. F. Wan, E. S. Cho, T. W. Heo, D. Prendergast, J. J. Urban, B. C. Wood, M. D. Allendorf, V. Stavila, "Nanostructured Metal Hydrides for Hydrogen Storage", *Chemical Reviews*, **118**, 10775-10839 (2018). 10.1021/acs.chemrev.8b00313
225. B. C. Wood, T. W. Heo, S. Kang, L. F. Wan, S. Li, "Beyond Idealized Models of Nanoscale Metal Hydrides for Hydrogen Storage", *Industrial & Engineering Chemistry Research*, **59**, 5786-5796 (2020). 10.1021/acs.iecr.9b06617
226. M. Sahlberg, D. Karlsson, C. Zlotea, U. Jansson, "Superior hydrogen storage in high entropy alloys", *Science Reports*, **6**, 36770-36775 (2016). 10.1038/srep36770
227. Y. Cho, S. Li, J. L. Snider, M. A. T. Marple, N. A. Strange, J. D. Sugar, F. El Gabaly, A. Schneemann, S. Kang, M.-H. Kang, H. Park, J. Park, L. F. Wan, H. E. Mason, M. D. Allendorf, B. C. Wood, E. S. Cho, V. Stavila, "Reversing the Irreversible: Thermodynamic Stabilization of $LiAlH_4$ Nanoconfined Within a Nitrogen-Doped Carbon Host", *ACS Nano*, **15**, 10163-10174 (2021). 10.1021/acsnano.1c02079
228. E. S. Cho, A. M. Ruminski, Y. S. Liu, P. T. Shea, S. Y. Kang, E. W. Zaia, J. Y. Park, Y. D. Chuang, J. M. Yuk, X. W. Zhou, T. W. Heo, J. H. Guo, B. C. Wood, J. J. Urban, "Hierarchically Controlled Inside-Out Doping of Mg Nanocomposites for Moderate Temperature Hydrogen Storage", *Advanced Functional Materials*, **27,** 1704316-1704326 (2017). 10.1002/adfm.201704316
229. Nature Research, **2021.** https://www.nature.com/articles/d42473-020-00542-w

230. F. Alhumaidan, D. Cresswell, A. Garforth, "Hydrogen Storage in Liquid Organic Hydride: Producing Hydrogen Catalytically from Methylcyclohexane", *Energy Fuels*, **25**, 4217-4234 (2011). 10.1021/ef200829x
231. H. Jorschick, P. Preuster, S. Dürr, A. Seidel, K. Müller, A. Bösmann, P. Wasserscheid, "Hydrogen storage using a hot pressure swing reactor", *Energy & Environmental Science*, **10**, 1652-1659 (2017). 10.1039/C7EE00476A
232. M. Niermann, A. Beckendorff, M. Kaltschmitt, K. Bonhoff, "Liquid Organic Hydrogen Carrier (LOHC) – Assessment based on chemical and economic properties", *International Journal of Hydrogen Energy*, **44**, 6631-6654 (2019). https://doi.org/10.1016/j.ijhydene.2019.01.199
233. P. T. Aakko-Saksa, C. Cook, J. Kiviaho, T. Repo, "Liquid organic hydrogen carriers for transportation and storing of renewable energy – Review and discussion", *Journal of Power Sources*, **396**, 803-823 (2018). https://doi.org/10.1016/j.jpowsour.2018.04.011
234. E. Gianotti, M. Taillades-Jacquin, J. Rozière, D. J. Jones, "High-Purity Hydrogen Generation via Dehydrogenation of Organic Carriers: A Review on the Catalytic Process", *ACS Catalysis*, **8**, 4660-4680 (2018). 10.1021/acscatal.7b04278
235. C. W. Hamilton, R. T. Baker, A. Staubitz, I. Manners, "B–N compounds for chemical hydrogen storage", *Chemical Society Reviews*, **38**, 279-293 (2009). 10.1039/B800312M
236. R. Kumar, A. Karkamkar, M. Bowden, T. Autrey, "Solid-state hydrogen rich boron–nitrogen compounds for energy storage", *Chemical Society Reviews*, **48**, 5350-5380 (2019). 10.1039/C9CS00442D
237. G. Severa, E. Rönnebro, C. M. Jensen, "Direct hydrogenation of magnesium boride to magnesium borohydride: demonstration of >11 weight percent reversible hydrogen storage", *Chemical Communications*, **46**, 421-423 (2010). 10.1039/B921205A
238. I. Saldan, "Decomposition and formation of magnesium borohydride", *International Journal of Hydrogen Energy*, **41**, 11201-11224 (2016). https://doi.org/10.1016/j.ijhydene.2016.05.062
239. A. Rossin, M. Peruzzini, "Ammonia–Borane and Amine–Borane Dehydrogenation Mediated by Complex Metal Hydrides", *Chemical Reviews*, **116**, 8848-8872 (2016). 10.1021/acs.chemrev.6b00043
240. P. Wang, F. Chang, W. Gao, J. Guo, G. Wu, T. He, P. Chen, "Breaking scaling relations to achieve low-temperature ammonia synthesis through LiH-mediated nitrogen transfer and hydrogenation", *Nature Chemistry*, **9**, 64-70 (2017). 10.1038/nchem.2595
241. J. W. Makepeace, T. He, C. Weidenthaler, T. R. Jensen, F. Chang, T. Vegge, P. Ngene, Y. Kojima, P. E. de Jongh, P. Chen, W. I. F. David, "Reversible ammonia-based and liquid organic hydrogen carriers for high-density hydrogen storage: Recent progress", *International Journal of Hydrogen Energy*, **44**, 7746-7767 (2019). https://doi.org/10.1016/j.ijhydene.2019.01.144
242. Q. Wang, J. Guo, P. Chen, "Recent progress towards mild-condition ammonia synthesis", *Journal of Energy Chemistry*, **36**, 25-36 (2019). https://doi.org/10.1016/j.jechem.2019.01.027
243. R. H. Crabtree, "Nitrogen-Containing Liquid Organic Hydrogen Carriers: Progress and Prospects", *ACS Sustainable Chemistry & Engineering*, **5**, 4491-4498 (2017). 10.1021/acssuschemeng.7b00983
244. R. Izquierdo, N. Cubillan, M. Guerra, M. Rosales, "Substituted heterocycles as new candidates for liquid organic hydrogen carriers: In silico design from DFT calculations", *International Journal of Hydrogen Energy*, **46**, 17853-17870 (2021). https://doi.org/10.1016/j.ijhydene.2021.02.201
245. M. H. Matus, S.-Y. Liu, D. A. Dixon, "Dehydrogenation Reactions of Cyclic $C_2B_2N_2H_{12}$ and C_4BNH_{12} Isomers", *Journal of Physical Chemistry A*, **114**, 2644-2654 (2010). 10.1021/jp9102838
246. J. Kothandaraman, S. Kar, A. Goeppert, R. Sen, G. K. S. Prakash, "Advances in Homogeneous Catalysis for Low Temperature Methanol Reforming in the Context of the Methanol Economy", *Topics in Catalysis*, **61**, 542-559 (2018). 10.1007/s11244-018-0963-9
247. Z. Li, Q. Xu, "Metal-Nanoparticle-Catalyzed Hydrogen Generation from Formic Acid", *Accounts of Chemical Research*, **50**, 1449-1458 (2017). 10.1021/acs.accounts.7b00132

248. L. Fan, C. Xia, P. Zhu, Y. Lu, H. Wang, "Electrochemical CO_2 reduction to high-concentration pure formic acid solutions in an all-solid-state reactor", *Nature Communications*, **11**, 3633-3641 (2020). 10.1038/s41467-020-17403-1
249. M. Ramdin, A. R. T. Morrison, M. de Groen, R. van Haperen, R. de Kler, E. Irtem, A. T. Laitinen, L. J. P. van den Broeke, T. Breugelmans, J. P. M. Trusler, W. d. Jong, T. J. H. Vlugt, "High-Pressure Electrochemical Reduction of CO2 to Formic Acid/Formate: Effect of pH on the Downstream Separation Process and Economics", *Industrial & Engineering Chemistry Reserach*, **58**, 22718-22740 (2019). 10.1021/acs.iecr.9b03970
250. O. Barrera, D. Bombac, Y. Chen, T. Daff, E. Galindo-Nava, P. Gong, D. Haley, R. Horton, I. Katzarov, J. Kermode, C. Liverani, M. Stopher, F. Sweeney, "Understanding and mitigating hydrogen embrittlement of steels: a review of experimental, modelling and design progress from atomistic to continuum (vol 53, pg 6251, 2018)", *Journal of Materials Research*, **53**, 10593-10594 (2018). 10.1007/s10853-018-2291-7
251. S. K. Dwivedi, M. Vishwakarma, "Hydrogen embrittlement in different materials: A review", *International Journal of Hydrogen Energy*, **43**, 21603-21616 (2018). 10.1016/j.ijhydene.2018.09.201
252. L. Y. Lan, X. W. Kong, C. L. Qiu, L. X. Du, "A Review of Recent Advance on Hydrogen Embrittlement Phenomenon Based on Multiscale Mechanical Experiments", *Acta Metallurgica Sinica*, **57**, 845-859 (2021). 10.11900/0412.1961.2020.00378
253. J. X. Li, W. Wang, Y. Zhou, S. G. Liu, H. Fu, Z. Wang, B. Kan, "A Review of Research Status of Hydrogen Embrittlement for Automotive Advanced High-Strength Steels", *Acta Metallurgical Sinica*, **56**, 444-458 (2020). 10.11900/0412.1961.2019.00427
254. X. F. Li, X. F. Ma, J. Zhang, E. Akiyama, Y. F. Wang, X. L. Song, "Review of Hydrogen Embrittlement in Metals: Hydrogen Diffusion, Hydrogen Characterization, Hydrogen Embrittlement Mechanism and Prevention", *Acta Metallurgical Sinica-English*, **33**, 759-773 (2020). 10.1007/s40195-020-01039-7
255. P. Sofronis, I. M. Robertson, "Viable mechanisms of hydrogen embrittlement-A review", *AIP Conference Proceedings*, **837**, 64-71 (2006). 10.1063/1.2213060
256. B. H. Sun, D. Wang, X. Lu, D. Wan, D. Ponge, X. C. Zhang, "Current Challenges and Opportunities Toward Understanding Hydrogen Embrittlement Mechanisms in Advanced High-Strength Steels: A Review", *Acta Metallurgical Sinica -English*, **34**, 741-754 (2021). 10.1007/s40195-021-01233-1
257. C. San Marchi, J. Ronevich, P. Bortot, Y. Wada, J. Felbaum, M. Rana, in *ASME 2019 Pressure Vessels & Piping Conference, Vol. Volume 1: Codes and Standards*, **2019** https://doi.org/10.1115/PVP2019-93907 10.1115/pvp2019-93907
258. H. S. Kwak, G. Y. Park, C. Kim, "Design of Compressed Natural Gas Pressure Vessel (Type II) to Improve Storage Efficiency and Structural Reliability", *Journal of Pressure Vessel Technology*, **142** 011303-011316 (2020). 10.1115/1.4045027
259. J. A. Ronevich, C. San Marchi, D. Brooks, J. M. Emery, P. Grimmer, E. Chant, J. R. Sims, A. Belokobyika, D. Farese, in *ASME 2019 Pressure Vessels & Piping Conference*, **2021.** 10.1115/PVP2021-61815
260. P. B. McLaughlin, S. C. Forth, L. R. Grimes-Ledesma, "Composite Overwrapped Pressure Vessels, A Primer", NASA, **2011.**
261. J. A. Ronevich, C. W. San Marchi, in *American Gas Association Sustainable Growth Committee* (Ed.: S. N. L. (SNL-CA)), **2019.** https://www.osti.gov/servlets/purl/1646101
262. G. Rawls, J. A. Ronevich, A. Slifka, **2017.** https://www.energy.gov/sites/default/files/2017/09/f37/fcto_webinarslides_lowering_costs_h2_pipelines_097217.pdf
263. A. Witkowski, A. Rusin, M. Majkut, K. Stolecka, "Analysis of compression and transport of the methane/hydrogen mixture in existing natural gas pipelines", *International Journal of Pressure Vessels and Piping*, **166**, 24-34 (2018). 10.1016/j.ijpvp.2018.08.002

264. Ł. Zabrzeski, P. Janusz, K. Liszka, M. Łaciak, A. Szurlej, "The Effect of Hydrogen Transported through a Gas Pipeline on the Functioning of Gas Compression Station Work", *AGH Drilling, Oil, Gas*, **33**, 959-967 (2017). http://dx.doi.org/10.7494/drill.2017.34.4.959
265. European Union, **2018.** https://www.hylaw.eu/database
266. Agency for the Cooperation of Energy Regulators (ACER), "ACER Report on NRAs Survey - Hydrogen, Biomethane, and Related Network Adaptations", **2020.** https://documents.acer.europa.eu/Official_documents/Acts_of_the_Agency/Publication/ACER%20Report%20on%20NRAs%20Survey.%20Hydrogen%2C%20Biomethane%2C%20and%20Related%20Network%20Adaptations.docx.pdf
267. I. Staffell, D. Scamman, A. V. Abad, P. Balcombe, P. E. Dodds, P. Ekins, N. Shah, K. R. Ward, "The role of hydrogen and fuel cells in the global energy system", *Energy & Environmental Science*, **12**, 463-491 (2019). 10.1039/c8ee01157e
268. F. Dolci, D. Thomas, S. Hilliard, C. F. Guerra, R. Hancke, H. Ito, M. Jegoux, G. Kreeft, J. Leaver, M. Newborough, J. Proost, M. Robinius, E. Weidner, C. Mansilla, P. Lucchese, "Incentives and legal barriers for power-to-hydrogen pathways: An international snapshot", *International Journal of Hydrogen Energy*, **44**, 11394-11401 (2019). 10.1016/j.ijhydene.2019.03.045
269. E. S. Henry, J. Bautista, I., J. D. Pendelton, D. R. Walsh, **2020.** https://www.socalgas.com/sites/default/files/2020-11/Utilities_Joint_Application_Prelim_H2_Injection_Standard_11-20-20.pdf
270. Y. Yoo, N. Glass, R. Baker, **2017** https://nrc-publications.canada.ca/eng/view/ft/?id=94a036f4-0e60-4433-add5-9479350f74de
271. From left to right: https://commons.wikimedia.org/wiki/File:Aerial_of_Badak_NGL_natural_gas_refinery.jpg; https://www.flickr.com/photos/warriorwoman531/8155235271/; https://www.flickr.com/photos/40132991@N07/7501108978; https://www.flickr.com/photos/nasakennedy/26172644733; https://www.flickr.com/photos/iip-photo-archive/22724718378
272. L. Decker, in *Hyper Closing Seminar*, Brussels, Belgium, **2019.**
273. P. Gerstl, in *Linde LH_2 Distribution Equipment*, PyeongChang, South Korea, **2019.**
274. G. Petitpas, "Simulation of boil-off losses during transfer at a LH_2 based hydrogen refueling station", *International Journal of Hydrogen Energy*, **43**, 21451-21463 (2018). 10.1016/j.ijhydene.2018.09.132
275. A. G. Krenn, D. W. Desenberg, in *Cryogenic Engineering Conference and International Cryogenic Materials Conference (CEC/ICMC)*, NASA, Hartford, CT, **2019**, pp. KSC-E-Daa-TN69387.
276. W. U. Notardonato, A. M. Swanger, J. E. Fesmire, K. M. Jumper, W. L. Johnson, T. M. Tomsik, Iop, in *Advances in Cryogenic Engineering, Vol. 278*, **2017**.
277. S. Kamiya, M. Nishimura, E. Harada, in *Proceedings of the 25th International Cryogenic Engineering Conference and International Cryogenic Materials Conference 2014, Vol. 67* (Eds.: H. J. M. TerBrake, H. H. J. TenKate, S. Vanapalli), **2015**, pp. 11-19.
278. F. Michel, H. Fiesler, L. Allidieres, in *WHEC*, Lyon, France, **2006**
279. R. K. Ahluwalia, H. S. Roh, J.-K. Peng, X. Wang, D. Papadias, S. Aceves, N. Killingsworth, B.Ehrhart, E. Hecht, J. Ronevich, C.Houchins, in *2021 DOE Hydrogen Program Annual Merit Review and Peer Evaluation Meeting*, **2021** https://www.hydrogen.energy.gov/pdfs/review21/st223_ahluwalia_2021_o.pdf
280. R. K. Ahluwalia, D. Papadias, W. Wang, in *2021 DOE Hydrogen Program Annual Merit Review and Peer Evaluation Meeting*, **2021.**
281. R. Tarkowski, "Underground hydrogen storage: Characteristics and prospects", *Renewable Sustainable Energy Review*, **105**, 86-94 (2019). 10.1016/j.rser.2019.01.051
282. N. Heinemann, J. Alcalde, J. M. Miocic, S. J. T. Hangx, J. Kallmeyer, C. Ostertag-Henning, A. Hassanpouryouzband, E. M. Thaysen, G. J. Strobel, C. Schmidt-Hattenberger, K. Edlmann, M. Wilkinson, M. Bentham, R. Stuart Haszeldine, R. Carbonell, A. Rudloff, "Enabling large-scale

hydrogen storage in porous media – the scientific challenges", *Energy & Environmental Science*, **14**, 853-864 (2021). 10.1039/D0EE03536J
283. N. Nanninga, A. Slifka, Y. Levy, C. White, "A Review of Fatigue Crack Growth for Pipeline Steels Exposed to Hydrogen", *Journal of Research of the National Institute of Standards and Technology*, **115**, 437-452 (2010). 10.6028/jres.115.030
284. A. Acht, in *Solution Mining Research Institute Conference*, Bremen, Germany, **2012.**
285. N. Dopffel, S. Jansen, J. Gerritse, "Microbial side effects of underground hydrogen storage - Knowledge gaps, risks and opportunities for successful implementation", *International Journal of Hydrogen Energy*, **46**, 8594-8606 (2021). 10.1016/j.ijhydene.2020.12.058
286. A. Ebigbo, F. Golfier, M. Quintard, "A coupled, pore-scale model for methanogenic microbial activity in underground hydrogen storage", *Advance in Water Resources*, **61**, 74-85 (2013). 10.1016/j.advwatres.2013.09.004
287. V. Reitenbach, L. Ganzer, D. Albrecht, B. Hagemann, "Influence of added hydrogen on underground gas storage: a review of key issues", *Environmental Earth Sciences*, **73**, 6927-6937 (2015). 10.1007/s12665-015-4176-2
288. P. O. Carden, L. Paterson, "Physical, chemical and energy aspects of underground hydrogen storage", *International Journal of Hydrogen Energy*, **4**, 559-569 (1979). 10.1016/0360-3199(79)90083-1
289. W. T. Pfeiffer, S. Bauer, in *European Geosciences Union General Assembly 2015 - Division Energy, Resources and Environment, Egu 2015, Vol. 76* (Eds.: M. Ask, S. Hangx, V. Bruckman, M. Kuhn), **2015**, pp. 565-572.
290. B. Hagemann, M. Rasoulzadeh, M. Panfilov, L. Ganzer, V. Reitenbach, "Mathematical modeling of unstable transport in underground hydrogen storage", *Environmental Earth Sciences*, **73**, 6891-6898 (2015). 10.1007/s12665-015-4414-7
291. M. Schlichtenmayer, A. Bannach, Solution Mining Research Institute, **2015**
292. A. Perez, E. Perez, S. Dupraz, J. Bolcich, in *21st World Hydrogen Energy Conference*, Zaragoza, Spain, **2016** https://hal-brgm.archives-ouvertes.fr/hal-01317467/document
293. R. Andrews, in *Energy Matters*, **2018**
294. International Energy Agency, **2019.** https://doi.org/10.1787/1e0514c4-en
295. E4tech, **2019.** http://www.afhypac.org/documents/publications/rapports/TheFuelCellIndustryReview2019.pdf
296. "California Plans to Ban Sales of new Gas-Powered Cars in 15 Years" in *New York Times*, New York, New York, **2020.**
297. B. Paul, J. Andrews, "PEM unitised reversible/regenerative hydrogen fuel cell systems: State of the art and technical challenges", *Renewable & Sustainable Energy Reviews*, **79**, 585-599 (2017). 10.1016/j.rser.2017.05.112
298. Y. F. Wang, D. Y. C. Leung, J. Xuan, H. Z. Wang, "A review on unitized regenerative fuel cell technologies, part-A: Unitized regenerative proton exchange membrane fuel cells", *Renewable & Sustainable Energy Reviews*, **65**, 961-977 (2016). 10.1016/j.rser.2016.07.046
299. S. Zhao, L. T. Yan, H. M. Luo, W. Mustain, H. Xu, "Recent progress and perspectives of bifunctional oxygen reduction/evolution catalyst development for regenerative anion exchange membrane fuel cells", *Nano Energy*, **47**, 172-198 (2018). 10.1016/j.nanoen.2018.02.015
300. B. Pivovar, Y. S. Kim, in *Anion Exchange Membrane Workshop* Dallas, Texas **2019.** https://www.nrel.gov/docs/fy20osti/77240.pdf
301. D. A. Cullen, K. C. Neyerlin, R. K. Ahluwalia, R. Mukundan, K. L. More, R. L. Borup, A. Z. Weber, D. J. Myers, A. Kusoglu, "New roads and challenges for fuel cells in heavy-duty transportation", *Nature Energy*, **6**, 462-474 (2021). 10.1038/s41560-021-00775-z
302. R. Borup, K. More, A. Weber, in *2018 Hydrogen and Fuel Cells Program Annual Merit Review, Vol. 2018*, Department of Energy, Energy Efficiency and Renewable Energy, Hydrogen and Fuel Cell Technologies Office, Arlington, VA, **2018** https://www.hydrogen.energy.gov/pdfs/review18/fc135_borup_2018_o.pdf

303. D. Banham, J. X. Zou, S. Mukerjee, Z. H. Liu, D. Yang, Y. Zhang, Y. Peng, A. G. Dong, "Ultralow platinum loading proton exchange membrane fuel cells: Performance losses and solutions", *Journal of Power Sources*, **490**, 229515-229532 (2021). 10.1016/j.jpowsour.2021.229515
304. J. S. Spendelow, in *2019 Hydrogen and Fuel Cells Program Annual Merit Review*, United States Department of Energy, Energy Efficiency and Renewable Energy, Hydrogen and Fuel Cell Technologies Office, Arlington, VA, **2019** https://www.hydrogen.energy.gov/pdfs/review19/fc161_spendelow_2019_o.pdf
305. L. Osmieri, J. Park, D. A. Cullen, P. Zelenay, D. J. Myers, K. C. Neyerlin, "Status and challenges for the application of platinum group metal-free catalysts in proton-exchange membrane fuel cells", *Current Opinions in Electrochemistry*, **25**, 100627-100638 (2021). 10.1016/j.coelec.2020.08.009
306. H. T. Chung, D. A. Cullen, D. Higgins, B. T. Sneed, E. F. Holby, K. L. More, P. Zelenay, "Direct atomic-level insight into the active sites of a high-performance PGM-free ORR catalyst", *Science*, **357**, 479-483 (2017). 10.1126/science.aan2255
307. P. Zelenay, D. J. Myers, in *2020 Hydrogen and Fuel Cells Program Annual Merit Review*, U.S. Department of Energy, Energy Efficiency and Renewable Energy, Hydrogen and Fuel Cell Technologies, On-line, **2020.** https://www.hydrogen.energy.gov/pdfs/review20/fc160_myers_zelenay_2020_o.pdf
308. R. Borup, J. Meyers, B. Pivovar, Y. S. Kim, R. Mukundan, N. Garland, D. Myers, M. Wilson, F. Garzon, D. Wood, P. Zelenay, K. More, K. Stroh, T. Zawodzinski, J. Boncella, J. E. McGrath, M. Inaba, K. Miyatake, M. Hori, K. Ota, Z. Ogumi, S. Miyata, A. Nishikata, Z. Siroma, Y. Uchimoto, K. Yasuda, K. I. Kimijima, N. Iwashita, "Scientific aspects of polymer electrolyte fuel cell durability and degradation", *Chemical Reviews*, **107**, 3904-3951 (2007). 10.1021/cr050182l
309. J. Chlistunoff, B. Pivovar, "Effects of Ionomer Morphology on Oxygen Reduction on Pt", *Journal of the Electrochemical Society*, **162**, F890-F900 (2015). 10.1149/2.0661508jes
310. A. Z. Weber, R. L. Borup, in *DOE Hydrogen and Fuel Cell Technologies Annual Merit Review*, **2021.** https://www.hydrogen.energy.gov/pdfs/review21/fc339_weber_2021_o.pdf.
311. C. S. Gittleman, H. Jia, E. S. De Castro, C. R. I. Chisholm, Y. S. Kim, "Proton Conductors for Heavy-duty Vehicle Fuel Cells", *Joule* (2021). 10.1016/j.joule.2021.05.016
312. S. A. Berlinger, G. S., A. Z. Weber, "Multicomponent, Multiphase Interactions in Fuel Cell Inks", *Current Opinion in Electrochemistry*, **29** (2021). 10.1016/j.coelec.2018.11.012
313. T. Van Cleve, S. Khandavalli, A. Chowdhury, S. Medina, S. Pylypenko, M. Wang, K. L. More, N. Kariuki, D. J. Myers, A. Z. Weber, S. A. Mauger, M. Ulsh, K. C. Neyerlin, "Dictating Pt-Based Electrocatalyst Performance in Polymer Electrolyte Fuel Cells, from Formulation to Application", *Acs Applied Materials & Interfaces*, **11**, 46953-46964 (2019). 10.1021/acsami.9b17614
314. D. G. Li, H. T. Chung, S. Maurya, I. Matanovic, Y. S. Kim, "Impact of ionomer adsorption on alkaline hydrogen oxidation activity and fuel cell performance", *Current Opinion in Electrochemistry*, **12**, 189-195 (2018). 10.1016/j.coelec.2018.11.012
315. W. E. Mustain, M. Chatenet, M. Page, Y. S. Kim, "Durability challenges of anion exchange membrane fuel cells", *Energy & Environmental Science*, **13**, 2805-2838 (2020). 10.1039/d0ee01133a
316. S. Maurya, A. S. Lee, D. G. Li, E. J. Park, D. P. Leonard, S. Noh, C. Bae, Y. S. Kim, "On the origin of permanent performance loss of anion exchange membrane fuel cells: Electrochemical oxidation of phenyl group", *Journal of Power Sources*, **436**, 9 (2019). 10.1016/j.jpowsour.2019.226866
317. M. Fallah Vostakola, B. A. Horri, "Progress in Material Development for Low-Temperature Solid Oxide Fuel Cells: A Review", *Energies*, **14** (2021). https://doi.org/10.3390/en14051280
318. W. Zhang, Y. H. Hu, "Progress in proton-conducting oxides as electrolytes for low-temperature solid oxide fuel cells: From materials to devices", *Energy Science & Engineering*, **9**, 984-1011 (2021). 10.1002/ese3.886
319. M. C. Williams, D. V. Shailesh, G. Jesionowski, "Worldwide Status of Solid Oxide Fuel Cell Technology", *Electrochemical Society Transactions*, **96**, 1-10 (2020).

320. M. Singh, D. Zappa, E. Comini, "Solid oxide fuel cell: Decade of progress, future perspectives and challenges", *International Journal of Hydrogen Energy* (2021). 10.1016/j.ijhydene.2021.06.020
321. L. Gagliani, A. Visibile, K. Ö. Gündüz, J.-E. Svensson, J. Froitzheim, "The Influence of Humidity Content on Ferritic Stainless Steels Used in Solid Oxide Fuel Cell Under Dual Atmosphere Conditions at 600° C.", *Electrochemical Society Transactions*, **103** (2021).
322. P. Burke, in *44th International Conference and Exposition on Advanced Ceramics and Composites (ICACC 2020)*, **2020.**
323. A. B. Sreedhar I, Goyal P, Agarwal A., "An overview of degradation in solid oxide fuel cells-potential clean power sources", *Journal of Solid State Electrochemistry* (2020). 10.1007/s10008-020-04584-4
324. K. O. Gunduz, A. Chyrkin, C. Goebel, L. Hansen, O. Hjorth, S. J.-E., "The effect of hydrogen on the breakdown of the protective oxide scale in solid oxide fuel cell interconnects", *Corrosion Sci.*, **179** 109112-109123 (2021). 10.1016/j.corsci.2020.109112
325. V. Philip, "Hydrogen as part of our value chain", Siemens Co., March 19, **2021.** https://assets.siemens-energy.com/siemens/assets/api/uuid:2a8c8b5c-a041-4faf-aaba-0d6f047f6145/se-hydrogen-day-presentation-vinod-philip.pdf
326. J. Goldmeer, J. Catillaz, J. Donohue, GE Gas Power, **2021.** https://www.ge.com/content/dam/gepower-new/global/en_US/downloads/gas-new-site/future-of-energy/hydrogen-fuel-for-gas-turbines-gea34979.pdf
327. R. Hamilton, O. Minervino and N. KV, "Next Generation Fuel Firing Combustion Technology for Gas Turbines," in Electrify Europe, 2018.
328. Solar Turbines, https://www.solarturbines.com/en_US/about-us/news-and-press-releases/converting-high-hydrogen-fuel-to-electricity.html
329. Solar Turbines, https://www.solarturbines.com/en_US/solutions/carbon-reduction/carbon-neutral-fuels/hydrogen.html
330. Ansaldo Energia, https://www.ansaldoenergia.com/PublishingImages/Idrogeno/Ansaldo%20Energia%20Solutions%20For%20Hydrogen%20Combustion.pdf
331. I. Glassman, *Combustion*, Academic Press, New York, New York, **1987.**
332. T. Asai, Y. Akiyama, K. Yunoki, N. Horii, K. Miura, M. Karishuku, S. Dodo, in *45th Turbomachinery & 32nd Pump Symposia*, Houston, TX, **2016**
333. A. Ciani, J. P. Wood, A. Wickstrom, G. J. Rortveit, R. Steeneveldt, J. Pettersen, N. Wortmann, M. J. Bothien, in *ASME TurboExpo*, Virtual, **2020.**
334. S. Dodo, T. Asai, H. Koizumi, H. Takahashi, S. Yoshida, H. Inoue, "Performance of a Multiple-Injection Dry Low NOx Combustor With Hydrogen-Rich Syngas Fuels", *Journal of Engineering for Gas Turbines and Power-Transactions ASME*, **135**, 7 (2013). 10.1115/1.4006691
335. M. Nose, T. Kawakami, H. Araki, N. Senba, S. Tanimura, in *Mitsubishi Heavy Industries Technical Review, Vol. 55(4)*, **2018**
336. Tekin, Nurettin & Ashikaga, Mitsugu & Horikawa, Atsushi & Funke, Dr.-Ing. Harald. (2019). "Enhancement of fuel flexibility of industrial gas turbines by development of innovative hydrogen combustion systems."
337. U. S. Department of Energy, https://www.netl.doe.gov/node/935
338. General Electric Gas and Power, Schenectady, NY, **2017.**
339. J. Goldmeer, in *Turbomachinery International, Vol. November/December*, **2020** https://www.turbomachinerymag.com/view/solving-the-challenge-of-lean-hydrogen-premix-combustion-with-highly-reactive-fuels
340. C. J. Goy, S. R. James, S. Rea, in *Combustion Instabilities in Gas Turbine Engines*, American Institute of Aeronautics and Astronautics, Reston, VA, **2005**, pp. 163-175.
341. M. Brower, E. L. Petersen, W. Metcalfe, H. J. Curran, M. Furi, G. Bourque, N. Aluri, F. Guthe, "Ignition Delay Time and Laminar Flame Speed Calculations for Natural Gas/Hydrogen Blends at

Elevated Pressures", *Journal of Engineering for Gas Turbines and Power-Transactions ASME*, **135**, 10 (2013). 10.1115/1.4007763
342. P. L. Spath, D. C. Dayton, (Ed.: National Renewable Energy Laboratory), **2003.** https://www.nrel.gov/docs/fy04osti/34929.pdf**.**
343. S. Garg, M. R. Li, A. Z. Weber, L. Ge, L. Y. Li, V. Rudolph, G. X. Wang, T. E. Rufford, "Advances and challenges in electrochemical CO2 reduction processes: an engineering and design perspective looking beyond new catalyst materials", *Journal of Materials Chemistry A*, **8**, 1511-1544 (2020). https://doi.org/10.1039/c9ta13298h
344. D. Higgins, C. Hahn, C. X. Xiang, T. F. Jaramillo, A. Z. Weber, "Gas-Diffusion Electrodes for Carbon Dioxide Reduction: A New Paradigm", *ACS Energy Letters*, **4**, 317-324 (2019). 10.1021/acsenergylett.8b02035
345. F. Y. Gao, R. C. Bao, M. R. Gao, S. H. Yu, "Electrochemical CO2-to-CO conversion: electrocatalysts, electrolytes, and electrolyzers", *Journal of Materials Chemistry A*, **8**, 15458-15478 (2020). 10.1039/d0ta03525d
346. D. M. Weekes, D. A. Salvatore, A. Reyes, A. X. Huang, C. P. Berlinguette, "Electrolytic CO2 Reduction in a Flow Cell", *Accounts of Chemical Research*, **51**, 910-918 (2018). 10.1021/acs.accounts.8b00010
347. T. T. Zheng, K. Jiang, H. T. Wang, "Recent Advances in Electrochemical CO2-to-CO Conversion on Heterogeneous Catalysts", *Advanced Materials*, **30**, 15 (2018). 10.1002/adma.201802066
348. Statista, **2021.** https://www.statista.com/statistics/974802/us-methanol-production-volume/
349. Statista, **2021.** https://www.statista.com/statistics/1065891/global-methanol-production-capacity/
350. International Renewable Energy Agency, **2021.** https://www.irena.org/-/media/Files/IRENA/Agency/Publication/2021/Jan/IRENA_Innovation_Renewable_Methanol_2021.pdf
351. Gas Processing News, **2021.** http://www.gasprocessingnews.com/features/201510/small-scale-methanol-technologies-offer-flexibility,-cost-effectiveness.aspx
352. U.S. Department of Energy, Office of Science, Basic Energy Sciences, Bethesda, MD, **2019.** https://science.osti.gov/-/media/bes/pdf/reports/2020/Chemical_Upcycling_Polymers.pdf
353. M. Solis, S. Silveira, "Technologies for chemical recycling of household plastics - A technical review and TRL assessment", *Waste Management*, **105**, 128-138 (2020). 10.1016/j.wasman.2020.01.038
354. Y. Miao, A. von Jouanne, A. Yokochi, "Current Technologies in Depolymerization Process and the Road Ahead", *Polymers*, **13**, 17 (2021). 10.3390/polym13030449
355. D. Munir, M. F. Irfan, M. R. Usman, "Hydrocracking of virgin and waste plastics: A detailed review", *Renewable & Sustainable Energy Reviews*, **90**, 490-515 (2018). 10.1016/j.rser.2018.03.034
356. M. Guttman, in *Conversion of Polymer Wastes and Energetics* (Eds.: H. H. Krause, J. M. L. Penniger), **1994**, pp. 57-65.
357. S. Oya, D. Kanno, H. Watanabe, M. Tamura, Y. Nakagawa, K. Tomishige, "Catalytic Production of Branched Small Alkanes from Biohydrocarbons", *Chemsuschem*, **8**, 2472-2475 (2015). 10.1002/cssc.201500375
358. Y. Nakaji, Y. Nakagawa, M. Tamura, K. Tomishige, "Regioselective hydrogenolysis of alga-derived squalane over silica-supported ruthenium-vanadium catalyst", *Fuel Processing Technology*, **176**, 249-257 (2018). 10.1016/j.fuproc.2018.03.038
359. G. Celik, R. M. Kennedy, R. A. Hackler, M. Ferrandon, A. Tennakoon, S. Patnaik, A. M. LaPointe, S. C. Ammal, A. Heyden, F. A. Perras, M. Pruski, S. L. Scott, K. R. Poeppelmeier, A. D. Sadow, M. Delferro, "Upcycling Single-Use Polyethylene into High-Quality Liquid Products", *ACS Central Science*, **5**, 1795-1803 (2019). 10.1021/acscentsci.9b00722
360. S. B. Liu, P. A. Kots, B. C. Vance, A. Danielson, D. G. Vlachos, "Plastic waste to fuels by hydrocracking at mild conditions", *Science Advances*, **7**, 9 (2021). 10.1126/sciadv.abf8283
361. A. Tennakoon, X. Wu, A. L. Paterson, S. Patnaik, Y. C. Pei, A. M. LaPointe, S. C. Ammal, R. A. Hackler, A. Heyden, Slowing, II, G. W. Coates, M. Delferro, B. Peters, W. Y. Huang, A. D. Sadow,

F. A. Perras, "Catalytic upcycling of high-density polyethylene via a processive mechanism", *Nature Catalysis*, **3**, 893-901 (2020). 10.1038/s41929-020-00519-4
362. F. Zhang, M. H. Zeng, R. D. Yappert, J. K. Sun, Y. H. Lee, A. M. LaPointe, B. Peters, M. M. Abu-Omar, S. L. Scott, "Polyethylene upcycling to long-chain alkylaromatics by tandem hydrogenolysis/aromatization", *Science*, **370**, 437-441 (2020). 10.1126/science.abc5441
363. V. R. Dufaud, J. M. Basset, "Catalytic hydrogenolysis at low temperature and pressure of polyethylene and polypropylene to diesels or lower alkanes by a zirconium hydride supported on silica-alumina: A step toward polyolefin degradation by the microscopic reverse of Ziegler-Natta polymerization", *Angewandte Chemie-International Edition*, **37**, 806-810 (1998). 10.1002/(sici)1521-3773(19980403)37:6<806::Aid-anie806>3.0.Co;2-6
364. S. Ghavam, M. Vahdati, I. A. G. Wilson, P. Styring, "Sustainable Ammonia Production Processes", *Frontiers in Energy Research*, **9**, 580808-580826, (2021). 10.3389/fenrg.2021.580808
365. S. Giddey, S. P. S. Badwal, A. Kulkarni, "Review of electrochemical ammonia production technologies and materials", *International Journal of Hydrogen Energy*, **38**, 14576-14594 (2013). 10.1016/j.ijhydene.2013.09.054
366. H. Xu, K. Ithisuphalap, Y. Li, S. Mukherjee, J. Lattimer, G. Soloveichik, G. Wu, "Electrochemical ammonia synthesis through N-2 and H2O under ambient conditions: Theory, practices, and challenges for catalysts and electrolytes", *Nano Energy*, **69** (2020). 10.1016/j.nanoen.2020.104469
367. R. Zhao, H. Xie, L. Chang, X. Zhang, X. Zhu, X. Tong, T. Wang, Y. Luo, P. Wei, Z. Wang, X. Sun, "Recent Progress in the Electrochemical Ammonia Synthesis under Ambient Conditions", *EnergyChem*, **1**, 100011-100039 (2019). 10.1016/j.enchem.2019.100011
368. Y. Yao, J. Wang, U. B. Shahid, M. Gu, H. Wang, H. Li, M. Shao, "Electrochemical Synthesis of Ammonia from Nitrogen Under Mild Conditions: Current Status and Challenges", *Electrochemical Energy Reviews*, **3**, 239-270 (2020). 10.1007/s41918-019-00061-3
369. J. Nash, X. Yang, J. J. Anibal, J. H. Wang, Y. S. X. Yan, B.J., "Electrochemical Nitrogen Reduction Reaction on Noble Metal Catalysts in Proton and Hydroxide Exchange Membrane Electrolyzers", *Journal of the Electrochemical Society*, **164**, F1712-F1716 (2017). 10.1149/2.0071802jes
370. S. J. Li, D. Bao, M. M. Shi, B. R. Wulan, J. M. Yan, Q. Jiang, "Amorphizing of Au Nanoparticles by CeOx -RGO Hybrid Support towards Highly Efficient Electrocatalyst for N2 Reduction under Ambient Conditions", *Advanced Materials*, **29,** 1700001-1700006 (2017). 10.1002/adma.201700001
371. https://ammoniaindustry.com/small-scale-ammonia-where-the-economics-work-and-the-technology-is-ready/
372. H. Liu, "Ammonia synthesis catalyst 100 years: Practice, enlightenment and Challenge", *Chinese Journal of Catalysis*, **35**, 1619-1640 (2014). 10.1016/S1872-2067(14)60118-2
373. U.S. Department of Energy, Office of Science, Basic Energy Sciences, **2016.** https://www.osti.gov/servlets/purl/1283146/
374. P. Wang, F. Chang, W. Gao, J. Guo, G. Wu, T. He, P. Chen, "Breaking scaling relations to achieve low-temperature ammonia synthesis through LiH-mediated nitrogen transfer and hydrogenation", *Nature Chemistry*, **9**, 64-70 (2017). 10.1038/nchem.2595
375. M. Malmali, Y. M. Wei, A. McCormick, E. L. Cussler, "Ammonia Synthesis at Reduced Pressure via Reactive Separation", *Industrial & Engineering Chemistry Research*, **55**, 8922-8932 (2016). 10.1021/acs.iecr.6b01880
376. D. K. Ojha, M. J. Kale, A. V. McCormick, M. Reese, M. Malmali, P. Dauenhauer, E. L. Cussler, "Integrated Ammonia Synthesis and Separation", *Acs Sustainable Chemistry & Engineering*, **7**, 18785-18792 (2019). 10.1021/acssuschemeng.9b03050
377. M. Y. Zhang, Y. L. Hu, H. Y. Wang, H. Y. Li, X. Han, Y. M. Zeng, C. C. Xu, "A review of bio-oil upgrading by catalytic hydrotreatment: Advances, challenges, and prospects", *Molecular Catalysis*, **504**, 20 (2021). 10.1016/j.mcat.2021.111438

378. Y. L. Han, M. Gholizadeh, C. C. Tran, S. Kaliaguine, C. Z. Li, M. Olarte, M. Garcia-Perez, "Hydrotreatment of pyrolysis bio-oil: A review", *Fuel Processing Technology*, **195**, 29 (2019). 10.1016/j.fuproc.2019.106140
379. G. Bagnato, A. Sanna, E. Paone, E. Catizzone, "Recent Catalytic Advances in Hydrotreatment Processes of Pyrolysis Bio-Oil", *Catalysts*, **11**, 19 (2021). 10.3390/catal11020157
380. M. Peplow, "The race for green steel", *Chemical Engineering News*, **99**, 22-29 (2021).
381. L. Holappa, "A General Vision for Reduction of Energy Consumption and CO(2)Emissions from the Steel Industry", *Metals*, **10**, 21 (2020). 10.3390/met10091117
382. Statista, **2020** https://www.statista.com/statistics/209343/steel-production-in-the-us/
383. W. G. Liu, H. B. Zuo, J. S. Wang, Q. G. Xue, B. L. Ren, F. Yang, S. L. Co, "The production and application of hydrogen in steel industry", *International Journal of Hydrogen Energy*, **46**, 10548-10569 (2021). 10.1016/j.ijhydene.2020.12.123
384. D. Spreitzer, J. Schenk, "Reduction of Iron Oxides with Hydrogen-A Review", *Steel Research International*, **90**, 17 (2019). 10.1002/srin.201900108
385. G. Y. Sun, B. Li, H. J. Guo, W. S. Yang, S. Y. Li, J. Guo, "Thermodynamic Study on Reduction of Iron Oxides by H-2 + CO + CH4 + N-2 Mixture at 900 degrees C", *Energies*, **13**, 18 (2020). 10.3390/en13195053
386. J. Tang, M. S. Chu, F. Li, C. Feng, Z. G. Liu, Y. S. Zhou, "Development and progress on hydrogen metallurgy", *Int. J. Miner. Metall. Mater.*, **27**, 713-723 (2020). 10.1007/s12613-020-2021-4
387. J. Ripke, in *H2@S*, U.S. Department of Energy University of Houston, Houston, TX, **2017** https://www.energy.gov/sites/default/files/2017/05/f34/fcto_may_2017_h2_scale_wkshp_ripke.pdf
388. DRI, **2018** https://www.midrex.com/wp-content/uploads/MIdrexDRI_ProductsBrochure_4-12-18-1.pdf
389. Midrex, **2018** https://www.midrex.com/wp-content/uploads/Midrex_STATSbookprint_2018Final-1.pdf
390. A. Bhaskar, M. Assadi, H. N. Somehsaraei, "Can Methane Pyrolysis-based Hydrogen Production Lead to the Decarbonisation of Iron and Steel Industry?", *Energy Conv. Manag.*, **10** (2021).
391. M. Åhman, O. Olsson, V. Vogl, B. Nyqvist, A. Maltais, L. J. Nilsson, K. Hallding, K. Skånberg, M. Nilsson, Miljö-och energisystem, LTH, Lunds Universitet https://portal.research.lu.se/portal/files/50948268/LU_SEI_HYBRIT_report.pdf
392. P. R. Behera, B. Bhoi, R. K. Paramguru, P. S. Mukherjee, B. K. Mishra, "Hydrogen Plasma Smelting Reduction of Fe2O3", *Metall Mater Trans B*, **50**, 262-270 (2019). 10.1007/s11663-018-1464-8
393. K. C. Sabat, A. B. Murphy, "Hydrogen Plasma Processing of Iron Ore", *Metall Mater Trans B*, **48**, 1561-1594 (2017). 10.1007/s11663-017-0957-1
394. I. R. Souza, Y. Ma, M. Kulse, D. Ponge, B. Gault, H. Springer, D. Raabe, "Sustainable steel through hydrogen plasma reduction of iron ore: Process, kinetics, microstructure, chemistry", *Acta Mater.*, **213**, 16 (2021). 10.1016/j.actamat.2021.116971
395. J. Goldmeer, J. Catillaz, "Hydrogen for Power Generation: Experience, Requirements, and Implications for Use in Gas Turbines," GE Gas Power, 2021. https://www.ge.com/content/dam/gepower-new/global/en_US/downloads/gas-new-site/future-of-energy/hydrogen-for-power-gen-gea34805.pdf.
396. M. Brower, E. Petersen, W. Metcalfe, H. Curran, M. Furi, G. Bourque, N. Aluri and F. Guthe, "Ignition delay time and laminar flame speed calculations for natural gas/hydrogen blends at elevated pressures," in ASME TurboExpo, Copenhagen, 2012.
397. J. Ripke, in *H2@Scale*, U.S. Department of Energy University of Houston, Houston, TX, **2017** https://www.energy.gov/sites/default/files/2017/05/f34/fcto_may_2017_h2_scale_wkshp_ripke.pdf

DISCLAIMER: This report was prepared as an account of work sponsored by an agency of the United States government. Neither the United States government nor any agency thereof, nor any of their employees, makes any warranty, express or implied, or assumes any legal liability or responsibility for the accuracy, completeness, or usefulness of any information, apparatus, product, or process disclosed, or represents that its use would not infringe privately owned rights. Reference herein to any specific commercial product, process, or service by trade name, trademark, manufacturer, or otherwise does not necessarily constitute or imply its endorsement, recommendation, or favoring by the United States government.

10.2172/1809223

U.S. DEPARTMENT OF ENERGY | Office of Science